SORPTION OF PHOSPHATE AND OTHER CONTAMINANTS ON BIOCHAR AND ITS ENVIRONMENTAL IMPLICATIONS

By

YING YAO

A DISSERTATION PRESENTED TO THE GRADUATE SCHOOL
OF THE UNIVERSITY OF FLORIDA IN PARTIAL FULFILLMENT
OF THE REQUIREMENTS FOR THE DEGREE OF
DOCTOR OF PHILOSOPHY

UNIVERSITY OF FLORIDA

2013

To my family

ACKNOWLEDGMENTS

I would like to express my deep appreciation and gratitude to my advisor, Dr. Bin Gao, for the patient guidance and mentorship he provided to me, all the way from when I was first considering applying to the Ph.D. program in the Agricultural and Biological Engineering Department, through to completion of this degree. Dr. Gao's intellectual heft is matched only by his genuinely good nature and down-to-earth humility, and I am truly fortunate to have had the opportunity to work with him.

I would also like to thank my co-chair Dr. Bruce Welt and committee members Dr. Willie G. Harris, Christopher J. Martinez, and Yuncong Li for the friendly guidance, thought-provoking suggestions, and the general collegiality that each of them offered to me over the years. I truly appreciate that Prof. Liuyan Yang at Nanjing University encouraged and guided me towards my academic life.

I extend my gratitude to my colleagues Mandu Inyang, Dr. Yuan Tian, Ming Zhang, Lei Wu in the Environmental Nanotechnology Research Group for their valuable advice and help in my research. I also thank my friends Dr. Congrong Yu, Dr. Hao Chen, Dr. Yanmei Zhou, Yining Sun, and Lin Liu for their kindly priceless help and support. I would like to acknowledge Paul Lane, Orlando Lanni, and Billy Duckworth for their lab support.

Finally, I'd be remiss if I didn't acknowledge the innumerable sacrifices made by my family. Special thanks go to my parents and grandparents for their tremendous love and support in my whole life. Without them, I could not pursue this final degree.

TABLE OF CONTENTS

page

LIST OF TABLES

LIST OF FIGURES

LIST OF ABBREVIATIONS

AC	Activated carbon
BB300/ 450/ 600	Bamboo biochar made at temperature 300/ 450/ 600 ^{o}C
BG300/ 450/ 600	Bagasse biochar made at temperature 300/ 450/ 600 ^{o}C
BP300/ 450/ 600	Peanut hull biochar made at temperature 300/ 450/ 600 ^{o}C
CaEC/ CaET	Ca-biochar composites/ corresponding raw material
DSTC	Digested sugar beet tailing biochar
FCC1/ FCT1	Biochar from Senibel farm control tomato tissues / corresponding raw material
FCC2/ FCT2	Biochar from Rocky Tops farm control tomato tissues / corresponding raw material
HTPH	Peanut hull hydrochar
HW300/ 450/ 600	Hickory wood biochar made at temperature 300/ 450/ 600 ^{o}C
KLN	Kaolinite
LCC/ LCT	Laboratory control biochar/ corresponding raw material
MB	Methylene blue
MgEC/ MgET	Mg-biochar composites/ corresponding raw material
MMT	Montmorillonite
P	Phosphate
PH300/ 450/ 600	Brazilian pepperwood biochar made at temperature 300/ 450/ 600 ^{o}C
SMX	Sulfamethoxazole
STC	Raw sugar beet tailing biochar

Abstract of Dissertation Presented to the Graduate School
of the University of Florida in Partial Fulfillment of the
Requirements for the Degree of Doctor of Philosophy

SORPTION OF PHOSPHATE AND OTHER CONTAMINANTS ON BIOCHAR AND ITS ENVIRONMENTAL IMPLICATIONS

By

Ying Yao

May 2013

Chair: Bin Gao
Major: Agricultural and Biological Engineering

Biochar converted from agricultural residues or other carbon-rich wastes may provide new solutions for environmental management, particularly with respect to carbon sequestration and contaminant remediation. This Ph.D. dissertation systematically investigated the application of various biochars to remove various contaminants, including nutrients, antibiotics, and cationic dye from aqueous solutions and its implications.

Thirteen biochars were first tested in laboratory sorption experiments to determine their sorption ability to nutrients and most of them showed little/no ability to sorb nitrate or phosphate. However, nine biochars could remove ammonium from aqueous solution. Column leaching experiment showed that the BP600 biochar effectively reduced the total amount of nitrate, ammonium, and phosphate (P) in the leachates by 34.0%, 34.7%, and 20.6%, respectively, relative to the soil alone. The PH600 biochar also reduced the leaching of nitrate and ammonium by 34% and 14%, respectively, but caused additional P release from the soil columns. Therefore, the nutrient sorption characteristics of a biochar should be studied prior to its use in a particular soil amendment project.

To enhance biochar's sorption ability to P, an engineered biochar (i.e., DSTC) was produced from anaerobically digested sugar beet tailings. Its P removal ability (73%) was the highest compared to as-is biochar (i.e., STC), an activated carbon (AC), and three Fe-modified biochar/AC adsorbents. Batch adsorption kinetic and equilibrium isotherm experiments, mathematical models study, and post-adsorption characterizations using SEM-EDS, XRD, and FTIR suggested that the enhanced P sorption ability of the DSTC is due to the presence of colloidal and nano-sized MgO (periclase) particles on its surface.

Another engineered biochar (i.e., MgEC) was prepared from magnesium (Mg) enriched tomato tissues and showed better sorption ability to P in aqueous solutions compared to the other four tomato tissue biochars. Mathematical modeling and post-sorption characterization results indicated that the sorption was mainly controlled by two mechanisms: precipitation of P through chemical reaction with Mg particles and surface deposition of P on Mg crystals on biochar surfaces. Most of the P retained in MgEC was bioavailable and significantly stimulated grass seed germination and growth.

To test the sorption ability of biochars to antibiotics, eight biochars derived from agricultural/forestry residuals were used to sorb SMX from aqueous solutions. Two biochars have dramatically decreased SMX leaching with only 2~14% of the SMX transported through biochar-amended soils. However, biochar with high accumulations of SMX was found to inhibit the growth of the bacteria. Thus, biochar with very high pharmaceutical sorption abilities may find use as a low-cost alternative sorbent for treating wastewater plant effluent, but should be used with caution.

Finally, clay-modified biochars were developed in laboratory, combining advantages of both biochar and clay, to remove cationic contaminants from water. The results showed that BG-MMT could effectively adsorb MB, a cationic dye, with removal rate around 84.3%. Eight commonly used mathematical models were used to fit the kinetics and isotherm data to investigate the sorption mechanisms and the findings showed ion-exchange was the governing sorption mechanism of MB on the biochars. The clay-modified biochars thus could be regenerated and reused after dye adsorption for multiple times.

The results of this dissertation indicate that biochar, as alternative sorbent, could effectively remove nutrients (P), antibiotics (SMX) and cationic dye (MB) from aqueous solutions. New preparation methods, such as anaerobically digestion, plant nutrient enrichment, and surface modification, could further enhance the sorption ability of biochars and thus promote their environmental applications.

CHAPTER 1
INTRODUCTORY REVIEWS

Background and Problem Statement

Biochar is a pyrogenic black carbon that has attracted increased attention in both political and academic arenas [1]. A number of studies have suggested that terrestrial land application of biochar could effectively sequester carbon in soils and thus mitigate global warming [1, 2]. When biochar is applied to soils, it may also present other potential advantages, including enhanced soil fertility and crop productivity [3], increased soil nutrients and water holding capacity [4], and reduced emissions of other greenhouse gases from soils [5].

In addition to its carbon sequestration and soil amelioration applications, studies have also indicated biochar's potential to be used as a low-cost adsorbent, storing chemical compounds including some of the most common environmental pollutants. It has been demonstrated that biochars made from a variety of sources had strong sorption ability to different types of pesticides and other organic contaminants [6-9]. The sorption ability of biochar has been shown to exceed that of the natural soil organic matter by a factor of 10-100 in some cases [10]. In addition to strong organic compounds sorption ability, biochars have also been shown to remove metal contaminants from water and showed strong affinity for a number of heavy metal ions [11-13].

This dissertation project was designed to determine the characteristics and mechanisms that control the ability of biochar as a low-cost adsorbent to remove nutrients (mainly phosphate), antibiotics, and cationic dyes from aqueous solutions.

Why Use Biochar to Remove Nutrients

The release of nutrients, such as phosphate, ammonia, and nitrate, from both point and non-point sources into runoff may impose a great threat on environmental health [14, 15]. The high level growth limiting nutrient can promote excessive production of photosynthetic aquatic microorganisms in natural water bodies and ultimately becomes a major factor in the eutrophication of many freshwater and marine ecosystems [16]. It is therefore very important to develop effective technologies to remove phosphate, ammonia and nitrate from aqueous solutions prior to their discharge into runoff and natural water bodies [17].

Typically raw domestic wastewater has a total phosphorus concentration of approximately 10 mg P/L, the principal forms of phosphate being orthophosphate (5 mg P/L), pyrophosphate (1 mg P/L), and tripolyphosphate (3 mg P/L), together with smaller amounts of organic phosphates. To meet the effluent quality standards, the removal of phosphate from wastewaters prior to discharge into natural waters is required [18].

Many nutrient removal technologies including biological, chemical, and physical treatment methods have been developed for water treatment applications, particularly for the removal of phosphate and nitrate from municipal and industrial effluents [16, 19]. Both biological and chemical treatments have been well documented and proven to be effective to remove nutrients from wastewater. Addition of chemicals, such as calcium, aluminum, and iron salts into wastewater is considered a simple phosphate removal technique, which separates the phosphate from aqueous system through precipitation [20-23]. However, the chemical precipitation methods require strict control of operating conditions and may potentially introduce new contaminants into the water such as chloride and sulfate ions [15, 20, 24]. Biological treatment of phosphate and nitrate in

waste effluents may have certain advantages over the chemical precipitation method because it does not require chemical additions and enhanced biological treatment has been reported effectively remove most of the nutrients in waste water [25, 26]. This technology, however, is very sensitive to the operation conditions and its removal efficiency may be, at times, much less [27]. Both the chemical and biological treatment methods are also subjected to the costs and risks associated with nutrient-rich sludge handling and disposal [28].Various physical methods have also been developed to remove phosphate, nitrate, and ammonia from aqueous solution such as electrodialysis, reverse osmosis, and ion exchange [20, 29-32]. However, most of these physical methods have proven to be either too expensive or inefficient. Simple physical adsorption might be comparatively more useful and cost-effective for nutrients removal [33, 34]. Several studies investigated activated carbons as nutrient adsorbents, but showed that the adsorption capacity was very low [14, 18, 35]. For example, Namasivayam et al. [18] reported that activated carbon made from coir pith with ZnCl2-activation had a phosphate adsorption capacity of only 5,100 mg/kg. Lower-cost materials, such as slag, fly ash, dolomite, red mud, and oxide tailings have also been explored by several studies as alternative adsorbents of phosphate from waste water [36-40].

Biochar is a low-cost adsorbent that is receiving increased attention recently because it has many potential environmental applications and benefits. While most of the current biochar studies are focused on biochar land application as an easy and cost-effective way to sequestrate carbon and increase fertility, a number of recent investigations suggest that biochar converted from agricultural residues have a strong

ability to bind chemical contaminants in water including heavy metals and organic contaminants [8, 11, 12, 41, 42]. Only few studies, however, have investigated the ability of biochar to remove nutrients from water [43].Ideally, if biochar can be used as a sorbent to reclaim nutrients such as phosphate and nitrate from water, there would be no need to regenerate the exhausted biochar because it can be directly applied to agricultural fields as a slow release fertilizer to improve soil fertility and build (sequester) soil carbon. But little research has been conducted to explore the nutrient removal potential of biochar [44].

Although almost all biomass can be converted into biochar through thermal pyrolysis, a life cycle assessment of pyrolysis-biochar systems suggested that it is more environmentally and financially viable to make biochar from waste biomass [45]. In this sense, agricultural residues (e.g. sugarcane bagasse, poultry litter, and manure) and other green waste have been proposed as good feedstock materials to make biochar [9, 46, 47]. However, the applications and functions of those biochars are highly depending on their physicochemical properties (e.g. elemental composition, surface charge, and surface area) [46]. Because biochar can be made of various waste biomass sources under different processing conditions, it is therefore very important to characterize their physicochemical properties before use. In a recent study, Inyang et al. [48] explored the production of biochar from the residue materials of anaerobic digestion of sugarcane bagasse. Comparison of the physicochemical properties of the biochar from anaerobically digested bagasse to that from raw bagasse suggested that the former has more desirable characteristics for soil amelioration, contaminant remediation, or water treatment. Using anaerobically digested residue materials (or the remains of biofuel

production) as feedstock to produce biochar could not only reduce the waste management cost, but also make bioenergy production more sustainable and eco-friendly. It is therefore very important to test the generality of this innovative approach by examining the feasibility of using other anaerobically digested materials for biochar production. It is anticipated that biochars converted from digested feedstock materials would have good ability to remove nutrients from water.

Although it is still a relatively unexplored concept, the use of biochar to remove nutrients from aqueous solutions presents an innovative and promising technology. Not only may biochar represent a low-cost waste water treatment technology for nutrient removal, but the nutrient-laden biochar may also be used as a slow-release fertilizer to enhance soil fertility that will also sequester carbon.

Why Use Biochar to Remove Antibiotics and Its Impact on Reclaimed Water Irrigation

Water stress and scarcity resulting from rapid population growth, global climate changes, and pollution is among the greatest environmental problems faced by many countries.[49] In the past decade, freshwater consumption in agricultures rising rapidly due to demand not only from water-thirsty vegetables and meat, but also from biofuel crops.[50] Reclaimed water therefore has been used in agricultural and landscape irrigations to satisfy the demand and to ease the water crisis. Globally, about 20 million ha of land were irrigated with reclaimed water and this has become undoubtedly a key strategy to fight water shortage.[51, 52]

On one hand, reclaimed water often contains some nutrient elements, so its application to agricultural field may bring additional benefit to soil and crop systems.[53] On the other hand, however, reclaimed-water irrigation may also pose serious

environmental risks by introducing various pollutants, such as organic compounds and heavy metals, to irrigated soils and groundwater underneath.[54] Pharmaceutical residues, which are recognized as emerging contaminants, are frequently detected in the discharge of treated effluent from wastewater-treatment facilities (WWTF).[55] Occurrences of pharmaceuticals in treated wastewater, surface water, and groundwater have been reported worldwide.[55-58] In a field study of pharmaceuticals in soil irrigated with treated urban wastewater, Furlong et al.[59] found that reclaimed-water irrigation may result in leaching of pharmaceuticals through the vadose zone to contaminate groundwater. Adverse effect of reclaimed-water irrigation in agriculture caused by pharmaceuticals has also been demonstrated in several other studies.[54, 56, 60, 61]

Sulfamethoxazole (SMX) is one the most frequently detected pharmaceuticals in reclaimed water.[56, 59] As a sulfonamide bacteriostatic antibiotic, it is extensively used for treatment and prevention of both human and animal diseases.[62] SMX is characterized as low reactive and shows high mobility in soils.[63] Consequently, if it is released into the aquatic systems through discharges from WWTF, SMX not only has toxic effect to aquatic organisms, but also may induce drug resistance to disease-causing bacteria.[64, 65] Occurrences of SMX in groundwater have been reported in many places, so it is important to inhibit SMX leaching through the vadose zone during reclaimed-water irrigation. As suggested by Munoz et al.[56], there is a critical need to develop new method or technology for reclaimed-water irrigation in agriculture to reduce the contamination risk of pharmaceuticals, particularly with respect to SMX in reclaimed water.

Recent development of biochar technology may provide such an opportunity to reduce the risk of pharmaceutical contamination of groundwater from reclaimed-water irrigation. When biochar is used in agriculture as a soil amendment, it can effectively increase soil fertility and create a carbon sink to mitigate global warming.[3, 66, 67] In addition, a number of investigations have also revealed biochar's potential to be a low-cost adsorbent to control pollutant migration in soils.[48, 68]It has been demonstrated that biochars converted from agricultural residues had strong sorption ability to different types of contaminants.[8, 69, 70] Previous studies have showed that biochar have strong affinities to soil organic matters and other organic pollutants such as phenanthrene (PHE), polycyclic aromatic hydrocarbons (PAHs), and polychlorinated biphenyls (PCBs).[8, 10] Although pharmaceuticals are emerging organic contaminants, very little research, if any, has been conducted to investigate the ability of biochar to remove pharmaceuticals from water. If it has good sorption ability to pharmaceuticals, such as SMX, then biochar, as a soil amendment, could prevent pharmaceuticals leaching from soil into groundwater as well as improve soil fertility and sequester carbon. This would increase the safety and feasibility of using reclaimed water for agricultural irrigation.

Why Use Biochar to Remove Cationic Dye (Methylene Blue)

Industrial dyes are produced more than 7×10^5 tons annually with over 100,000 commercial types. A considerable fraction of the industrial dyes have been discharged directly in aqueous effluent [71]. This poses a serious hazard to aquatic living organisms as well as diminishing the transparency of the water, because many dyes are toxic and even carcinogenic [71, 72]. Adsorption techniques have been widely applied to treat the dye polluted wastewater. The removal of cationic dyes, such as methylene blue (MB),

by clays and their interaction have been extensively studied in the literature [38, 73]. As one of the most popular dyes, MB has long been used as a model compound to study the interactions between organic dyes and adsorbents. It has been reported that MB can be attracted toward clays' anionic layers and are thus suitable in this dissertation project to determine the sorption characteristics and properties of the clay-modified biochars [74].

Research Objectives

The main objectives of this Ph.D. dissertation were as follows:

Objective 1: Determine the Effect of Biochar Amendment on Leaching of Nitrate, Ammonium, and Phosphate in Sandy Soils

The specific objectives were to: 1) access the overall aqueous nitrate, ammonium, and phosphate sorption ability of the biochars by conducting laboratory batch sorption experiments, and 2) examine the leaching dynamics of the three nutrients in a sandy soil amended with two selected biochars by running laboratory column experiments.

Objective 2: Develop a Low-Cost Biochar Made from Anaerobically Digested Sugar Beet Tailings to Effectively Remove Phosphate from Wastewater

The specific objectives were to: 1) determine whether the anaerobically digested sugar beet tailings can be efficiently used as feedstock for biochar and bioenergy production, 2) compare the physicochemical properties of biochar obtained from digested feedstock to those of biochar obtained from pyrolysis of sugar beet tailings directly, and 3) assess the phosphate removal ability of the biochars produced.

Objective 3: Determine the Mechanisms and Characteristics of Phosphate Adsorption onto the Digested Sugar Beet Tailing Biochar (DSTC)

The specific objectives were to: 1) identify the mechanisms governing the adsorption of phosphate onto the DSTC; 2) measure the kinetics and equilibrium isotherms of phosphate adsorption onto DSTC; and 3) determine the effect of initial solution pH and coexisting anions on the adsorption of phosphate onto the DSTC.

Objective 4: Determine Whether Engineered Mg-Biochar Nanocomposites Could Be Prepared by Direct Pyrolysis of Mg-Accumulated Tomato Tissues.

The specific objectives were to: 1) develop a novel approach to produce engineered biochar from Mg-enriched plant tissues through direct pyrolysis, 2) characterize the physicochemical properties of the engineered biochar, and 3) assess the potential role of Mg enrichment on P sorption on the engineered biochar.

Objective 5: Determine Whether Engineered Biochars from Mg-Enriched Tomato Tissues Can Be Used to Reclaim Aqueous P and Then Be Applied To Soils as a P-Fertilizer

The specific objectives were to: 1) measure the sorption characteristics of P to the engineered biochar, 2) characterize the post-sorption biochar to identify the governing P sorption/desorption mechanisms, 3) measure the release characteristics of P from the post-sorption biochar, and 4) determine the biological effects of the post-sorption biochar on seed germination and seedling growth.

Objective 6: Develop a Biochar Technology to Reduce the Contamination Risk of Reclaimed-Water Irrigation

The specific objectives were to: 1) test the ability of different types of biochar to sorb aqueous SMX, 2) determine the leaching and retention of SMX in simulated reclaimed water through soils amended with selected biochar; and 3) evaluate the effect of SMX-laden biochar on the growth of *E. coli*.

Objective 7: Develop Low-Cost, Clay-Modified Biochars for the Removal of Cationic Dyes from Wastewater

The specific objectives were to: 1) develop a novel approach to prepare clay-modified biochars, 2) characterize the physicochemical properties of the clay-modified biochars, 3) assess the MB removal ability of the clay-modified biochars, and 4) determine the sorption mechanisms.

Organization of the Dissertation

This Ph.D. dissertation has nine chapters, including the present introductory chapter (Chapter 1). Chapter 2 discusses the effect of biochar amendment on leaching of nitrate, ammonium, and phosphate in sandy soils. Biochars were produced from a range of commonly used feedstock materials. Laboratory batch sorption experiments were conducted to access the overall aqueous nitrate, ammonium, and phosphate sorption ability of the biochars. Laboratory column experiments were used to examine the leaching dynamics of the three nutrients in a sandy soil amended with two selected biochars. Chapter 3 investigates phosphate removal ability of biochar made from anaerobically digested sugar beet tailings. Physicochemical properties of the biochar produced were characterized and a simple adsorption experiment was conducted as a preliminary assessment of the phosphate removal ability of the biochars. As a follow-up study of Chapter 3, Chapter 4 applies laboratory adsorption experiments and mathematical models to determine the mechanisms and characteristics of phosphate adsorption onto the digested sugar beet tailing biochar. Chapter 5 explores whether engineered Mg-biochar nanocomposites could be prepared by direct pyrolysis of Mg-accumulated tomato tissues and its phosphate removal ability. An innovative approach was used to produce engineered biochars directly from tissues of tomato, a commonly

used model plant, enriched with Mg/Ca through bioaccumulation. Greenhouse experiments were conducted using a sand-zeolite culture system to produce tomato tissues (leaves) containing high concentration of Mg/Ca for production of the engineered biochars. Physicochemical properties of the biochars produced were characterized in details. A preliminary adsorption experiment was conducted to assess the P removal ability of the biochars and together with the published results to determine potential relations between biochar's P removal ability and its metal contents. Chapter 6 describes the potential of engineered Mg-biochar nanocomposites to reclaim aqueous P and then be applied to soils as a P-fertilizer. A series of laboratory experiments were conducted to determine the mechanisms and characteristics of P adsorption on the engineered biochar. The bioavailability, desorption characteristics, and seed germination ability of the adsorbed P within the spent (i.e. P-laden) biochar were also evaluated. Chapter 7 studies biochar's ability to remove antibiotics (SMX) from reclaimed water in order to reduce the contamination risk of reclaimed-water irrigation and protect the groundwater. A series of laboratory experiments were conducted to study the adsorption of SMX, a common pharmaceutical contaminant in reclaimed water, on biochar and its impact on reclaimed-water irrigation. Chapter 8 describes the effect of clay-modified biochar on the removal of cationic contaminants (MB) from wastewater, using a low-cost method combining biochar and clay together. Six new clay-modified engineered biochar were produced in laboratory through slow pyrolysis of clay (montmorillonite and kaolinite) pretreated biomass (bamboo, bagasse, hickory chips). Physicochemical properties of the clay-modified biochar were characterized and MB adsorption experiment was conducted. Chapter 9 summarizes

the results of all the previous chapters and makes recommendations on future work.

References are included at the end of this document.

CHAPTER 2
EFFECT OF BIOCHAR AMENDMENT ON SORPTION AND LEACHING OF NITRATE, AMMONIUM, AND PHOSPHATE IN A SANDY SOIL[1]

Introduction

Excessive application of fertilizer has caused the release of nutrient elements, such as nitrogen and phosphorus, from agricultural fields to aquatic systems. Leaching of nutrients from soils may deplete soil fertility, accelerate soil acidification, increase fertilizer costs for the farmers, reduce crop yields, and most importantly impose a threat to environmental health [14, 15, 75]. High nutrient levels in surface and/or groundwater can promote eutrophication, excessive production of photosynthetic aquatic microorganisms in freshwater and marine ecosystems [16]. It is therefore very important to develop effective technologies to hold nutrients in soils.

An option to reduce nutrient leaching could be the application of biochar to soils. Biochar, sometimes called agrichar, is a charcoal derived from the thermal decomposition of a wide range of carbon-rich biomass materials, such as grasses, hard and soft woods, and agricultural and forestry residues. The approach of land application of biochar in agriculture is receiving increased attention as a way to create a carbon sink to mitigate global warming, increase soil water holding capacity, and reduce emissions of NO_x and CH_4, as well as to control the mobility of a variety of environmental pollutants, such as heavy metals, pesticides and other organic contaminants [1, 66, 76, 77]. In addition, it is suggested that application of biochar can

[1] Reprint with permission from Yao, Y.; Gao, B.; Zhang, M.; Inyang, M.; Zimmerman, A. R., Effect of biochar amendment on sorption and leaching of nitrate, ammonium, and phosphate in a sandy soil. Chemosphere 2012, 89, (11), 1467-1471.

increase soil fertility and crop productivity by reducing the leaching of nutrients or even supplying nutrients to plants [3, 4, 78].

Only a few studies, however, have investigated the ability of biochars to retain nutrients, particularly for a range of different biochars. For example, Lehmann et al.[78] reported that amendment of biochar produced from secondary forest residuals significantly reduced the leaching of fertilizer N and increased plant growth and nutrition. Ding et al. [79] showed that bamboo biochar sorbed ammonium ions by cation exchange and retarded the vertical movement of ammonium into deeper soil layers within the 70-day observation time. Laird et al [75] reported the addition of biochar produced from hardwood to typical Midwestern agricultural soil significantly reduced total N and P leaching by 11% and 69%, respectively.

The overarching objective of this work was to determine the effect of biochar amendment on leaching of nitrate, ammonium, and phosphate in sandy soils. Biochars were produced from a range of commonly used feedstock materials. Laboratory batch sorption experiments were conducted to access the overall aqueous nitrate, ammonium, and phosphate sorption ability of the biochars. In addition, laboratory column experiments were used to examine the leaching dynamics of the three nutrients in a sandy soil amended with two selected biochars.

Materials and Methods

Materials

Biochar samples were produced from commonly used biomass feedstock materials: sugarcane bagasse (BG), peanut hull (PH), Brazilian pepperwood (BP), and bamboo (BB). The raw materials were oven dried (80 ˚C) and converted into biochar through slow pyrolysis using a furnace (Olympic 1823HE) in a N_2 environment at

temperatures of 300, 450 and 600˚C. The resulting twelve biochar samples are henceforth referred to as BG300, BG450, BG600, PH300, PH450, PH600, BP300, BP450, BP600, BB300, BB450, and BB600. Another biochar (hydrochar) was produced through the hydrothermal carbonization of PH submerged in deionized (DI) water in an autoclave at 300 ^{o}C for 5 hours and is referred to as HTPH. All biochar samples were then crushed and sieved yielding a uniform 0.5-1 mm size fraction. After rinsing with DI water several times to remove impurities, such as ash, the biochar samples were oven dried (80˚C) and sealed in containers for later use. Detailed information about biochar production procedures were reported previously [80].

Sandy soil was collected from an agricultural field at the University of Florida in Gainesville, FL. The soil was sieved through a 1mm mesh (No. 18) and dried (60˚C) in an oven. Basic properties of the soil are listed in Table 2-1.

Nitrate, ammonium, and phosphate solutions were prepared by dissolving ammonium nitrate (NH_4NO_3) or potassium phosphate dibasic anhydrous (K_2HPO_4) in deionized (DI) water. All the chemicals used in the study were A.C.S certified and obtained from Fisher Scientific.

Characterization of Sorbents

A range of physicochemical properties of the biochar samples produced were determined. The pH of the biochars was measured using a biochars to deionized (DI) water mass ratio of 1:20 followed by shaking and an equilibration time of 5 minutes before measurement with a pH meter (Fisher Scientific Accumet Basic AB15). Elemental C, N, and H abundances were determined, in duplicate, using a CHN Elemental Analyzer (Carlo-Erba NA-1500) via high-temperature catalyzed combustion followed by infrared detection of the resulting CO_2, H_2 and NO_2 gases, respectively.

Major inorganic elements were determined by acid digestion of the samples followed by inductively-coupled plasma atomic emission spectroscopic (ICP-AES) analysis. The surface area of the biochars was determined on Quantachrome Autosorb1 at 77 K using the Brunauer-Emmett-Teller (BET) method in the 0.01 to 0.3 relative pressure range of the N_2 adsorption isotherm.

Sorption of Nitrate, Ammonium, and Phosphate

Batch sorption experiments were conducted in 68 mL digestion vessels (Environmental Express) at room temperature (22±0.5 ˚C). About 0.1 g of each biochar sample was added into the vessels and mixed with 50 mL 34.4 mg/L nitrate and 10.0 mg/L ammonium solution or 30.8 mg/L phosphate solution. Vessels without either biochar or nutrient elements were included as experimental controls. The mixtures were shaken at 55 rpm in a mechanical shaker for 24 h, and then filtered through 0.22 μm nylon membrane filters (GE cellulose nylon membrane).

In addition to pH, concentrations of nitrate in the supernatants were determined using an ion chromatograph (Dionex Inc. ICS90). Concentrations of ammonium and phosphate in the supernatants were measured using the phenate method [81] and the ascorbic acid method (ESS Method 310.1; [82]), respectively using a dual beam UV/VIS spectrophotometer (Thermo Scientific, EVO 60). Nutrient elements concentrations on the solid phase were calculated based on the initial and final aqueous concentrations. All the experimental treatments were carried out in duplicate and the average values are reported. The variance between any duplicate measurements in this study was smaller than 5%.

Leaching of Nutrients from Soil Columns

Two biochar samples, PH600 and BP600, were selected to study their effect on nutrients retention and transport in a sandy soil. Soil columns were made of acrylic cylinders measuring 16.5 cm in height and 4.0 cm in diameter, and the bottom of the columns were covered with a stainless steel mesh with 60 μm pore size to prevent soil loss. The sandy soil with (2% by weight) or without biochars was wet-packed into the column (200 g total) following procedures reported previously [83]. These columns were flushed with 10 pore-volumes of DI water before use to precondition the column. A nutrient solution containing 34.4 mg/L nitrate, 10.0 mg/L ammonium and 30.8 mg/L phosphate was then applied to these laboratory soil columns to study biochar effect on nutrients retention and transport. About one pore-volume of DI water was poured into the soil columns on the first day. On days 2 and 3, same amount of nutrient solution was applied to the soil columns. After that, the columns were flushed with one pore-volume DI water each day for another four days. All the leachate samples were collected from the outlet at the bottom of the columns and immediately filtered through 0.22 μm filters for further analyses. The nitrate, ammonium and phosphate concentrations in leachate samples were measured using the same method described above.

Results and Discussion

Biochar Properties

The biochar production rate ranged 21.7-51.5% on a mass basis (Table 2-2). In general, more biochar was yielded at the lower pyrolysis temperatures due to lower losses of volatile components [84, 85]. The pH of the biochars ranged from 5.2 to 9.1 (Table 2-2). Most of the biochars were alkaline, which is common for thermally

produced biochars [86]. While two biochars had considerable N_2 surface area (BP600 and BB600, 234.7 and 470.4 m^2/g, respectively), the surface areas of most biochars were relatively very small ranging from 0.70 to 81.1 m^2/g (Table 2-2). Positive correlation between N_2-measured surface area and pyrolytic temperature was found for all tested biochars, which is consistent with the results of several previous biochar studies [87-89].

Elemental composition analysis indicated all the biochar samples to be carbon-rich with carbon compositions ranging 56.4-86.4% carbon (Table 2-2), which is typical of pyrolyzed biomass [67, 90]. The oxygen and hydrogen contents of all the samples ranged 10.0 -36.7% and 1.4 -5.6%, respectively. As reported in the literature, some of these oxygen and hydrogen contents are likely in organic functional groups on biochar surface [90, 91]. The biochar samples contained relatively small amount of nitrogen (0.1 -1.6%) and relatively low levels of phosphorous (0.03 -0.5%) and metal elements (Table 2-2).

Adsorption of Nitrate, Ammonium and Phosphate by Biochars

The four biochars made at a higher temperature (600 ^oC), BG600, BB600 PH600, and BP600 could remove nitrate from aqueous solution with removal rates of 3.7%, 2.5%, 0.2%, and 0.12%, respectively (Figure 2-1a). The rest of the biochars (nine) showed no nitrate removal ability, and even released nitrate into the solution. Thus, increase in pyrolysis temperature may improve the sorption ability of biochars to aqueous nitrate. Mizuta et al.[92] reported that bamboo biochar made at 900℃ had relatively higher nitrate adsorption capacity even compared to a commercial activated carbon, which is consistent with the findings of this study.

Nine of the thirteen tested biochars showed some ammonium sorption ability, with removal rate ranged 1.8 -15.7% (Figure 2-1b). The BP biochars had the best overall ammonium sorption performance with removal rates of 3.8%, 15.7% and 11.9% for BP300, BP450 and BP600, respectively. There was no apparent pyrolysis temperature trend in the ammonium sorption data.

Only five biochars had any ability to remove phosphate from aqueous solution, with the rest of the biochars releasing phosphate into the solution (Figure 2-1c). The BG450 biochar had the highest removal rate of 3.1%. The HTPH, BG300, PH600, and the three bamboo biochars released relatively large amount of phosphate into the solution (> 2%). The hydrothermally produced biochar, HTPH, showed no nutrient sorption ability and released the greatest amount of nitrate and phosphate.

It is well accepted that biochar can be used as a soil amendment to improve soil fertility and crop productivity. Some previous studies attributed this function to the ability of biochar to retain nutrients in soils [93-96]. The sorption experimental results in this work, however, showed that the ability of biochar to adsorb nutrient elements is not universal, but depends on both the nutrient and the biochar type. In fact, most of the biochars tested in this work showed little/no sorption ability to phosphate or nitrate, but performed slightly better in removing ammonium from aqueous solutions. Perhaps it not surprising that biochars are more effective at removing cationic species from solution given that most biochars have been reported to have a net negative surface charge [93, 94].

Transport in Soil Columns

Two biochars (PH600 and BP600) with relatively good sorption ability for nutrients were selected for the soil column leaching study. When applied to the sandy

soil, the two biochars reduced the leaching of both nitrate and ammonium ions from the column (Figure 2-2a & 2b). Compared to the columns without biochar, after 6 days, the PH600 and BP600 amended soil columns released about 34.3% and 34.0% less of total nitrate and 14.4% and 34.7% less ammonium, respectively. These results are in line with findings of the batch sorption experiment that both biochars could remove nitrate and ammonium from aqueous solutions (Figure 2-1).

The two biochar's effect on the leaching of phosphate from the soils columns was different (Figure 2-2c). BP600 reduced the total amount of phosphate in the leachates by about 20.6%, whereas PH600 increased the amount of phosphate leached from the soil columns by about 39.1%. These results are also consistent with the results of the batch sorption experiment (Figure 2-1). Although multiple mechanisms could be responsible to the enhanced or reduced retention of nutrients in the biochar amended soil [97], several recent studies have suggested that, when applied to soils, biochar may not only affect soil ion exchange capacity but also provide refugia for soil microbes to influence the binding of nutritive cations and anions [98, 99]. Further investigations are still needed to unveil the governing mechanisms of nutrient retention and leaching in biochar amended soils.

Implications

Biochar land application is commonly assumed to be an effective way to sequester carbon and improve soil fertility by reducing nutrient leaching. The finding from this work, however, suggests that the effect of biochar on the retention and release of nutrient ions (i.e., nitrate, ammonium, and phosphate) varies with nutrient and biochar type. Of the thirteen biochars tested in this study, most of them showed little to no nitrate or phosphate sorption ability. However, nine biochars removed aqueous

ammonium. When two selected biochars with relatively good sorption ability were used in soil columns, they could effective reduce the leaching of nitrate and ammonium. Only one biochar, however, could reduce the leaching of phosphate from the soil columns. The results obtained from the leaching column study were consistent with finding from the sorption experiments, suggesting the effect of biochar on nutrients in soils could be determined through laboratory batch sorption studies. It is also recommended that sorption ability of biochars to nutrients should be determined before their applications to soils as amendment.

Table 2-1. Basic properties of the sandy soil used in this study.

Texture	Sand (%)	Silt (%)	Clay (%)	Density (g/cm^3)	Organic Matter (%)
Sandy	94.0	3.0	3.0	2.4	1.0

Table 2-2. Properties and elemental composition of biochars used in this study.

	Production rate (%,mass based)	BET surface area(m^2/g)	pH	Elemental composition (%, mass based)										
				C	H	O [a]	N	P	K	Ca	Mg	Zn	Cu	Fe	Al
BG300	33.4	5.2	7.2	69.5	4.2	24.5	0.9	0.05	0.27	0.46	0.14	0.01	0.00	0.02	0.10
BG450	28.0	15.3	7.9	78.6	3.5	15.5	0.9	0.07	0.25	0.83	0.18	0.01	0.00	0.06	0.11
BG600	26.5	4.2	7.9	76.5	2.9	18.3	0.8	0.08	0.15	0.91	0.21	0.01	0.00	0.05	0.11
PH300	38.4	0.8	7.8	73.9	3.9	19.1	1.6	0.09	0.86	0.32	0.13	0.00	0.00	0.00	0.06
PH450	21.7	21.8	8.2	81.5	2.9	13.0	1.0	0.09	0.94	0.33	0.13	0.00	0.00	0.00	0.06
PH600	30.8	27.1	8.0	86.4	1.4	10.0	0.9	0.10	0.71	0.34	0.12	0.00	0.00	0.00	0.06
HTPH300	44.9	5.6	6.8	56.4	5.6	36.7	0.9	0.08	0.00	0.20	0.02	0.00	0.00	0.07	0.07
BP300	51.5	81.1	6.6	59.3	5.2	34.1	0.3	0.03	0.10	0.73	0.12	0.01	0.00	0.04	0.03
BP450	32.0	0.7	7.3	75.6	3.6	17.2	0.3	0.07	0.25	1.32	0.23	0.00	0.00	0.05	0.03
BP600	28.9	234.7	9.1	77.0	2.2	17.7	0.1	0.09	0.12	1.81	0.29	0.00	0.00	0.08	0.03
BB300	73.2	1.3	6.7	66.2	4.7	27.7	0.4	0.24	0.30	0.22	0.14	0.01	0.00	0.00	0.08
BB450	26.3	18.2	5.2	76.9	3.6	18.1	0.2	0.36	0.35	0.29	0.19	0.01	0.00	0.00	0.04
BB600	24.0	470.4	7.9	80.9	2.4	14.9	0.2	0.50	0.52	0.34	0.23	0.01	0.00	0.00	0.04

a: Determined by weight difference assuming that the total weight of the samples was made up of the tested elements only. b: < 0.01%.

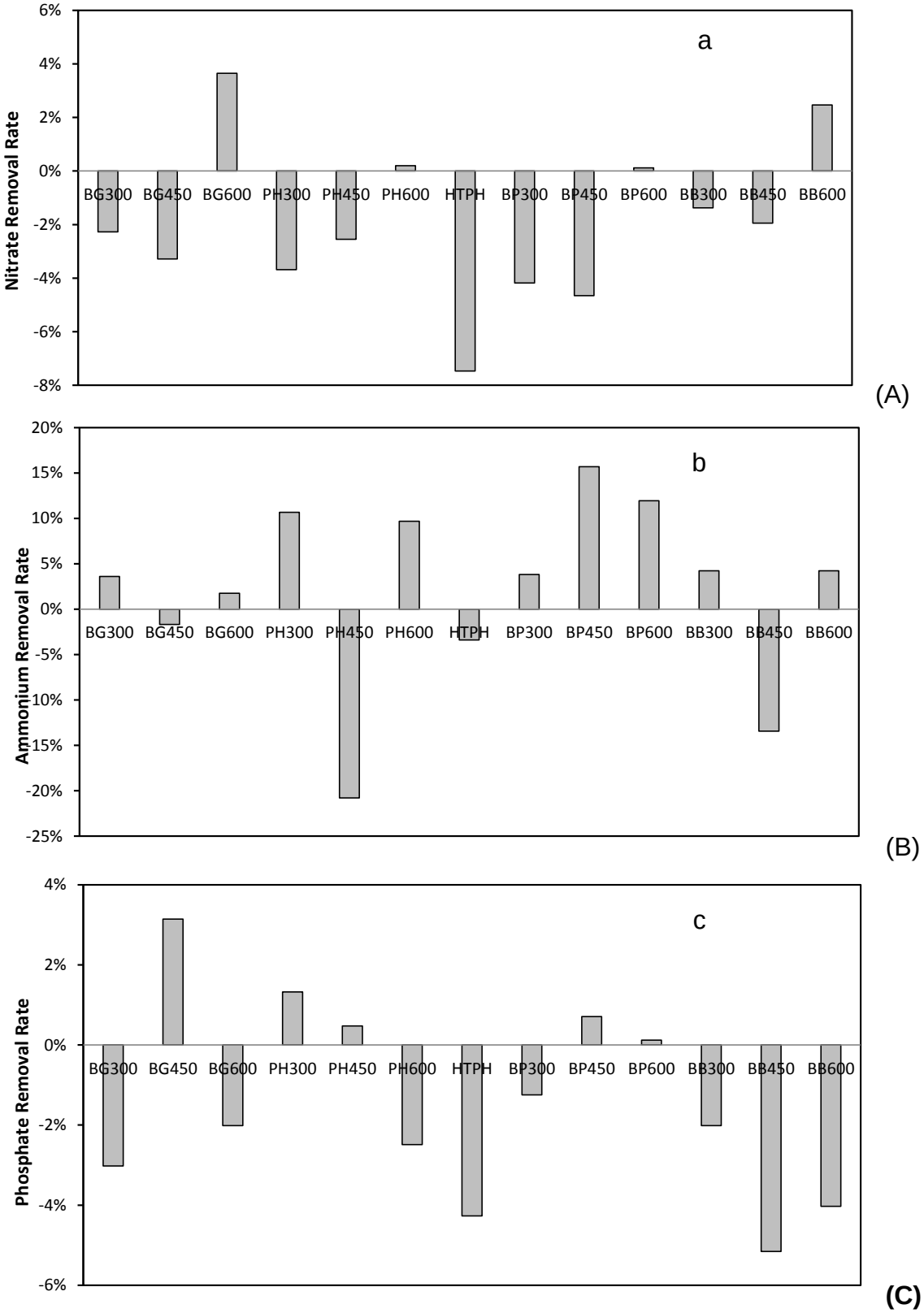

Figure 2-1. Removal of nitrate (A), ammonium (B), and phosphate (C) from aqueous solution by different types of biochars.

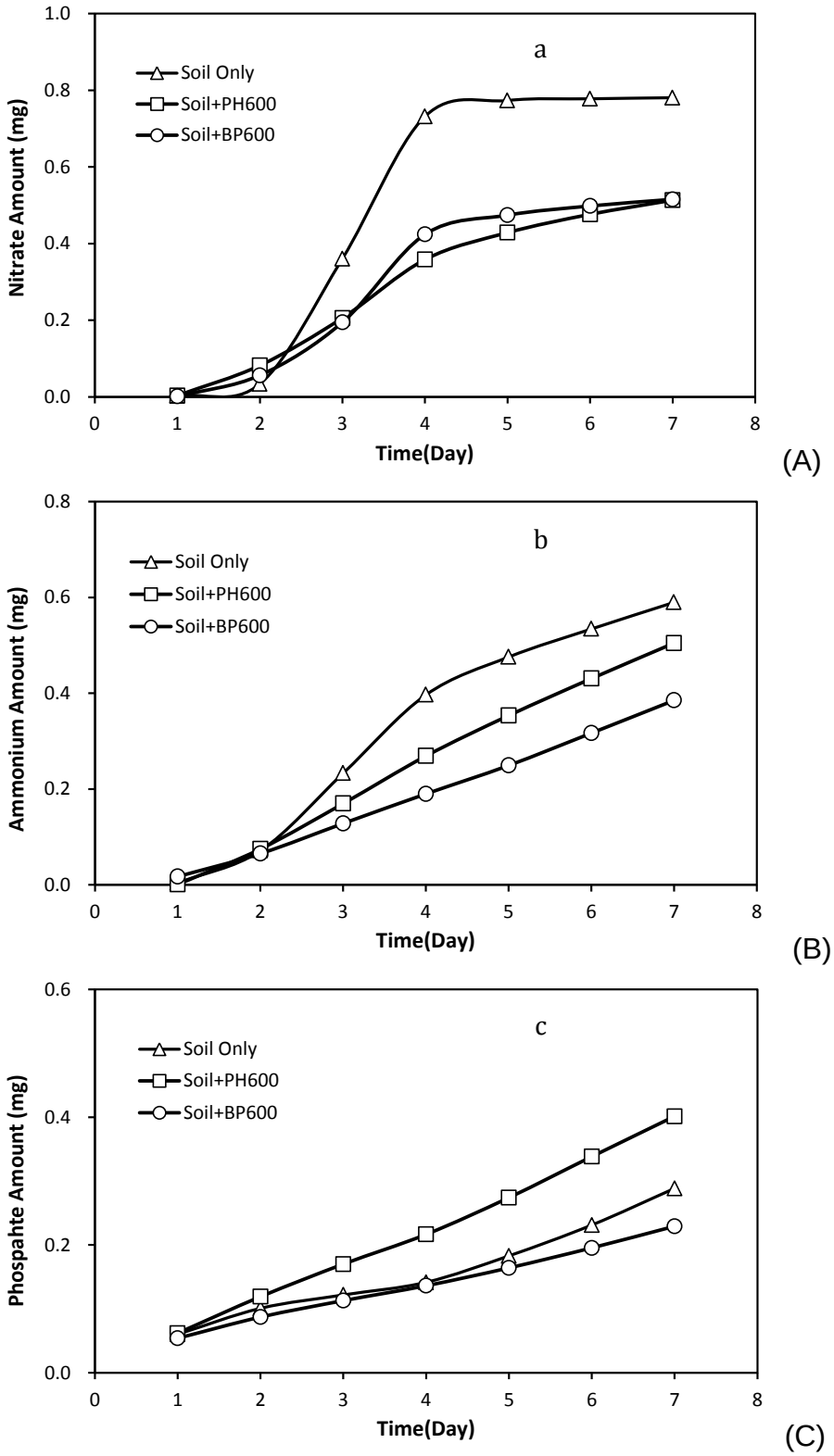

Figure 2-2. Cumulative amounts of nitrate (A), ammonium (B), and phosphate (C) in the leachates from biochar-amended and unamended soil columns.

CHAPTER 3
REMOVAL OF PHOSPHATE FROM AQUEOUS SOLUTION BY BIOCHAR DERIVED FROM ANAEROBICALLY DIGESTED SUGAR BEET TAILINGS: I. BIOCHAR CHARACTERIZATION AND PRELIMINARY ASSESSMENT[1]

Introduction

Biochar is a pyrogenic black carbon that has attracted increased attention in both political and academic arenas [1]. A number of studies have suggested that terrestrial land application of biochar could effectively sequester carbon in soils and thus mitigate global warming [1, 2]. When biochar is applied to soils, it may also present other potential advantages including enhanced soil fertility and crop productivity [3], increased soil nutrients and water holding capacity [4], and reduced emissions of NO_x and CH_4, two other greenhouse gases from soils [5].

In addition to its carbon sequestration and soil amelioration applications, studies have also indicated biochar's potential to be used as a low-cost adsorbent, storing chemical compounds including some of the most common environmental pollutants. It has been demonstrated that biochars made from a variety of sources had strong sorption ability to different types of pesticides and other organic contaminants [6-9]. The sorption ability of biochar has been shown to exceed that of the natural soil organic matter by a factor of 10-100 in some cases [10]. In addition to strong organic compounds sorption ability, biochars have also been shown to remove metal contaminants from water and showed strong affinity for a number of heavy metal ions [11-13]. Only few studies, however, have investigated the ability of biochar to remove nutrients from water, particularly with respect to phosphate [43]. Ideally, if biochar can

[1] Reprinted with permission from Yao, Y.; Gao, B.; Inyang, M.; Zimmerman, A. R.; Cao, X.; Pullammanappallil, P.; Yang, L., Biochar derived from anaerobically digested sugar beet tailings: Characterization and phosphate removal potential. Bioresource Technology 2011, 102, (10), 6273-6278

be used as a sorbent to reclaim nutrients such as phosphate from water, there would be no need to regenerate the exhausted biochar because it can be directly applied to agricultural fields as a slow release fertilizer to improve soil fertility and build (sequester) soil carbon. Although almost all biomass can be converted into biochar through thermal pyrolysis, a life cycle assessment of pyrolysis-biochar systems suggested that it is more environmentally and financially viable to make biochar from waste biomass [45]. In this sense, agricultural residues (e.g. sugarcane bagasse, poultry litter, and manure) and other green waste have been proposed as good feedstock materials to make biochar [9, 46, 47]. However, the applications and functions of those biochars are highly depending on their physicochemical properties (e.g. elemental composition, surface charge, and surface area) [46]. Because biochar can be made of various waste biomass sources under different processing conditions, it is therefore very important to characterize their physicochemical properties before use.

In a recent study, Inyang et al. [48] explored the production of biochar from the residue materials of anaerobic digestion of sugarcane bagasse. Comparison of the physicochemical properties of the biochar from anaerobically digested bagasse to that from raw bagasse suggested that the former has more desirable characteristics for soil amelioration, contaminant remediation, or water treatment. Using anaerobically digested residue materials (or the remains of biofuel production) as feedstock to produce biochar could not only reduce the waste management cost, but also make bioenergy production more sustainable and eco-friendly. It is therefore very important to test the generality of this innovative approach by examining the feasibility of using another anaerobically digested material for biochar production.

Sugar beet tailings are the waste byproducts from the production of beet sugar, which have been mainly managed by landfill disposal or direct land applications. Because beet sugar accounts for almost 40% of all refined sugar consumed in the U.S., significant amount of sugar beet tailings are generated by the sugar industry as solid waste every day. It has been demonstrated that sugar beet tailings can be anaerobically digested to generate bioenergy (biogas) [100]. Although this practice may also reduce the volume of the sugar beet tailing waste, disposal of residue materials from the anaerobic digestion still poses significant economic and environmental problems.

In this chapter, biochars were made from both undigested and anaerobically digested sugar beet tailings at 600 ^{o}C through slow pyrolysis. Physicochemical properties of the biochar produced were characterized and a simple adsorption experiment was conducted as a preliminary assessment of the phosphate removal ability of the biochars. Our objectives were to: 1) determine whether the anaerobically digested sugar beet tailings can be efficiently used as feedstock for biochar and bioenergy production, 2) compare the physicochemical properties of biochar obtained from digested feedstock to those of biochar obtained from pyrolysis of sugar beet tailings directly, and 3) assess the phosphate removal ability of the biochars produced.

Materials and Methods

Biochar Production

Raw sugar beet tailings and anaerobically digested sugar beet tailing residues were obtained from American Crystal Sugar Company (East Grand Forks, MN). These samples were rinsed with water and oven dried (80 ˚C). A bench-scale slow pyrolyzer was used to convert the samples into biochars. For each experiment, about 500 g of the dried samples were fed into a stainless cylinder reactor (50 cm diameter, 30 cm height)

designed to fit inside of a furnace (Olympic 1823HE). The cylinder reactor was first purged with nitrogen gas (10 psi) and an oxygen sensor attached to the reactor ensured that the oxygen content in the reactor was less than 0.5% before it was inserted into the furnace. The reactor was purged again with N_2 along with the furnace and sealed for pyrolysis. Stainless steel tubing and fittings were installed on the furnace and the reactor to collect the oil and the non-condensable gases evolved during the slow pyrolysis. The controller of the furnace was programmed to drive the internal biomass chamber temperature to 600 ^{o}C at a rate of 10 ^{o}C/min and held at the peak temperature for 2 h before cooling to room temperature. Biochar produced from the pyrolysis was gently crushed and sieved into two size fractions: <0.5 mm and 0.5-1mm. Only the latter was used in the experiments to minimize the presence of residual ash particles. In addition, the biochar samples were then washed with deionized (DI) water for several times, oven dried (80 ˚C), and sealed in a container before use.

Biochar Properties

Elemental C, N, and H abundances were determined using a CHN Elemental Analyzer (Carlo-Erba NA-1500) via high-temperature catalyzed combustion followed by infrared detection of the resulting CO_2, H_2 and NO_2 gases, respectively. Major inorganic elements were determined using the AOAC method of acid digesting the samples for multi-elemental analysis by inductively-coupled plasma emission spectroscopy (ICP-AES).

A range of physicochemical properties of the digested sugar beet tailing biochar (DSTC) and the undigested sugar beet tailing biochar (STC) were determined. The pH of the biochar was measured by adding biochar to deionized water in a mass ratio of 1:20. The solution was then hand shaken and allowed to stand for 5 minutes before

measuring the pH with a pH meter (Fisher Scientific Accumet Basic AB15). The surface area of the biochar was determined using N_2 sorption isotherms run on NOVA 1200 and the Brunauer-Emmett-Teller (BET) method to determine mesopore-enclosed surfaces and using CO_2 sorption isotherms run on a Quantachrome Autosorb measured at 273 K an interpreted using grand canonical Monte Carlo simulations of the non-local density functional theory for micropore–enclosed (<1.5 nm) surfaces.

The surface charge of the samples was determined by measuring the zeta potential (ζ) of colloidal biochar according to the procedure of Johnson et al. [101]. About 1g of each sample was added to 100ml of DI water and the solution was shaken at 250 rpm for 30 minutes using a mechanical shaker. The shaken solution was then placed in a sonic bath to break the particles into colloids and the solution filtered using a 0.45 µm filter paper. The electric mobility of each supernatant solution was determined using a Brookhaven Zeta Plus (Brookhaven Instruments, Holtsville, NY) and Smoluchowski's formula was used to convert the electric mobility into zeta potential.

Scanning electron microscope (SEM) imaging analysis was conducted using a JEOL JSM-6400 Scanning Microscope. Varying magnifications were used to compare the structure and surface characteristics of the two biochar samples. Surface element analysis was also conducted simultaneously with the SEM at the same surface locations using energy dispersive X-ray spectroscopy (EDS, Oxford Instruments Link ISIS). The EDS can provide rapid qualitative, or with adequate standards, semi-quantitative analysis of elemental composition with a sampling depth of 1-2 microns [102].

X-ray diffraction (XRD) analysis was carried out to identify any crystallographic structure in the two biochar samples using a computer-controlled X-ray diffractometer (Philips Electronic Instruments) equipped with a stepping motor and graphite crystal monochromator. Crystalline compounds in the samples were identified by comparing diffraction data against a database compiled by the Joint Committee on Powder Diffraction and Standards.

Fourier Transform Infrared (FTIR) analysis of the biochars was carried out to characterize the surface organic functional groups present on these samples. To obtain the observable FTIR spectra, STC and DSTC were ground and mixed with KBr to 0.1 wt% and then pressed into pellets. The spectra of the samples were measured using a Bruker Vector 22 FTIR spectrometer (OPUS 2.0 software).

Other Adsorbents

Granulated activated carbon (AC, from coconut shell) was obtained from Fisher Scientific and was gently crushed, sieved, and washed using the same procedures as the biochar samples. In addition, each of the three biochars were modified by impregnating ferric hydroxide onto the AC (i.e., FeAC), STC (i.e., FeSTC), and DSTC (i.e., FeDSTC) samples according to the procedure employed by Thirunavukkarasu et al. [103] and Chen et al.[104]. Briefly, 6 grams of AC, STC, and DSTC were added to 30 mL of 2M $Fe(NO_3)_3 \cdot 9H_2O$ solution separately, and pH was then adjusted to 4-5 with NaOH to create an iron precipitate. The mixture was then heated at 105 ^{0}C overnight and the grains were separated, sieved, and washed thoroughly with DI water. The FeAC, FeSTC, and FeDSTC samples were then oven dried for further use.

Phosphate Adsorption

Phosphate solutions were prepared by dissolving Potassium Phosphate Dibasic Anhydrous (K_2HPO_4, certified A.C.S, Fisher Scientific) in DI water. The experiments were carried out in 68 mL digestion vessels (Environmental Express) at room temperature (22±0.5 ˚C). To initiate the adsorption experiments, 50 mL phosphate solutions of 61.5 mg/L (i.e., 20 mg/L P) and 0.1 g of each adsorbent (DSTC, FeDSTC, STC, FeSTC, AC, or FeAC) were added into the vessels. The pH of the solution was then adjusted to 7, which is not only the typical pH of secondary wastewater, but also among the optimal pH values for phosphate adsorption as reported by previous studies [35, 105]. After being shaken at 200 rpm in a mechanical shaker for 24 h, the vials were withdrawn and the mixtures were filtered through 0.22 μm pore size nylon membrane filters (GE cellulose nylon membrane). The phosphate concentrations of the liquid phase samples were then determined by the ascorbic acid method (ESS Method 310.1; [82]) with aid of a spectrophotometer (Thermo Scientific EVO 60). The phosphate removal rates were calculated based on the initial and final aqueous concentrations. All the experimental treatments were performed in duplicate and the average values are reported. Additional analyses were conducted whenever two measurements showed a difference larger than 5%.

Results and Discussion

Biochar and Bioenergy Production Rates

On a weight basis, about nine percent more biochar was produced from digested sugar beet tailing residue feedstock than from the undigested sugar beet tailings. The biochar production rates of the digested and undigested materials were 45.5% and 36.3% of initial dry weight, respectively. Although studies have shown that increased

biochar production through slow pyrolysis is often accompanied by decreased yield in bio-oil [106], the bio-oil production rates were similar for the digested and undigested sugar beet tailings with values of 12.5% and 10.9%, respectively. By summing to 100%, it follows that the amount of the non-condensable gases extracted from the digested sugar beet tailings (43.6%) must have been lower than that from the undigested sugar beet tailings (51.2%). These results suggest that residue materials from anaerobic digestion of sugar beet tailings are comparable with undigested sugar beet tailings, and thus can be used as feedstock for both biochar and further bioenergy production.

Elemental Composition

Elemental analysis of the feedstock materials showed that the residue of the anaerobically digested sugar beet tailings were carbon rich and had carbon content around 34% (Table 3-1). This carbon content was only slightly lower than that of the undigested feedstock (Table 3-1), confirming that the residue of anaerobically digested sugar beet tailings can be used as feedstock for biochar production. Compared to the undigested sugar beet tailings, the digested feedstock contained more hydrogen and nitrogen, but less oxygen element. It is notable that, after the anaerobic digestion, most of the inorganic elements in the residue materials increased except potassium. For instance, the magnesium content of the digested sugar beet tailings increased from about one-half percent to above one percent. The calcium content also increased dramatically from above one percent to about ten percents. These results are consistent with findings of published studies that anaerobic digestion may concentrate exchangeable cations, such as calcium and magnesium, into the residue materials [107, 108].

After being converted into biochar through slow pyrolysis, the carbon content of DSTC (31.81%) was slightly lower than that of the feedstock, but the carbon content of STC increased dramatically to more than 50% (Table 3-1). This indicates that the two biochars could be very different because of the effects of anaerobic digestion on the feedstock materials. The hydrogen, oxygen, and nitrogen contents of the two biochars were similar to each other (Table 3-1). But some of the nutrient elements including phosphorous, calcium, and magnesium were much higher in the DSTC than in the STC (Table 3-1). High levels of calcium and phosphorous were also found in studies of some other biochars [46]. However, the DSTC had a surprisingly high level of magnesium of about 10%, which is more than 6 times of the STC. These results suggest that the digested sugar beet tailing biochar may, when applied to soils, provide a more concentrated source of nutrients to crops.

Zeta Potential and pH

The surface of charcoals (biochar, activated carbon) is often negatively charged, which makes them unlikely to sorb negatively charged ions such as phosphate [109, 110]. The measured zeta potentials of the STC (-54.23 mV) and DSTC (-18.11 mV) were both negative, confirming that the two biochars are negatively charged at circum-neutral conditions. The STC had a much lower zeta potential than the DSTC, however, suggesting that it might be more difficult for STC than for DSTC to adsorb phosphate. Measurements of the pH of the two biochars were alkaline (9.45 and 9.95 for STC and DSTC, respectively), which are similar to the reported values of other biochars produced at high temperatures [46, 48]. The high pH of the two biochar samples suggests their potential to be used as amendments to reduce soil acidity [1].

Surface Area

Two methods were used to determine the surface area of the biochars. The liquid N_2 adsorption BET method (77 K) is more commonly used. However, this method may be inaccurate for materials that include micropores (< 1.5 nm pore diameter) as N_2 may be kinetically limited in their diffusion into smaller pores at the low temperatures at which the measurement must be carried out [111-113]. The CO_2 adsorption method (273 K) has, therefore, been promoted to be a better way to determine the true surface area of biochar samples [8, 114].

The CO_2 surface area measurements showed that the surface area of DSTC (449 m^2/g) was much higher than that of STC (351 m^2/g). While the DSTC had significant N_2 surface area (336 m^2/g, indicating the presence of mesopores), the N_2 surface area of the STC was very small (2.6 m^2/g), indicating that its surface was dominated by the micropores only. The surface area of DSTC is comparable to that of many commercial activated carbon (AC) adsorbents [115]. Because surface area is one of most important factors that control a material's ability to adsorb chemical compounds, the digested sugar beet tailing biochar (i.e., DSTC) may be useful for water treatment or environmental remediation.

SEM-EDS

The SEM imaging of the STC (500 X) showed that the undigested sugar beet tailing biochar had smooth surfaces (Figure 3-1a). This is consistent with the findings from the N_2 surface area measurement, which suggested that micropores dominated the STC surface. The EDS spectrum of the STC surface (Figure 3-1a) identified the same elements detected in the elemental analysis (Table 3-1). The SEM imaging of the DSTC (500 X), however, showed knaggy surfaces (Figure 3-1b), perhaps reflecting the

presence of mesopores indicated by the N_2 surface area measurement. The EDS spectrum of the STC surface (Figure 3-1b) also showed many elements detected in the elemental analysis (Table 3-1). Although the element analysis suggested that the DSTC had similar amount calcium and magnesium (i.e., about 10%), the EDS spectrum of the DSTC indicated a magnesium content greater than that of calcium, suggesting more magnesium may present on the biochar surfaces. This was further confirmed by the SEM-EDS analysis at a high resolution (7000 X). The SEM image of the DSTC taken at the high resolution showed evidence of mineral crystals on the biochar surface (Figure 3-1c). These crystals were mainly magnesium minerals as evidenced in the EDS spectrum at the same location (Figure 3-1c), which showed an extremely high peak of magnesium. The magnesium crystals are colloidal or nano-sized and could contribute to the high surface area of the digested sugar beet tailing biochar.

XRD

The XRD spectra of the DSTC and STC showed several peaks (Figure 3-2), indicating the presence of mineral crystals. In the DSTC spectrum, the two strong peaks at 43.2^o (d = 2.09 Å) and 62.2^o (d = 1.49 Å) were identified as periclase (MgO), suggesting that the colloidal and nano-sized magnesium crystals on the DSTC surface (as shown in the SEM-EDS analysis) were MgO. Quartz (SiO_2) and calcite ($CaCO_3$) were found in both the DSTC and STC, which is also consistent with the elemental analyses and EDS spectra of the two biochars.

Surface Functional Groups

The infrared spectra of the DSTC and STC were very similar (Figure 3-3) with both biochars showing three significant bands at: 1) wave number near 1427, which could be attributed to O-H bending or C-O stretching vibration of phenol [109], 2) wave

number near 1049, which could be attributed to C–O stretching vibrations of polysaccharides [116], and 3) wave near 874, which is characteristic of C-H bending vibration in a β-glucosidic linkage [109]. All of the observed functional groups have been reported as chemical groups characterizing many other carbon based adsorbents including biochars and activated carbons [117-120].

Phosphate Removal

Both AC and STC showed very low phosphate removal and AC even released a small amount of phosphate back into the solution (Figure 3-4). This is consistent with the literature [109, 110] and the fact that STC has very high negative zeta potential. Although the zeta potential measurements showed that the surface of DSTC was also negatively charged, the DSTC demonstrated the highest phosphate removal with a rate about 73%, which was much higher than the phosphate removal rates of all the other adsorbents tested. The ferric hydroxide impregnation did increase the phosphate removal for the AC and STC, with FeAC and FeSTC removal of about 10% and 8% of phosphate, respectively. The Fe surface modification, however, reduced the phosphate removal rate of DSTC dramatically from around 73% to 22%. This preliminary assessment suggests that anaerobically digested sugar beet tailing biochar could be used as low-cost adsorbent to effectively remove phosphate from aqueous solution without any modification.

The enhanced removal of phosphate by the DSTC was probably because of the large amount of colloidal and nano-sized periclase (MgO) on its surface, which has a strong ability to bind phosphate in aqueous solution [121, 122]. Precipitation of ferric hydroxide onto the SDTC might cover the colloidal and nano-sized periclase, thus reducing the phosphate sorption ability of the biochar. Detailed discussion about the

adsorption mechanisms and characteristics of phosphate onto the SDTC can be found in the part II of this study [123].

Implications

Based on the characterization of DSTC biochar physicochemical properties and the preliminary phosphate sorption assessment, it is evident that (1) residue from the anaerobic digestion of sugar beet tailings can be used as a feed stock for biochar production, (2) some of the physicochemical properties (e.g., pH and surface functional groups) of the two biochars are similar, but only the anaerobically digested sugar beet tailing biochar has colloidal and nano-sized periclase (MgO) on its surface, and (3) anaerobic digestion enhances the phosphate adsorption ability of biochar produced from digested sugar beet tailings relative to undigested ones.

Table 3-1. Elemental analysis of raw and digested sugar beet tailings, and their associated biochars, STC and DSTC, respectively (mass %)[a].

Sample	C	H	O [b]	N	P	S	Ca	Mg	K	Fe	Al	Zn	Na	Cu
Digested Tailing	33.94	4.53	46.89	2.35	0.34	0.28	9.68	1.20	0.79	-[c]	-	-	-	-
Raw Tailing	36.06	3.43	55.82	1.23	0.16	0.09	1.80	0.53	0.88	-	-	-	-	-
DSTC	30.81	1.38	39.87	2.74	2.18	0.46	9.78	9.79	1.97	0.75	0.24	0.03	-	-
STC	50.78	2.08	36.70	1.83	0.35	0.05	4.41	1.53	1.04	0.59	0.64	-	-	-

a: Expressed on a total dry weight basis. b: Determined by weight difference assumed that the total weight of the samples was made up of the tested elements only. c: Below 0.01%.

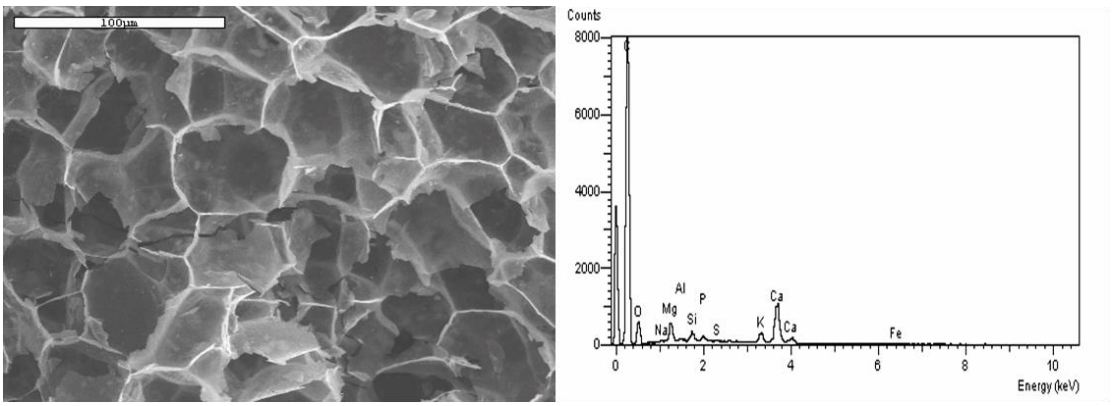

(A) STC 500X

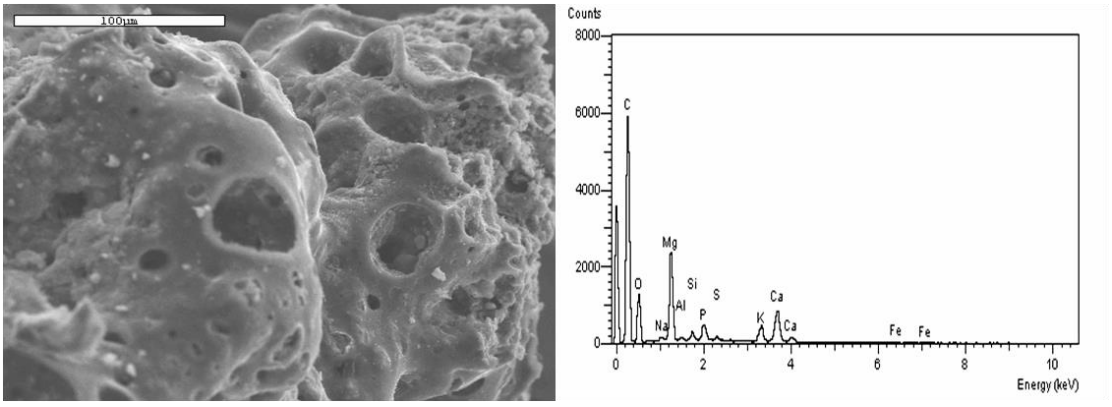

(B) DSTC 500X

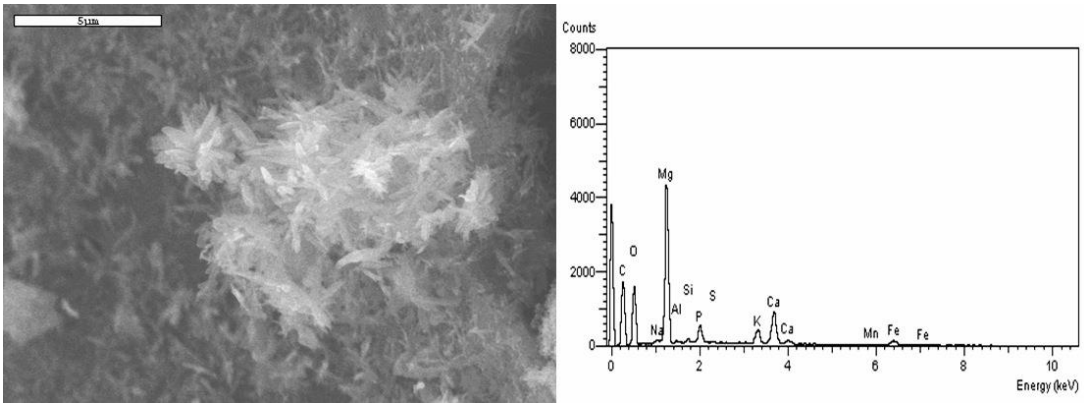

(C) DSTC 7000X

Figure 3-1. SEM images (left) and corresponding EDS spectra (right) of the two biochar samples: A) STC, 500X; B) DSTC, 500X; and C) DSTC, 7000X. The EDS spectra were obtained at the same location as shown in the SEM images.

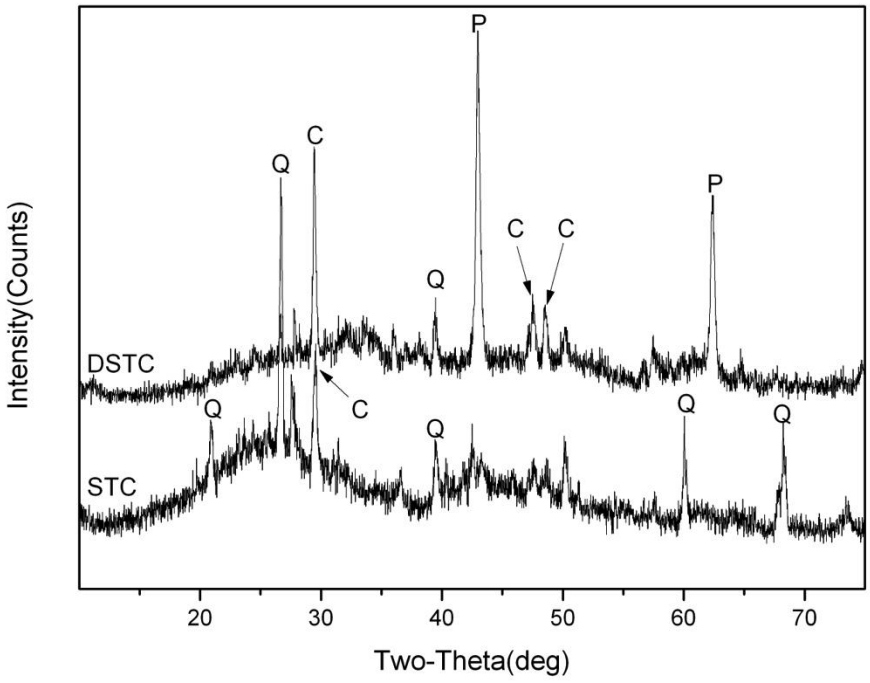

Figure 3-2. XRD spectra of the two biochars. Crystallites were detected with peaks labeled as Q for quartz (SiO2), C for calcite (CaCO3), and P for periclase (MgO).

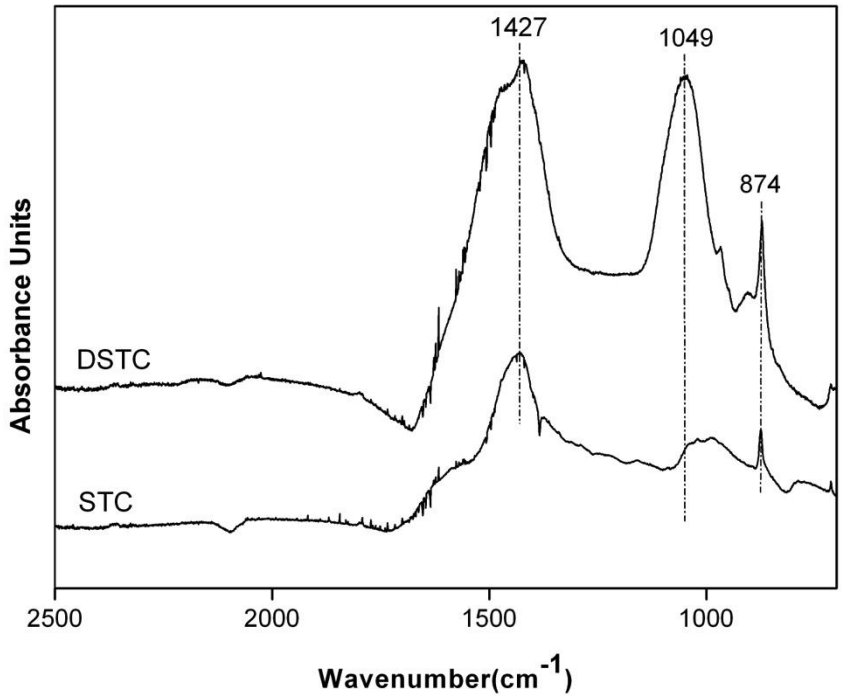

Figure 3-3. FTIR spectra of the two biochar samples.

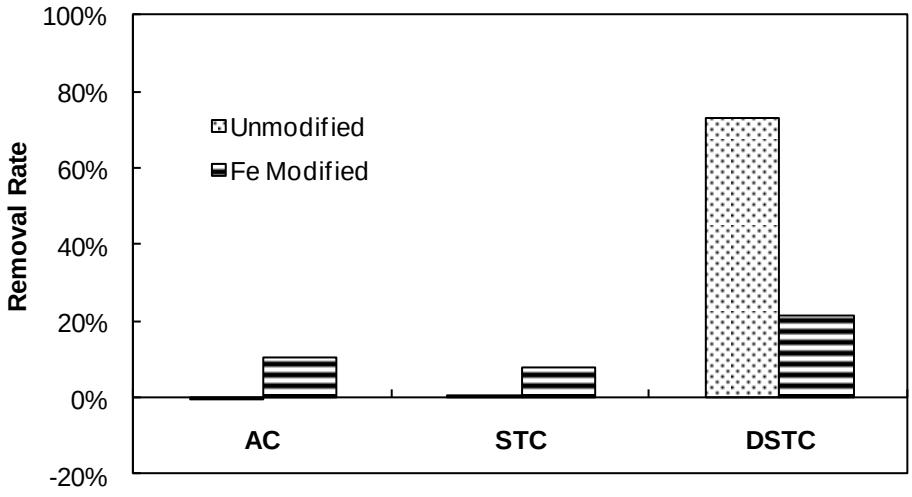

Figure 3-4. Comparison of phosphate removal by different adsorbents.

CHAPTER 4
REMOVAL OF PHOSPHATE FROM AQUEOUS SOLUTION BY BIOCHAR DERIVED FROM ANAEROBICALLY DIGESTED SUGAR BEET TAILINGS: II. ADSORPTION MECHANISMS AND CHARACTERISTICS[1]

Introduction

The release of phosphate from both point and non-point sources into runoff may impose a great threat on environmental health [14, 15]. As a growth limiting nutrient, high level phosphate can promote excessive production of photosynthetic aquatic microorganisms in natural water bodies and ultimately becomes a major factor in the eutrophication of many freshwater and marine ecosystems [16]. It is therefore very important to develop effective technologies to remove phosphate from aqueous solutions prior to their discharge into runoff and natural water bodies [17].

Many phosphate removal technologies including biological, chemical, and physical treatment methods have been developed for various applications, particularly for the removal of phosphate from municipal and industrial effluents [16]. Both biological and chemical treatments have been well documented and proven to be effective to remove phosphate from wastewater. Addition of chemicals, such as calcium, aluminum, and iron salts into wastewater is considered a simple phosphate removal technique, which separates the phosphate from aqueous system through precipitation [20-23]. However, the chemical precipitation methods require strict control of operating conditions and may potentially introduce new contaminants into the water such as chloride and sulfate ions [15, 20, 24]. Biological treatment of phosphate in waste effluents may have certain advantages over the chemical precipitation method because

[1] Reprinted with permission from Yao, Y.; Gao, B.; Inyang, M.; Zimmerman, A. R.; Cao, X. D.; Pullammanappallil, P.; Yang, L. Y., Removal of phosphate from aqueous solution by biochar derived from anaerobically digested sugar beet tailings. J Hazard Mater 2011, 190, (1-3), 501-507.

it does not require chemical additions and enhanced biological treatment has been reported to remove up to 97% of the total phosphorus in waste water [25]. This technology, however, is very sensitive to the operation conditions and its phosphate removal efficiency may be, at times, much less [27]. Both the chemical and biological treatment methods are also subjected to the costs and risks associated with phosphate-rich sludge handling and disposal [28].

Various physical methods have also been developed to remove phosphate from aqueous solution such as electrodialysis, reverse osmosis, and ion exchange [20, 29, 30]. However, most of these physical methods have proven to be either too expensive or inefficient. Simple physical adsorption might be comparatively more useful and cost-effective for phosphate removal. Several studies investigated activated carbons as phosphate adsorbents, but showed that the adsorption capacity was very low [14, 18, 35]. For example, Namasivayam et al. [18] reported that activated carbon made from coir pith with $ZnCl_2$-activation had a phosphate adsorption capacity of only 5,100 mg/kg. Lower-cost materials, such as slag, fly ash, dolomite, red mud, and oxide tailings have also been explored by several studies as alternative adsorbents of phosphate from waste water [36-40].

Biochar is a low-cost adsorbent that is receiving increased attention recently because it has many potential environmental applications and benefits. While most of the current biochar studies are focused on biochar land application as an easy and cost-effective way to sequestrate carbon and increase fertility, a number of recent investigations suggest that biochar converted from agricultural residues have a strong ability to bind chemical contaminants in water including heavy metals and organic

contaminants [8, 11, 12, 41, 42]. The use of biochar to remove phosphate from aqueous solutions, however, is still a relatively unexplored, though promising concept. Not only may biochar represent a low-cost waste water treatment technology for phosphate removal, but the phosphate-laden biochar may be used as a slow-release fertilizer to enhance soil fertility that will also sequester carbon. But little research has been conducted to explore the phosphate removal potential of biochar [44].

In the Chapter 3 of this dissertation, we characterize the physicochemical properties of two biochars and compared their phosphate removal abilities with activated carbon and their Fe-impregnated forms [44]. Our results showed that biochar derived from the residues of anaerobically digested sugar beet tailings had much better phosphate removal ability than all the other tested adsorbents. As a follow-up, laboratory adsorption experiments and mathematical models were used in this study to determine the mechanisms and characteristics of phosphate adsorption onto the digested sugar beet tailing biochar (DSTC). The specific objectives were to: a) identify the mechanisms governing the adsorption of phosphate onto the DSTC; b) measure the kinetics and equilibrium isotherms of phosphate adsorption onto DSTC; and c) determine the effect of initial solution pH and coexisting anions on the adsorption of phosphate onto the DSTC.

Materials and Methods

Materials

The biochar sample (DSTC) used in this study was obtained by pyrolyzing residues of anaerobically digested sugar beet tailings at 600 ^{o}C inside a furnace (Olympic 1823HE) in a N_2 environment. The DSTC was then crushed and sieved to give a 0.5-1 mm size fraction. After washing with deionized (DI) water to remove impurities,

the biochar samples were oven dried (80˚C) and sealed in container before use. Detailed information about biochar production its physiochemical properties can be found in part I of this study [44]

Phosphate solutions were prepared by dissolving Potassium Phosphate Dibasic Anhydrous (K_2HPO_4) in DI water. All the chemicals used in the study are A.C.S certified and from Fisher Scientific.

Adsorption Kinetics

Adsorption kinetics of phosphate onto DSTC were examined by mixing 0.1 g of the biochar with 50 ml phosphate solutions of 61.5 mg/L (20 mg/L P) in 68 mL digestion vessels (Environmental Express) at room temperature (22±0.5 ˚C). The pH was then adjusted to close to 7 prior to the measurements of the adsorption kinetics. The vessels were then shaken at 200 rpm in a mechanical shaker. At appropriate time intervals, the vessels were withdrawn and the mixtures were immediately filtered through 0.22 μm pore size nylon membrane filters (GE cellulose nylon membrane). The phosphate concentrations in the liquid phase samples were determined by the ascorbic acid method (ESS Method 310.1; [82]) and a spectrophotometer (Thermo Scientific EVO 60). Phosphate concentrations on the solid phase were calculated based on the initial and final aqueous concentrations. All the experimental treatments were performed in duplicate and the average values are reported. Additional analyses were conducted whenever two measurements showed a difference larger than 5%.

Adsorption Isotherm

Adsorption isotherm of phosphate onto DSTC was determined similarly by mixing 0.1 g DSTC with 50 ml phosphate solutions of different concentrations ranging from 15 to 640 mg/L in the digestion vessels. After pH adjustment to about 7, the vessels were

shaken in the mechanical shaker for 24 h at room temperature, this time periods having been previously determined by kinetic experiments as sufficient for adsorption equilibrium to be established. The samples were then withdrawn and filtered to determine adsorbed phosphate concentrations by the same method. Following the experiments, the post-adsorption DSTC were collected, rinsed with deionized water, and dried at 80 ˚C in an oven for further characterizations.

Effect of pH and Coexisting Anions

The effect of initial solution pH on phosphate removal was studied over a range of 2 to11 (i.e., 2.0, 4.0, 6.2, 7.1, 8.1, and 10.4). In addition, the effect of the common coexisting anions, chloride, nitrate, and bicarbonate, was also investigated by adding 0.01M of NaCl, $NaNO_3$, or $NaHCO_3$ to the 61.5 mg/L phosphate solutions into separate digestion vessels. The adsorbent to initial solution phosphate concentration were the same as the kinetics experiment. The vessels were shaken in the mechanical shaker for 24 h at room temperature. The same procedures were then used to determine aqueous and adsorbed phosphate concentrations.

Post-adsorption Biochar Characterization

To investigate the crystallographic structures on the post-adsorption DSTC, X-ray diffraction (XRD) patterns were acquired with a computer-controlled X-ray diffractometer (Philips APD 3720) equipped with a stepping motor and graphite crystal monochromator. Fourier Transform Infrared (FTIR) spectra were collected using a Bruker Vector 22 FTIR spectrometer (OPUS 2.0 software) to identify the surface functional groups of post-adsorption DSTC samples. The P-loaded DSTC was ground and mixed with KBr to approximately 0.1 wt% and pressed into a pellet using a mechanical device. Scanning electron microscopy (SEM, JEOL JSM-6400) coupled with

dispersive X-ray spectroscopy (EDS, Oxford Instruments Link ISIS) was used to the surface of the post-adsorption DSTC and to determine its surfacial elemental composition. These characteristics of the phosphate-loaded DSTC were compared with those of the original biochar [44] to determine the adsorption mechanisms.

Results and Discussion

Main Adsorption Mechanism

The Chapter 3 of this study [44] showed that DSTC had a relatively high surface area measured with N_2 (336 m^2/g) and CO_2 (449 m^2/g), which is generally desirable for phosphate adsorption. In addition, characterization results from elemental, SEM-EDS, and XRD analyses revealed that the DSTC surface was covered with colloidal or nano-sized MgO (periclase) particles, which could serve as the main adsorption sites for phosphate removal [44].

SEM-EDS analysis of the post-adsorption DSTC samples confirmed the hypothesis that the MgO particles on the DSTC surface may dominate the phosphate adsorption. At a high resolution of 7000X, when the SEM was focused on the MgO crystals on the P-loaded DSTC surface, the corresponding EDS spectrum showed an elevated peak of phosphorus (Figure 4-1). Although phosphorus was also detected in the original DSTC (Chapter 3), its EDS signal of phosphorus was much lower [44]. For the P-loaded DSTC, the phosphorus signal was even higher than those of the magnesium and oxygen, which showed the second and third highest EDS peaks (Figure 4-1).

Metal oxides have showed strong ability to adsorb negative charged compounds, such as phosphate and arsenate [124]. When in contact with water, the metal oxide surface becomes hydroxylated and thus introduces either a positive or negative surface

charge, depending on the solution pH. The charge development of MgO on the biochar surface can be described in a simplified manner as [125]:

$$S_{MgO} - OH_2^+ \Leftrightarrow S_{MgO} - OH \Leftrightarrow S_{MgO} - O^- \quad (2\text{-}1)$$

where S_{MgO} denotes the MgO surface. The point of zero charge (PZC) of MgO is very high (PZC_{MgO}=12, [126]), thus its surface is expected to be positively charged in most natural aqueous conditions. In aqueous solution, phosphate exists in four species with pKa values of 2.12 (pKa_1), 7.21(pKa_2), and 12.67 (pKa_3). When solution pH is lower than PZC_{MgO}, the hydroxylated MgO surface can electrostatically attract negatively charged phosphate species to form mono-, and polynuclear complexes [125, 127]:

$$S_{MgO} - OH_2^+ + H_2PO_4^- \Leftrightarrow S_{MgO}H_2PO_4 + H_2O \quad \text{mononuclear (0.12<pH<9.21) (4-2a)}$$

$$2S_{MgO} - OH_2^+ + HPO_4^{2-} \Leftrightarrow (S_{MgO})_2 HPO_4 + 2H_2O \quad \text{binuclear (5.21<pH<10.67) (4-2b)}$$

$$3S_{MgO} - OH_2^+ + PO_4^{3-} \Leftrightarrow (S_{MgO})_3 PO_4 + 3H_2O \quad \text{trinuclear (10.67<pH<12) (4-2c)}$$

Although most of the initial solution pH values in this study were around 7, the reductions of aqueous phosphate during the experiments would affect the dynamics of solution pH [35, 127]. This would increase the heterogeneity of the adsorption processes of phosphate onto the biochar to trigger both mono-and polynuclear interactions (i.e., equation 2.1-2.3).

Other Potential Adsorption Mechanisms

Element analysis indicated that there were large amount of calcium in both DSTC and STC [44]. If the calcium was released from the biochars into the solution as free ions, they may remove phosphate through precipitation. However, the preliminary assessment of STC showed almost no ability to remove aqueous phosphate [44]. In addition, the XRD spectra of the original and P-loaded DSTC were almost identical and showed no evidence of calcium-phosphate precipitates in the P-loaded biochar (Figure

4-2a), suggesting that the precipitation might not be an important mechanism for phosphate removal. This could be explained by two reasons: 1) some of the calcium in the biochar was in form of calcite (Figure 4-2a), which has a very low solubility; and 2) a portion of the calcium might be incorporated inside of the biochar and could not be released into the solution [46].

Because there was abundance of surface functional groups on the DSTC surface [44], phosphate could also be removed by the biochar through interacting with the functional groups. However, again, the similarity between the FTIR spectra of the original and P-loaded DSTC provides no evidence of adsorption of phosphate onto the surface functional groups in the P-loaded biochar (Figure 4-2b).

Adsorption Kinetics

The adsorption of phosphate onto the DSTC increased smoothly over time and reached equilibrium after 24 h (Figure 4-3a). The slow kinetics further suggests that precipitation might not play an import role in the removal of phosphate by the biochar. Mathematical models were used to simulate the experimental kinetics. In addition to the commonly used pseudo-first-order and pseudo-second order models, the Ritchie N_th-order model and Elevich model were also tested [128] and are represented by the following equations:

$$\frac{dq_t}{dt} = k_1(q_e - q_t) \quad \text{first-order (4-3a)}$$

$$\frac{dq_t}{dt} = k_2(q_e - q_t)^2 \quad \text{second-order (4-3b)}$$

$$\frac{dq_t}{dt} = k_n(q_e - q_t)^N \quad \text{N\_th-order (4-3c)}$$

$$\frac{dq_t}{dt} = \alpha \exp(-\beta q_t) \quad \text{Elevich (4-3d)}$$

where q_t and q_e are the amount of phosphate adsorbed at time t and at equilibrium, respectively (mg kg^{-1}), and k_1, k_2 and k_n are the first-order, second-order, and N_th-order apparent adsorption rate constants (h^{-1}), respectively. Also, α is the initial adsorption rate (mg kg^{-1}) and β is the desorption constant (kg mg^{-1}). The first-order, second-order, and N_th-order models describe the kinetics of the solid-solution system based on mononuclear, binuclear, and N-nuclear adsorption, respectively, with respect to the sorbent capacity [128], while the Elevich model is an empirical equation considering the contribution of desorption.

All the models closely reproduced the kinetic data (Figure 4-3a), with all correlation coefficients (R^2) exceeding 0.98 (Table 4-1). However, the first-order, second-order, and N_th-order (N=1.14) models fitted the data slightly better than the Elevich model and N_th-order model had the highest R^2 (0.9970). This result is consistent with the proposed predominant mechansim that phosphate removal by the biochar was mainly through adsorption onto the colloidal and nano-sized MgO crystals on DSTC surface. Both mononuclear and polynuclear adsorption of phosphate would be favored in the kinetics experiment, perhaps explaining why fittings from the N_th-order model were slightly better than that of either the first-or second-order model.

Previous studies on the kinetic behaviors of microporous sorbents showed that intraparticle surface diffusion may be important to the adsorption process [129, 130]. In this study, the adsorption of phosphate onto DSTC also showed diffusion limitation. The pre-equilibrium (i.e. before 24 h) phosphate adsorption showed a strong linear dependency (R^2=0.9959) on the square root of time (Figure 4-3b). This result suggests

that intraparticle surface diffusion may play an important role in controlling the adsorption of phosphate onto the biochar, likely due to its abundance of mesopores.

Adsorption Isotherms

With the maximum observed phosphate adsorption of greater than 100,000 mg/kg (Figure 4-4), the DSTC showed phosphate sorption ability to superior to most of the reported values of other carbonaceous adsorbents [15, 18, 35]. Three isotherm equations were tested to simulate the phosphate adsorption onto the biochar [128]:

$$q_e = \frac{KQC_e}{1 + KC_e} \quad \text{Langmuir (4-4a)}$$

$$q_e = K_f C_e^{\,n} \quad \text{Freundlich (4-4b)}$$

$$q_e = \frac{KQC_e^{\,n}}{1 + KC_e^{\,n}} \quad \text{Langmuir-Freundlich (4-4c)}$$

where *K and* K_f represents the Langmuir bonding term related to interaction energies (L mg^{-1}) and the Freundlich affinity coefficient ($mg^{(1-n)}$ L^n kg^{-1}), respectively, *Q* denotes the Langmuir maximum capacity (mg kg^{-1}), C_e is the equilibrium solution concentration (mg L^{-1}) of the sorbate, and *n* is the Freundlich linearity constant. The Langmuir model assumes monolayer adsorption onto a homogeneous surface with no interactions between the adsorbed molecules. The Freundlich and Langmuir-Freundlich models, however, are empirical equations, which are often used to describe chemisorptions onto heterogeneous surface.

All the models reproduced the isotherm data fairly well (Figure 4-4), with correlation coefficients (R^2) exceeding 0.95 (Table 4-1). However, fittings of the Freundlich and Langmuir-Freundlich matched the experimental data better than those of the Langmuir model, suggesting the adsorption of phosphate onto the DSTC was controlled by heterogeneous processes. This result is consistent with the proposed

predominant adsorption mechanism of phosphate removal by the biochar through both mononuclear and polynuclear adsorption onto the colloidal and nano-sized MgO particles on DSTC surface.

Effect of pH and Coexisting Anions

The adsorption of phosphate onto the DSTC depended on initial solution pH (Figure 4-5a). The phosphate adsorption was lowest when pH equaled 2.0. When pH was increased from 2.0 to 4.1, the adsorption of phosphate by the biochar increased. Further increases in pH from 4.1 to 6.2, 7.1, 8.1, and 10.4, however, decreased the adsorption of phosphate onto the DSTC (Figure 4-5a), suggesting the existence of an optimum pH for the maximum phosphate adsorption. Similar results were found in studies of the pH effect on phosphate removal from aqueous solution by other carbon-based adsorbents [35].

Although molecular concentrations of the coexisting anions were about 15.5 times of the phosphate, chloride and nitrate had little effect on the adsorption of phosphate (4.3 and 11.7 percent decrease, respectively) onto the biochar (Figure 4-5b), suggesting low competitions between phosphate and these two ions for the MgO sites on the DSTC surface. The existence of high concentrations of bicarbonate in the solution, however, reduced the phosphate adsorption for about 41.4% (Figure 4-5b). Two factors could be responsible for the reduction: 1) the competition for the adsorption site between bicarbonate and phosphate; and 2) the increase of solution pH due to the addition of bicarbonate.

Implications

Biochar converted from anaerobically digested sugar beet tailings (DSTC) demonstrated superior ability to remove phosphate from water under a range of pH and

competitive ion conditions. Batch sorption experiments and post-sorption characterizations suggested that phosphate removal was mainly controlled by adsorption onto colloidal and nano-sized MgO particles on the DSTC surface. Because both the original and anaerobically digested sugar beet tailings are waste materials, the cost to make DSTC should be very low. However, the use of pre-digested sugar beet tailings has the benefit of additional energy generation and more efficient production (with less CO_2 release during production). Thus, DSTC should be considered a promising alternative water treatment or environmental remediation technology for phosphate removal. In addition, when used as an adsorbent to reclaim phosphate from water, the exhausted biochar can be directly applied to agricultural fields as a fertilizer to improve soil fertility because the P-loaded biochar contains abundance of valuable nutrients. Potential additional environmental benefits from this approach include fuel or energy produced during both the anaerobic digestion and pyrolysis and carbon sequestration due to biochar's refractory nature. Because arsenate and molybdate are phosphate analogues [124], it is expected that the digested sugar beet tailing biochar would also be an effective adsorbent for them.

Table 4-1. Best-fit parameter values for models of kinetic and isotherm data

Model	Parameter 1	Parameter 2	Parameter 3	R^2
First-order	k_1 = 0.1554 (h^{-1})	q_e = 23474.94 (mg kg^{-1})	--	0.9968
Second-order	k_2 = 5.211x10^{-6} (kg mg^{-1} h^{-1})	q_e = 28771.04 (mg kg^{-1})	--	0.9949
N_th-order	k_N = 0.000701 (kg^N mg^{-N} h^{-1})	q_e = 23927.64 (mg kg^{-1})	N = 1.1359	0.9970
Elevich	β = 0.000139 (mg kg^{-1})	α = 5967.70 (mg kg^{-1})	--	0.9855
Langmuir	K = 0.02551 (L mg^{-1})	Q = 133084.7 (mg kg^{-1})	--	0.9526
Freundlich	K_f = 11642.39 ($mg^{(1-n)}$ L^n kg^{-1})	n = 0.4527	--	0.9781
Langmuir-Freundlich	K = 0.01562 (L^n mg^{-n})	Q = 705873.6 (mg kg^{-1})	n = 0.4954	0.9785

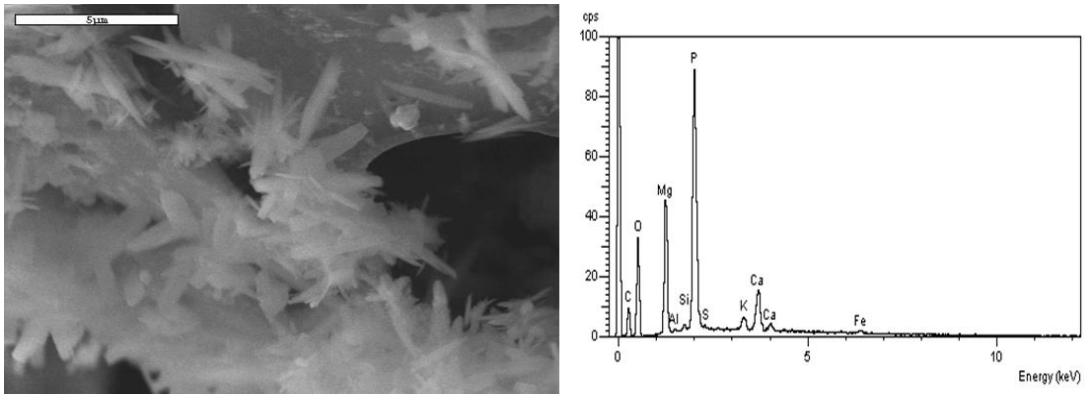

(A) (B)

Figure 4-1. SEM image (A) and corresponding EDS spectra (B) of the post-adsorption DSTC at 7000X. The EDS spectra were recorded at the same location as showing in the SEM image.

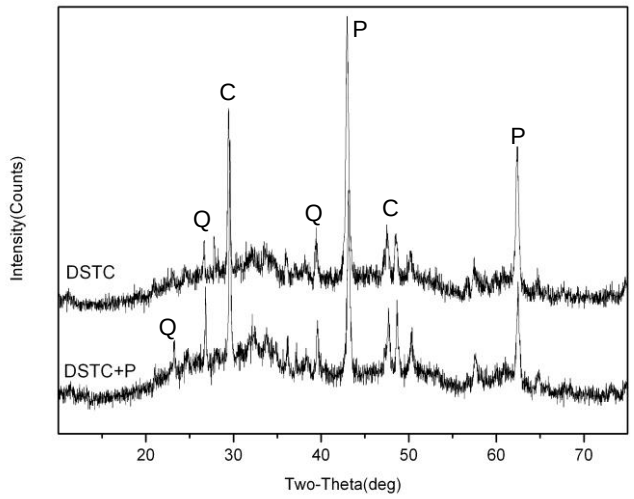

(A)

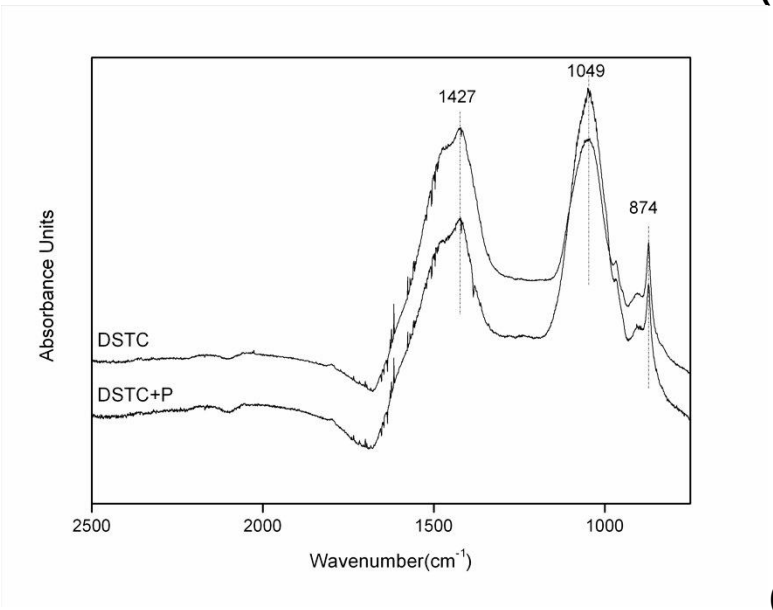

(B)

Figure 4-2. XRD (A) and FTIR (B) spectra of the original and post-adsorption DSTC. Crystallites were detected with peaks labeled in the XRD spectra as Q for quartz (SiO_2), C for calcite ($CaCO_3$), and P for periclase (MgO).

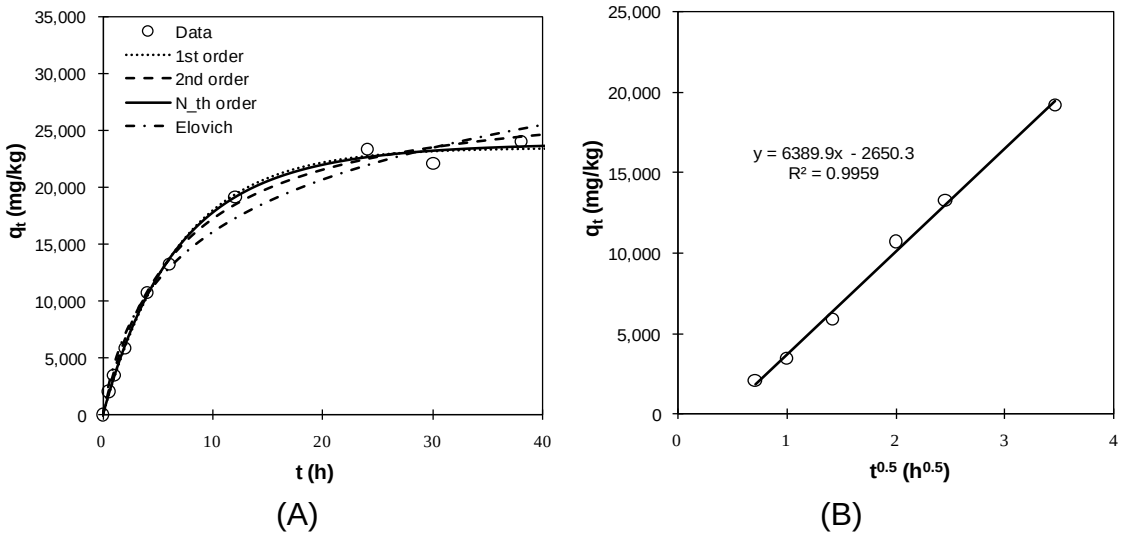

(A) (B)

Figure 4-3. Adsorption kinetic data and modeling for phosphate onto DSTC (A) full, and (B) pre-equilibrium adsorption versus square root of time.

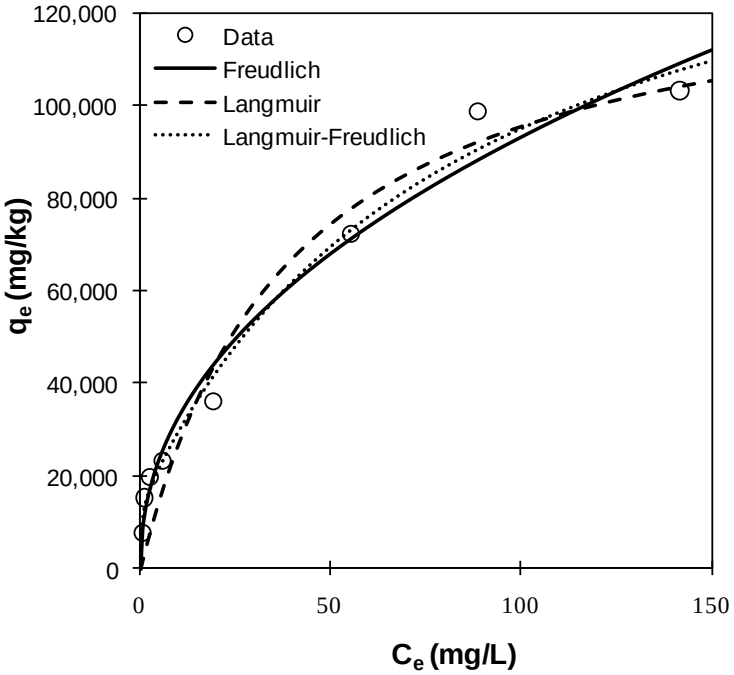

Figure 4-4. Adsorption isotherm for phosphate on DSTC.

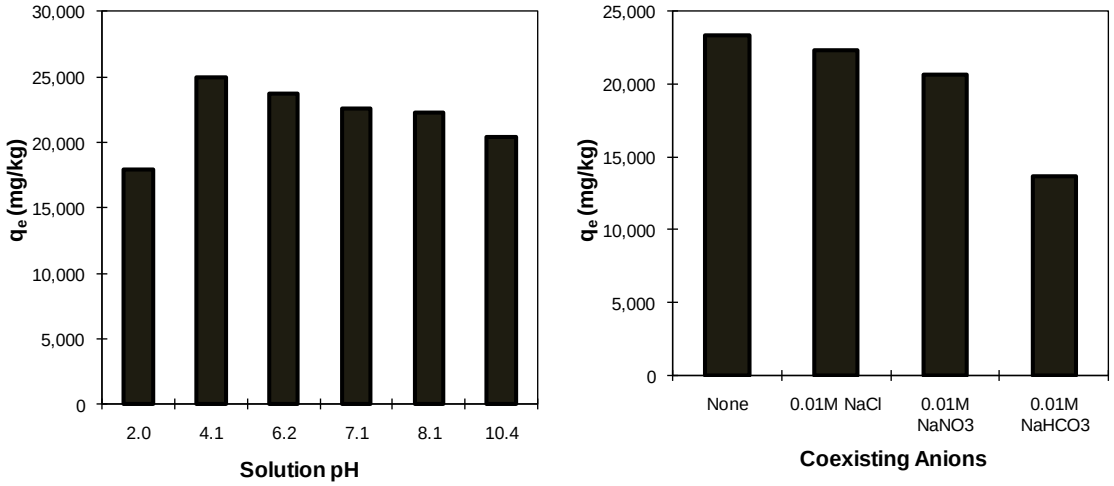

Figure 4-5. Effect of (A) pH and (B) coexisting anions on phosphate adsorption onto DSTC.

CHAPTER 5
ENGINEERED CARBON (BIOCHAR) PREPARED BY DIRECT PYROLYSIS OF MG-ACCUMULATED TOMATO TISSUES: CHARACTERIZATION AND PHOSPHATE REMOVAL POTENTIAL[1]

Introduction

Biochar is an engineered carbon that can be created from various biomass materials including agricultural and forestry residues through pyrolysis in an oxygen-limited environment. The role of biochar in political and academic arenas has received much attention in recent years because of its potential to be used as a carbon fixer and soil amendment for land applications that benefit the environment [131-133]. In addition, biochar has also been recognized as an alternative sorbent to remove aqueous chemical contaminants including heavy metals and organic compounds [8, 134-137]. Relatively little research, however, has been devoted to evaluate the application of biochar or other engineered carbon for removal of nutrients from aqueous solutions. Excessive nutrients, such as phosphate (P), are the main contributor to the eutrophication that not only affects the aquatic ecosystems but also indirectly hinders the economic progress [138, 139].

As a relatively new concept, using engineered carbon/biochar derived from biomass residues to sorb phosphate from water is considered as an eco-friendly and sustainable approach that may bring about multiple environmental and economic benefits. Particularly, spent biochar with sorbed P can be used as a fertilizer when applied to agricultural soils in addition to its benefits to enhance soil quality as well as a carbon sink. Unfortunately, most of the engineered carbons, including biochar, have

[1] Reprinted with permission from Yao, Y.; Gao, B.; Chen, J.; Zhang, M.; Inyang, M.; Li, Y.; Alva, A.; Yang, L., Engineered carbon (biochar) prepared by direct pyrolysis of mg-accumulated tomato tissues: Characterization and phosphate removal potential. Bioresource Technol 2013, doi: 10.1016/j.biortech.2013.03.057

limited ability to adsorb P or other anionic nutrients [140, 141]. Although several methods have been developed to modify the surface of engineered carbons to improve their affiliations to negatively charged ions [142, 143], only limited amount of studies have evaluated the sorption of P.

Recent studies suggested that biochar based composites with colloidal or nanosized MgO particles impregnated within carbon matrix have strong affiliation to aqueous P under various conditions [80, 144, 145]. The maximum sorption capacity of this new type of engineered biochar to P can reach more than 100 mg/g, which is greater than that of any other carbon-based sorbents reported in the literature (all lower than 20 mg/g). For instance, activated carbon is the most popular engineered carbon used in separation processes; however, its reported sorption capacity to P was still lower than 15.1 mg/g even after surface modification with iron or other metal elements [18, 146, 147]. The superior P sorption ability of the engineered biochar could be attributed to the large amount of colloidal or nanosized MgO particles distributed on the carbon surfaces within the pores of the biochar matrix [80].

In previous studies, the engineered Mg-biochar nanocomposites were synthesized through pyrolyzing anaerobically digested biomass residues or $MgCl_2$-pretreated agricultural residues [80]. In both cases, the feedstock materials contained high amount of Mg, a common element in plant tissues, after the pretreatment of the original biomass. This suggests that the engineered biochar nano-composites may be produced directly from selected plant tissues that are rich in Mg. In addition, recent advances in plant nutrient enrichment and phytoremediation technologies make it possible to envision the development of an innovative method to create high-efficiency

P removal biochars from plant biomass residues enriched with Mg element through bioaccumulation. If feasible, this innovative method may not only develop a much more convenient production method for engineered Mg-biochar nanocomposites (no pretreatment is required), but also makes it possible to create alternative opportunities for the plant nutrient enrichment and phytoremediation technologies to produce value-added by-products.

In this study, an innovative approach was used to produce engineered biochars directly from tissues of tomato, a commonly used model plant, enriched with Mg/Ca through bioaccumulation. Greenhouse experiments were conducted using a sand-zeolite culture system to produce tomato tissues (leaves) containing high concentration of Mg/Ca for production of the engineered biochars. Physicochemical properties of the biochars produced were characterized in details. A preliminary adsorption experiment was conducted to assess the P removal ability of the biochars and together with the published results to determine potential relations between biochar's P removal ability and its metal contents. The overarching objective of this study was to determine whether engineered Mg-biochar nanocomposites could be prepared by direct pyrolysis of Mg-accumulated tomato tissues. The specific objectives were as follows: 1) develop a novel approach to produce engineered biochar from Mg-enriched plant tissues through direct pyrolysis, 2) characterize the physicochemical properties of the engineered biochar, and 3) assess the potential role of Mg enrichment on P sorption on the engineered biochar.

Materials and Methods

Biochar production

Five tomato tissues (leaves) were used in this study, including three samples obtained in the laboratory: Mg-enriched (MgET), calcium-enriched (CaET), and a lab control (LCT), and two field samples (FCT1 and FCT2). For Mg and Ca enrichment, tomato plants grown in a peat-based medium were respectively irrigated with Hoagland solution at 25 mM Mg and 50 mM Ca twice a week. FCT1 and FCT2 were collected from farms in Senibel and Rocky Top in South Florida, respectively. The biomass samples were oven dried and grounded into 1-2 mm pieces as feedstocks for biochar production. A tube furnace (MTI, Richmond, CA) was used to convert them into biochar samples in a N_2 environment at temperatures of 600 °C for one hour. The resulting biochar samples were washed several times with DI water and oven dried for further tests. The resulting five biochar samples were henceforth referred to as MgEC, CaEC, LCC, FCC1 and FCC2.Detailed information about biochar production procedures can be found in previous studies [80, 141].

Besides the five biochars produced in this study, additional twenty biochars were used to determine the correlation between their phosphate remove ability and element contents. Eight biochars were produced from Canadian peat (one), composted dairy manure (one), and tomato stems and roots (six, including Ca- and Mg-enriched and control) using the same method. Other twelve biochars were produced from agricultural residues (e.g., bagasses, sugarbeet tailings, and peanut hulls) under various conditions as reported in published studies [80, 141].

Characterization

Major elements of biochar and corresponding feedstock were determined by acid digestion of the samples followed by inductively-coupled plasma atomic emission spectroscopy (ICP-AES) analysis. The pH of the biochar (i.e. equilibrium pH of biochar/ water suspension) was measured in a biochar (dry sample) / deionized water mass ratio of 1:20 with a pH meter (Fisher Scientific Accumet Basic AB15). Scanning electron microscope (SEM) imaging analysis of the original and P-sorbed Mg-biochar was conducted using a JEOL JSM-6400 Scanning Microscope. Surface elemental analysis was also conducted simultaneously with the SEM at the same surface locations using energy dispersive X-ray spectroscopy (EDX, Oxford Instruments Link ISIS). X-ray diffraction (XRD) analysis was carried out using a computer-controlled X-ray diffractometer (Philips Electronic Instruments) equipped with a stepping motor and graphite crystal monochromator. Crystalline compounds in the samples were identified by comparing diffraction data against a database compiled by the Joint Committee on Powder Diffraction and Standards. X-ray photoelectron spectroscopy (XPS) measurements were conducted with a PHI 5100 series ESCA spectrometer (Perkin-Elmer) to determine the elemental composition on the sample surface. Thermogravimetric analysis (TGA) of original and P-loaded MgEC was carried out under a stream of air at a heating rate of 10 ^{o}C/min using a Mettler Toledo's TGA/DSC1 thermogravimetric analyzer.

P sorption

P solutions were prepared by dissolving Potassium P Dibasic Anhydrous (K_2HPO_4, certified A.C.S, Fisher Scientific) in DI water. The P sorption ability of 9 biochars were examined using 68 mL digestion vessels (Environmental Express) at room temperature

(22±0.5 ˚C) with a 1:500 (0.1g biochar in 50ml solution) biochar / solution (30 mg/L P) ratio for 24 h. The samples were withdrawn from a mechanical shaker and immediately filtered through 0.22 μm pore size nylon membrane filters (GE cellulose nylon membrane) to determine adsorbed P concentrations by inductively-coupled plasma atomic emission spectroscopic (ICP-AES). All the experimental treatments were performed in duplicate and the average values are reported. Additional analyses were conducted whenever two measurements showed a difference larger than 5%.

Statistical Methods

The least squares method was used to study the relationship of phosphate removal ability and 7 metal contents (Mg, Ca, K, Fe, Zn, Cu, and Al) of 25 engineered biochars produced by various methods from current and previous studies. The coefficient of determination (R^2), *p-value*, standard deviation, and other statistics were analyzed by OriginPro 8.5. R^2 was then compared to measure the effect of each metal content on variation of phosphate removal ability. Error bars represent SD of duplicate or triplicate determinations.

Results and Discussion

Mg and Ca in Feedstock and Biochar

Compared to the controls, the Mg/Ca treatments showed no notable effects on the growth of the tomato plants, probably because both Mg and Ca are belonging to the essential mineral elements necessary for plant growth. In addition, previous studies have shown that this kind of treatment may even enhance the nutrient values of tomato fruits to be used as a principal dietary mineral source for humans because of the accumulation of Mg and Ca in the edible tissues [148]. Tomato plants treated with 25 mM Mg accumulated much higher level of Mg in tissue compared to plants from the

laboratory control treatment and the two field sampled plants (Table 5-1), indicating Mg can be substantially enriched in tomato plants. The Ca content in tomato plants treated with 50 mM Ca was also greater than that of the lab control, but much lower than that of the two field samples. These results further confirmed the plant bioaccumulation ability to metal elements because the two field samples were collected from farms in south Florida, where the soils mainly consist of Miami limestone ($CaCO_3$). In the literature, a number of naturally occurring or genetically engineered plants have been reported to hyperaccumulate metals, such as arsenic, lead, cadmium, and mercury [149-151].

As shown in Table 5-1, pyrolysis process further concentrated Mg and Ca in the engineered biochar samples. Biochar produced from the Mg-enriched biomass had a Mg level of 8.8%, which is the highest among all the biochar samples in this study. Similarly, biochar samples produced from the Ca-enriched and two field samples contained more than 12% of Ca. These results demonstrated that the new method could successfully produce engineered biochar composites (carbon-metal composites) from plant biomass enriched with cationic nutrient elements, such as Mg and Ca, through growth enrichment.

Effect of Mg Enrichment of P Removal by Biochar

Phosphate removal rate varies significantly among biochar samples. The correlations between P removal rate and metal element contents of the biochars were analyzed statistically. Comparison of the P sorption ability of all the 5 biochar samples produced in this study (Figure 5-1) showed that biochars with high Mg level removed greater percent of P from the solution (88.5%). This result is consistent with findings from previous studies that Mg-biochar composites have strong sorption ability to aqueous P [80].

Figure 5-2 shows the correlations between the phosphate removal rates of a total of 25 engineered biochars produced by various methods from current and previous studies and their Mg, Ca, K, Fe, Zn, Cu, and Al contents. Statistical analysis based on the results showed a strong and statistically significant correlation between P removal rate and biochar Mg content (Figure 5-2a, R^2 = 0.78, and p< 0.001). On the contrary, the other metal elements (Ca, K, Fe, Zn, Cu, and Al) are not important to P removal by the biochars and no significant correlations were identified (R^2 <0.364). The regression results were listed in Table 5-2. Thus, it can be concluded that the sorption of P by the engineered biochar is governed by the presence of Mg in the carbon matrix. This also explains why the innovative approach that enriches plant tissues with Mg element was successful in producing P removal biochar. Previous studies suggested that the Mg in the biochar may form large amount of colloidal or nanosized oxides particles on carbon surface within the biochar, and those fine particles can electrostatically attract P in aqueous solution to form mono-, and polynuclear complexes through the surface deposition mechanism [125, 127, 145].

Characterization of Mg-Enriched Biochar (MgEC).

Among all the biochars produced in this work, the Mg-enriched one had the highest P remove rate; it was then selected for further investigations. In previous work, strong P sorption ability of the engineered biochars converted from digested and Mg-pretreated biomass was attributed to the presence of colloidal or nanosized MgO particles on the carbon surface within the pores [145]. XRD analysis of the Mg-enriched biochar obtained in the current work, however, showed both MgO and $Mg(OH)_2$ (Figure 5-3). Diffraction peaks at (001), (100), (101), (102), (110), (111), (103) and (201) are readily recognized from the XRD pattern of the $Mg(OH)_2$ powder, and the peaks at (200)

and (220) match the peak in the diffractions of MgO. The particle sizes of MgO and $Mg(OH)_2$ within the biochar matrix were calculated using the Scherrer formula which was designed in 1918 for determination of the mean size of single-crystal nanoparticles or crystallites in nanocrystalline bulk materials in the form as [152, 153]:

$$\tau = \frac{K\lambda}{\beta \cos\theta}$$

where K is the shape factor with a typical value of about 0.9, λ is the x-ray wavelength, β is the line broadening at half the maximum intensity (FWHM) in radians, and θ is the Bragg angle; τ is the mean size of the ordered (crystalline) domains. The particle sizes of MgO and $Mg(OH)_2$ within the biochar matrix in this study were about 46.0 nm and 6.3 nm, respectively.

SEM imaging of the biochar showed a wide spread of nanoscale Mg flakes (nanoplatelet) on the carbon surface, which is a common structural morphology of Mg hydroxide (Figure 5-4). The EDX spectrum of the biochar surface identified an extremely high peak of Mg, which further confirmed the dominance of those nanoparticles on the biochar. The presence of large quantity of nano-sized flakes could contribute to the high surface area of the biochar. The SEM-EDX analyses concurred to the XRD results that the engineered biochar produced from Mg-enriched plant tissues was a biochar composites with Mg oxyhydroxides particles on carbon surfaces within the biochar matrix. Further characterization of the engineered biochar MgEC with the XPS showed strong signals of Mg on the surface (Figure 5-5), further confirming previous results. The XPS results also suggested that there might be more $Mg(OH)_2$ than MgO on the surface of the engineered biochar, suggesting $Mg(OH)_2$ particles could also play an important role in controlling the surface interactions between P and the Mg-biochar composites.

Because the points of zero charge (PZCs) of $Mg(OH)_2$ and MgO are both higher than 12 [126], their surfaces should be positively charged in most natural aqueous conditions and thus could adsorb P through electrostatic attractions [144, 145]. Based on this mechanism, it is anticipated that solution pH could play an important role in controlling the adsorption of P on this new engineered biochar though altering surface charge of the biochar and P speciation. A recent study on P adsorption on MgO-biochar composites derived from anaerobic digested sugar beet tailings also showed that P removal by the MgO-biochar decreased with increasing bicarbonate concentration in solution due to the competition for adsorption sites [145]. If not optimized, those two factors (i.e., pH and coexisting anions) could inhibit the removal ability of the engineered biochar to P in aqueous solutions, particularly in real-life wastewater.

Comparison of the TGA curves between the Mg-biochar and the laboratory control biochar showed almost no difference (Figure 5-6), indicating that the new method has no impact on the thermal stability of the biochar. The Mg-biochar composite (MgEC), therefore, can also be used as a carbon sequester to soils due to its high recalcitrance, particularly after being laden with P (spent/exhausted biochar).

Implications

As a first study of its kind, an innovative method has been developed to produce engineered biochar directly (without pretreatment) from plant tissues enriched with Mg. The results from the initial P sorption evaluation and biochar characterization indicated that this novel approach successfully created Mg-biochar composites, containing both nanosized MgO and $Mg(OH)_2$ particles within the matrix, which can be used as a high-efficiency adsorbent to remove P form aqueous solutions.

Table 5-1. Elemental analysis of feedstocks and biochars produced in this study (mass %)a. Feedstocks: Ca-enriched tomato tissues (CaET), Mg-enriched tomato tissues (MgET), laboratory control of tomato tissues (LCT), farm control from Senibel (FCT1), and farm control from Rocky Tops (LCT2). CaEC, MgEC, LCC, FCC1, and FCC2 are biochars produced form these feedstocks, respectively.

	%, mass based														
	P	K	Na	Mg	Ca	Cu	Cr	Fe	Al	As	Cd	Ag	Mn	Pb	Zn
Feedstocks															
CaET	0.18±0.04	2.22±0.03	0.11±0.03	0.89±0.14	4.90±0.50	0.00±0.00	-	-	0.01±0.01	-	-	-	0.01±0.00	-	0.01±0.00
MgET	0.22±0.03	3.82±0.17	0.18±0.01	3.11±0.32	2.56±0.50	0.00±0.00	-	0.00±0.00	0.00±0.00	-	-	0.00	0.02±0.01	0.00	0.00±0.00
LCT	0.21±0.03	3.70±0.15	0.28±0.04	1.51±0.16	2.55±0.49	0.00±0.00	-	0.00±0.00	0.01±0.00	-	-	-	0.01±0.00	-	0.00±0.00
FCT1	0.18±0.02	0.10±0.02	0.01±0.00	0.62±0.09	8.25±0.70	0.05±0.01	-	0.02±0.01	0.03±0.00	-	-	0.00	0.01±0.00	-	0.02±0.00
FCT2	0.15±0.02	0.15±0.01	0.01±0.00	0.53±0.10	8.17±0.73	0.05±0.01	-	0.13±0.02	0.03±0.00	-	-	0.00	0.03±0.01	0.00	0.02±0.00
Biochars															
CaEC	0.46±0.06	0.35±0.01	0.06±0.03	2.10±0.20	12.32±0.97	0.00±0.00	-	0.01±0.00	0.01±0.00	-	-	-	0.06±0.01	-	0.01±0.00
MgEC	0.74±0.06	1.25±0.10	0.14±0.01	8.79±0.82	1.68±0.01	0.00±0.00	-	0.02±0.00	0.01±0.00	-	-	-	0.09±0.01	-	0.03±0.00
LCC	0.60±0.10	0.85±0.03	0.11±0.01	3.53±0.33	3.28±0.63	0.00±0.00	-	0.01±0.01	0.01±0.00	-	-	-	0.07±0.02	-	0.01±0.00
FCC1	0.58±0.08	0.02±0.00	0.00±0.00	1.30±0.21	18.77±1.15	0.32±0.04	0.00	0.08±0.02	0.07±0.01	-	-	0.00	0.07±0.01	0.00	0.04±0.02
FCC2	0.48±0.05	0.02±0.01	0.00±0.00	1.32±0.08	19.20±1.08	0.29±0.02	-	0.05±0.02	0.08±0.02	-	-	0.00	0.04±0.01	-	0.04±0.02

'-' below detection limit.

Table 5-2. Correlation between biochar phosphate removal rate (P) and different metal content (C), where P= a· C+ b.

Metal	R^2	Metal content coefficient (a)	Constant (b)
Mg	0.779	0.101	0.019
Ca	0.364	0.031	0.043
K	0.251	0.298	0.027
Fe	0.085	0.453	0.122
Zn	0.011	0.667	0.151
Cu	0.106	1.139	0.135
Al	0.013	-0.247	0.194

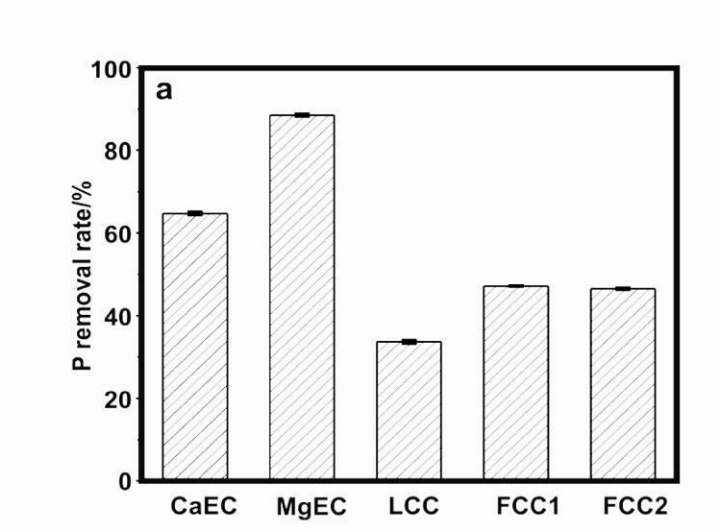

Figure 5-1. Comparison of phosphate adsorption ability of five biochars produced in this study. CaEC, Ca-enriched biochar; MgEC, Mg-enriched biochar; LCC, laboratory control biochar; FCC, farm control biochar.

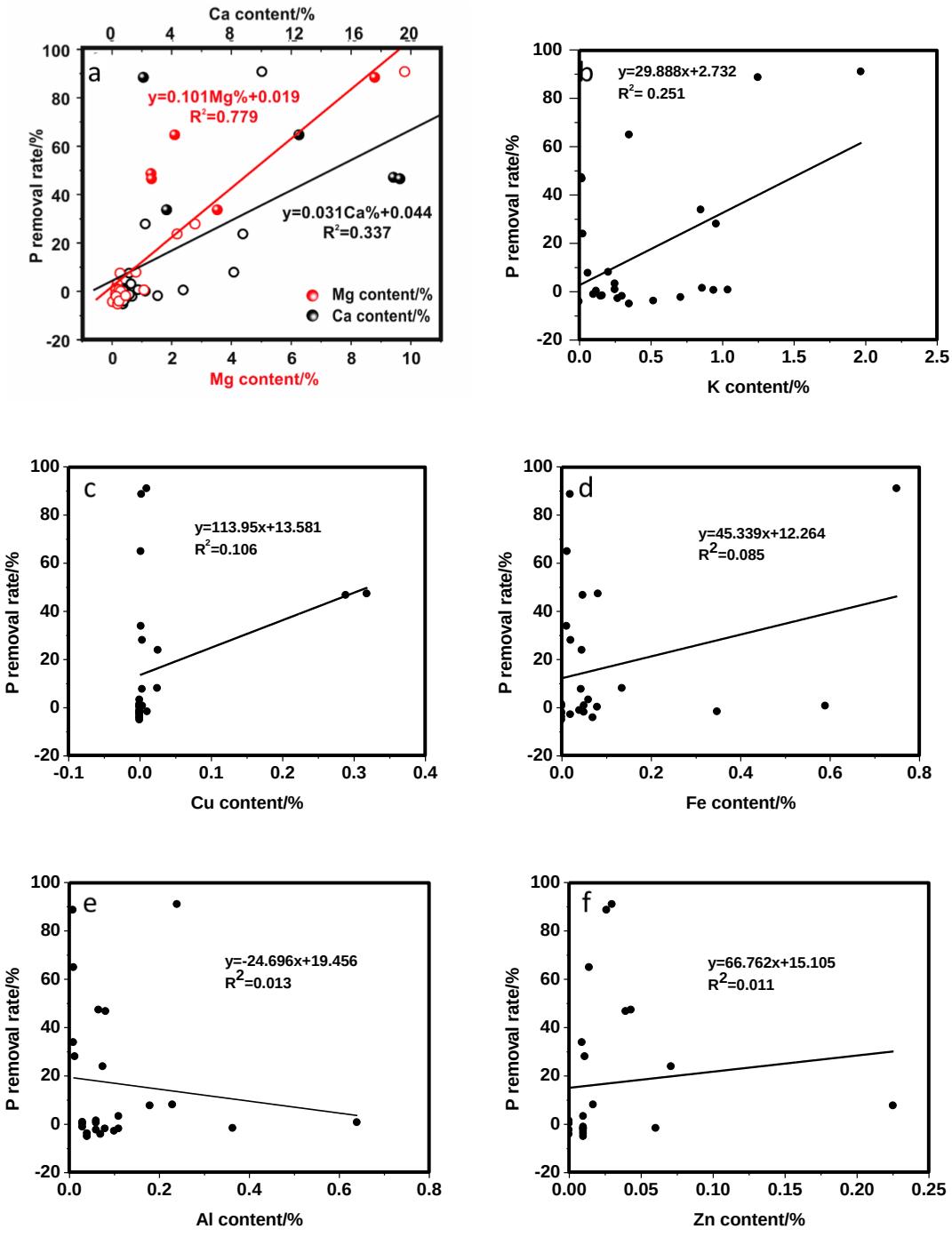

Figure 5-2. Correlation between phosphate removal rate and Mg/ Ca (a) and other metal contents (Cu, Fe, Al, Zn, K) (b-f) of a total of 25 biochars. Red and black colors represent Mg and Ca, respectively.

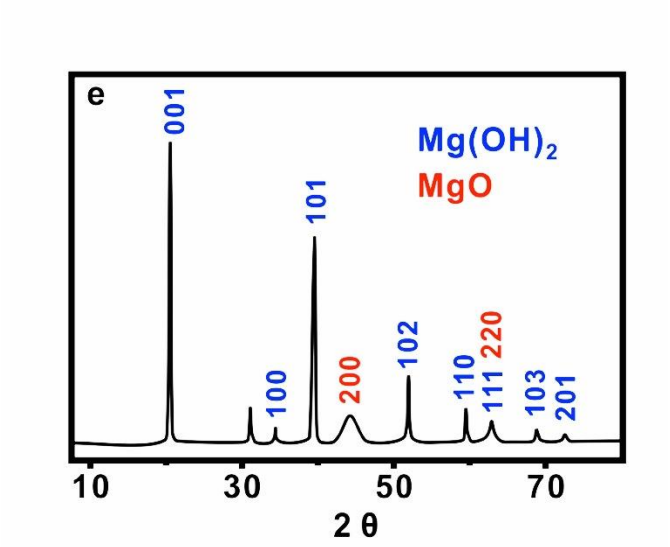

Figure 5-3. XRD spectrum of MgEC.

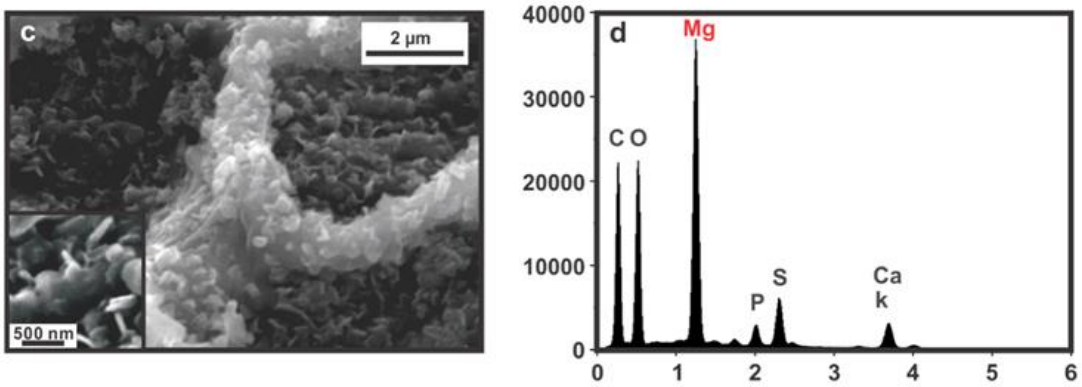

Figure 5-4. SEM image and EDS spectrum of MgEC morphological structures, the insert is at a higher resolution.

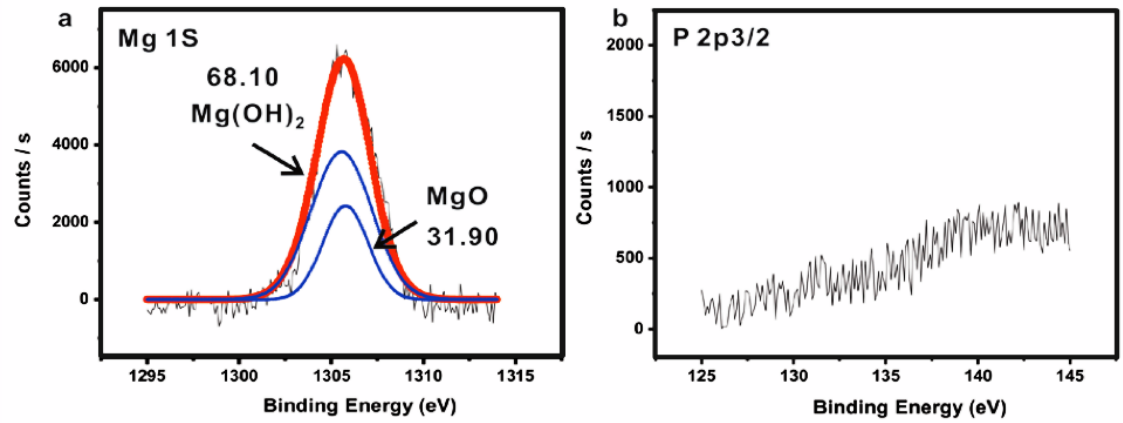

Figure 5-5. XPS scan of magnesium (a) and phosphorus (b) on MgEC surfaces.

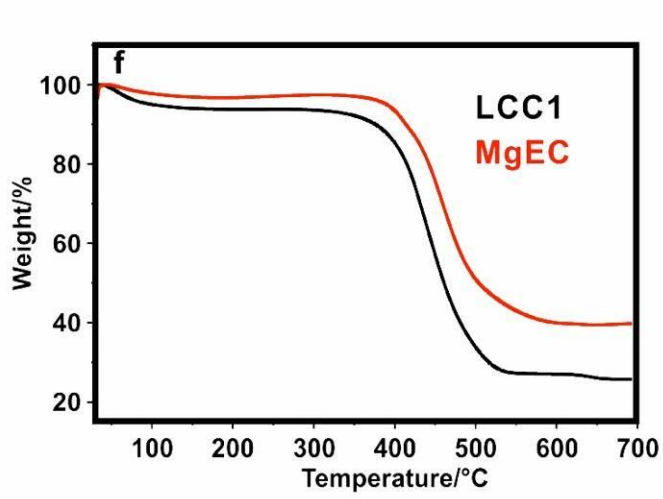

Figure 5-6. TGA curves of MgEC and LCC1.

CHAPTER 6
AN ENGINEERED BIOCHAR RECLAIMS PHOSPHATE FROM AQUEOUS SOLUTIONS: MECHANISMS AND POTENTIAL APPLICATION AS A SLOW-RELEASE FERTILIZER

Introduction

Phosphorus is a limiting nutrient for the growth of organisms and plants and is an indicator of surface water quality [154]. Excessive phosphorus from both point and non-point sources into natural waters is known to cause eutrophication which is occurring throughout the world [14, 15, 155, 156]. Dissolved phosphate of ~0.02 $mg \cdot L^{-1}$ is considered to have potential that lead to profuse algal growth in waters [157]. Accelerated eutrophication not only affects the aquatic ecosystems but also indirectly hinders the economic progress. The combined costs were approximately $2.2 billion annually as a result of eutrophication in U.S. freshwaters [158]. It is therefore very important to develop effective technologies to remove phosphate from aqueous solutions prior to their discharge into runoff and natural water bodies.

The role of biochar (pyrogenic black carbon derived from incomplete biomass combustion) in political and academic arenas has received much attention in recent years. Biochar is widely recognized as important cost-effective adsorbent storing chemical contaminants including heavy metals, organic compounds and other environmental pollutions [8, 93, 135, 137, 159]. The use of carbon/biochar to remove phosphate from aqueous solutions is an emerging and promising concept with plenty of advantages over traditional wastewater treatment technologies (i.e., chemical, biological and physical processes). Most of the traditional engineered carbons (e.g., activated carbon and biochar), however, have limited ability to adsorb P or other anionic nutrients. For example, Namasivayam et al. [18] and Bhargava et al. [146] reported that the P

adsorption capacity of activated carbons derived from coir pith and tamarind nut shell was only about 5.1 $mg \cdot g^{-1}$ and 5.0 $mg \cdot g^{-1}$, respectively. Yao et al. [160] tested thirteen biochars made from different biomass feedstocks and found most of them had little/no ability to sorb phosphate from aqueous solutions. Chen et al. [161] reported that magnetic biochars made from iron-treated orange peel powders had a P adsorption capacity of only around 1.2 $mg \cdot g^{-1}$.

In order to improve the sorption ability of biochars to aqueous P, several investigations have been conducted to synthesize engineer biochars with novel structures and surface properties [80, 145, 161-165]. In particular, it has been reported that engineered Mg-biochar nanocomposites with nanosized magnesium oxides (MgO) attached on carbon surfaces within the biochar matrix have superior sorption ability to aqueous P [80, 145, 163]. For example, the MgO-biochar nanocomposites synthesized through pyrolyzing anaerobically digested sugar beet tailings [145] or $MgCl_2$-pretreated agricultural residues [163] both showed an extremely high sorption capacity to P (> 100 $mg \cdot g^{-1}$), which is much higher than that of many carbon-based and other commercial adsorbents reported in the literature (<20 $mg \cdot g^{-1}$) [15, 36, 43, 109, 166-169]. The superior P sorption ability of these MgO-biochar nanocomposites is attributed to the presence of the nanosized MgO particles on the biochar surfaces, which can serve as active adsorption sites for aqueous P [145, 163]. Because the production of the MgO-biochar nanocomposites involves either chemical or microbial pretreatment procedures, an innovative approach was recently developed to synthesize a new P-removal engineered biochar by direct pyrolysis of plant biomass residues enriched with Mg element through bioaccumulation [162]. The new engineered biochar has nanosized

$Mg(OH)_2$ and MgO particles on its surfaces and showed promising potential to adsorb P from aqueous solutions [162]. However, the sorption characteristics and mechanisms of P on this engineered biochar prepared from Mg-enriched plant tissues have not been examined previously.

Previous studies of the P-removal biochars also have proposed that the post-sorption biochars could potentially be applied directly to cropland as a fertilizer because the spent biochars may contain high amount of P. For example, the P contents in the post-sorption MgO-biochar nanocomposites derived from anaerobically digested sugar beet tailings and $MgCl_2$-treated biomass were all greater than 10%, comparable to or even greater than that of commercial phosphorus fertilizers. In addition to P-fertilizer supply, the P-laden biochars, when applied to soils, would also be a carbon sink because of their relatively high recalcitrance, or resistance to abiotic and biotic degradation [67, 170-174]. Nevertheless, the bioavailability of the adsorbed P in the spent engineered biochars is still unknown. To the authors' best knowledge, no investigations have been conducted previously to determine desorption mechanisms, release characteristics, or biological effects of adsorbed P in spent engineered biochars.

The overarching objective of this study was to determine whether engineered biochars can be used to reclaim aqueous P and then be applied to soils as a P-fertilizer. A series of laboratory experiments were conducted to determine the mechanisms and characteristics of P adsorption on an engineered biochar prepared from Mg-enriched tomato tissues. The bioavailability, desorption characteristics, and seed germination ability of the adsorbed P within the spent (i.e. P-laden) biochar were also evaluated. The specific objectives were as follows: 1) measure the sorption characteristics of P to the

engineered biochar, 2) characterize the post-sorption biochar to identify the governing P sorption/desorption mechanisms, 3) measure the release characteristics of P from the post-sorption biochar, and 4) determine the biological effects of the post-sorption biochar on seed germination and seedling growth.

Materials and Methods

Materials

The engineered biochar used in this study is a Mg-biochar nanocomposite prepared by pyrolyzing Mg-enriched tomato leaves inside a furnace under a N_2 environment at 600 ˚C. After washing with deionized (DI) water to remove impurities, the biochar was oven dried (80˚C) and sealed in a container prior to use. More information about the preparation and characterization of the engineered biochar can be found in Yao et al. [162]. Phosphate solutions were prepared by dissolving Potassium Phosphate Dibasic Anhydrous (K_2HPO_4) in DI water. All the chemicals used in the study are A.C.S certified and from Fisher Scientific.

P Adsorption

Adsorption kinetics of P on the biochar were examined by mixing 0.1 g of the sorbent with 50 mL 10 $mg \cdot L^{-1}$ P solutions in 68 mL digestion vessels (Environmental Express) at room temperature (22 ± 0.5 ˚C). The vessels were then shaken at 55 rpm in a mechanical shaker. At appropriate time intervals, the vessels were withdrawn and the mixtures were immediately filtered through 0.22 μm pore size nylon membrane filters (GE cellulose nylon membrane). Adsorption isotherm of phosphate on the biochar was determined similarly by mixing 0.1 g biochar with 50 mL phosphate solutions of different concentrations ranging from 3.1 to 588.1 $mg \cdot L^{-1}$ in the digestion vessels. The vessels were shaken in the mechanical shaker for 24 h at room temperature (sufficient to reach

adsorption equilibrium). The samples were then withdrawn and filtered to determine adsorbed phosphate concentrations. Phosphate concentrations on the solid phase were calculated based on the initial and final aqueous concentrations, which were determined by inductively-coupled plasma atomic emission spectroscopic (ICP-AES). The post-adsorption biochar samples were collected, rinsed with deionized water, and dried at 80 ˚C for further experiments. All the adsorption experiments were conducted in duplicate and the average experimental data are reported. Additional measurements were obtained when the duplicates had a difference larger than 5%.

Post-Sorption Characterization

Scanning electron microscope (SEM) imaging analysis was conducted using a JEOL JSM-6400 Scanning Microscope. Varying magnifications were used to examine the structure and surface characteristics of the post-sorption engineered biochar. Surface element analysis was also conducted simultaneously with the SEM at the same surface locations using energy dispersive X-ray spectroscopy (EDX, Oxford Instruments Link ISIS). The EDX can provide rapid qualitative, or with adequate standards, semi-quantitative analysis of elemental composition with a sampling depth of 1-2 microns [102]. X-ray diffraction (XRD) analysis was carried out to identify any crystallographic structure in the post-sorption biochar using a computer-controlled X-ray diffractometer (Philips Electronic Instruments) equipped with a stepping motor and graphite crystal monochromator. Crystalline compounds in the samples were identified by comparing diffraction data against a database compiled by the Joint Committee on Powder Diffraction and Standards. In addition, X-ray photoelectron spectroscopy (XPS) measurements were carried out with a PHI 5100 series ESCA spectrometer (Perkin-Elmer) to determine the elemental composition on the sample surface.

P Release

Bioavailable phosphorus test was carried out using the Mehlich 3 soil test method [175]. P was extracted at a soil: extractant volumetric ratio of 1:10. Mehlich 3 extractant consists of 0.2 M CH_3COOH, 0.25 M NH_4NO_3, 0.015 M NH_4F, 0.013 M HNO_3, 0.001 M EDTA. The final pH of the extracting solution was about 2.5 ± 0.1. The samples were shaken at 200 epm for 5 min at room temperature (22 ± 0.5 ˚C), and then filtered through Whatman No. 42 filter paper to determine the extractable P concentrations. The extraction experiment was replicated three times and the average data and standard deviations are reported.

Kinetics of phosphorus release from the post-sorption biochar into DI water was measured by mixing 0.3 g of the sample with 120 mL DI water at room temperature (22 ± 0.5 ˚C). The contents of P in the aqueous solution were then determined after 1, 2, 3, 6, 10, 24, 48, 120, and 144 h. For the next 11 days, the biochar sample was filtered out from the solution and added to 120 mL fresh DI water every day to release P. The kinetics and release experiments were replicated three times and the average data and standard deviations are reported.

Seeds Germination and Early Stage Seedling Growth Bioassay

Seeds germination assay was carried out by spreading same number of grass seeds (Brown Top Millot) on a layer of filter paper moistened with DI water in containers with or without 0.1g P-laden biochar with ≥ 4 replicates. All replicates were incubated at room temperature and successfully emerged seeds (those with shoots longer than 0.5 cm) were counted once significant germination was observed. The early stage (first 13 days) seedling growth was also determined and 10 seedlings from each group were randomly collected for statistical analysis.

Statistics

The coefficient of determination (R^2), *p-value*, standard deviation, and other statistics were analyzed by OriginPro 8.5. Matlab Toolbox was used to fit all kinetics and isotherm data. Differences between the numbers of seeds germination were statistically analyzed with the t-test and one-way ANOVA with a significance level of 0.05 ($p < 0.05$). Error bars were used to represent standard deviations of multiple determinations.

Results and Discussion

Adsorption Kinetics and Isotherms

Kinetics study indicated that the sorption of P on the engineered biochar increased smoothly over time and reached equilibrium at around 24 hrs (Figure 6-1a). This result is similar to the sorption kinetics of P on the MgO-biochar nanocomposites produced from digested sugar beet tailings, although the biochar used in this study contained both MgO and $Mg(OH)_2$ particles. Different mathematical models were applied in this study to describe the adsorption kinetics of P on the biochar. In addition to the commonly used pseudo-first-order and pseudo-second order models, the Ritchie n_th-order model and the Elovich model were also used and the governing equations are [145]

$$\frac{dq_t}{dt} = k_1(q_e - q_t) \quad \text{first-order (6-1a)}$$

$$\frac{dq_t}{dt} = k_2(q_e - q_t)^2 \quad \text{second-order (6-1b)}$$

$$\frac{dq_t}{dt} = k_n(q_e - q_t)^N \quad \text{N\_th-order (6-2c)}$$

$$\frac{dq_t}{dt} = \alpha \exp(-\beta q_t) \quad \text{Elovich (6-3d)}$$

where q_t ($mg \cdot g^{-1}$) and q_e ($mg \cdot g^{-1}$) are the amount of P adsorbed at time t and at equilibrium, respectively, k_1 (h^{-1}), k_2 ($g \cdot mg^{-1} \cdot h^{-1}$), and k_n ($g^{n-1} \cdot mg^{1-n} \cdot h^{-1}$) are the first-order,

second-order, and n_th-order adsorption rate constants, α ($mg \cdot g^{-1} \cdot h^{-1}$) is the initial adsorption rate, and β ($g \cdot mg^{-1}$) is the desorption constant. The first-order, second-order, and n_th-order models describe the kinetics of the solid-solution system based on mononuclear, binuclear, and n-nuclear adsorption, respectively, with respect to the sorbent capacity and the Elovich model is an empirical equation considering the contribution of desorption [145].

The best-fit parameters of the kinetics models are listed in Table 6-1. All these models closely reproduced the kinetic data (Figure 6-1a) with R^2 exceeding 0.97. The n_th-order (n=1.74) models fitted the data slightly better than other models with a R^2 of 1.00, suggesting that the adsorption of P on the engineered biochar could be controlled by multiple mechanisms. Previous studies showed that intraparticle diffusion processes could play an important role in controlling the sorption of contaminants on carbon materials [129, 176]. In this study, the sorption kinetics of P on the engineered biochar might also affect by the intraparticle diffusion mechanism because the pre-equilibrium P adsorption data showed a linear dependency (R^2=0.891) on the square root of time (Figure 6-2).

The maximum P sorption capacity of the engineered biochar obtained from the isotherm study was greater than 100 $mg \cdot g^{-1}$ (Figure 6-1b), indicating the biochar could be used as an effective sorbent to remove P from aqueous solutions. In addition, this high sorption capacity also suggests that the spent engineered biochar, which was laden with more than 10% of P, could potentially be used as a P-fertilizer. Five commonly used isotherm equations were used to simulate the experimental isotherms and the governing equations are [128, 145]

$$q_e = \frac{KQC_e}{1+KC_e} \quad \text{Langmuir (6-2a)}$$

$$q_e = K_f C_e^{\,n} \quad \text{Freundlich (6-2b)}$$

$$q_e = \frac{KQC_e^{\,n}}{1+KC_e^{\,n}} \quad \text{Langmuir-Freundlich (6-2c)}$$

$$q_e = \frac{K_r C_e}{1+aC_e^{\,n}} \quad \text{Redlich-Peterson (6-2d),}$$

$$q_e = \frac{RT}{b}\ln(AC_e) \quad \text{Temkin (6-2e),}$$

where K ($L \cdot mg^{-1}$), K_f ($mg^{(1-n)} \cdot L^n \cdot g^{-1}$), K_{lf} ($L^n \cdot mg^{-n}$), and K_r ($L^n \cdot mg^{-n}$) represents the Langmuir bonding term related to interaction energies, the Freundlich affinity coefficient, Langmuir-Freundlich affinity parameter, and the Redlich–Peterson isotherm constants, respectively, Q ($mg \cdot g^{-1}$) denotes the Langmuir maximum capacity, C_e ($mg \cdot L^{-1}$) is the equilibrium solution concentration of the sorbate, n (dimensionless) is the Freundlich linearity constant, a ($L \cdot g^{-1}$) is the Redlich-Peterson isotherm constant, and b ($J \cdot g \cdot mg^{-1}$) and A ($L \cdot mg^{-1}$) are the Temkin isotherm constants [128, 145]. The Langmuir model assumes monolayer adsorption onto a homogeneous surface with no interactions between the adsorbed molecules, while the other models are empirical or semi-empirical equations, which are often used to describe heterogeneous sorption processes.

Almost all the isotherm models reproduced the adsorption data well, except the Freundlich equation (Figure 6-1b). The best-fit model parameters are also listed in Table 6-1. Fittings of the Langmuir-Freundlich and Redlich-Peterson (R^2=0.994) matched the experimental data better than other models, indicating that the interaction between P and the biochar could be affected by both the Langmuir and the Freundlich processes.

This result is consistent with the kinetics study results that the sorption of P on the engineered biochar could be govern by multiple mechanisms.

Adsorption/Desorption Mechanisms

In previous studies of P sorption on MgO-biochar nanocomposites prepared from anaerobically digested biomass, the interaction was mainly attributed to the surface deposition mechanism between P ions and the MgO particles on carbon surfaces within the matrix [145]. Because surfaces of the engineered biochar used in this study were dominated by both $Mg(OH)_2$ and MgO particles [162], the P sorption mechanism could be different from previous studies. In this study, the XRD spectra of the post-sorption biochar (i.e., P-laden biochar) showed strong signals of not only the pre-exist Mg oxyhydroxides but also new Mg-P crystals in the forms of $MgHPO_4$ and $Mg(H_2PO_4)_2$ with calculated particle sizes of 30.3 nm and 32.4 nm respectively (Figure 6-3). This suggested that, in addition to surface deposition mechanism as reported previously, precipitation of P by Mg released from the engineered biochar could also play an important role in the P removal from aqueous solutions. The SEM-EDX analysis confirmed the formation of the new Mg-P crystals within the biochar matrix (Figure 6-4). As shown in the SEM image, the post-sorption biochar showed clusters of nanosized Mg-P flakes on the carbon surface, which were not observed in the original biochar samples.

The precipitation of P on the biochar was further confirmed by XPS analysis (Figure 6-5). The Mg 1s spectrum (Figure 6-5a) clearly demonstrates the presences of four compounds on the P-laden biochar surface [177]. The molar percentage of Mg oxyhydroxides, $MgHPO_4$, and $Mg(H_2PO_4)_2$ on the biochar surface were around 21.9%, 25.8% and 52.3%, respectively. The Mg oxyhydroxides on the carbon surface

decreased dramatically after the sorption, because they reacted with the P ions to form the Mg-P precipitates. Although both MgO and $Mg(OH)_2$ have low solubility, the presence of P anions in the solution may facilitate their dissolution to form more insolubility of P salt, such as $Mg(H_2PO_4)_2$ and $MgHPO_4$. The newly formed P salts prefer to nucleate and grow on the carbon surface within the biochar because of lower surface energy [178], which often can be confirmed by examining morphology and crystallization of the salt particles. In this study, the nanoplatelet particles on the original biochar surface [162], which is a common structural morphology of Mg hydroxide, were converted into nanorods growing in bunches after P sorption experiment [179, 180]. The significant altering in morphology of nanoparticles before and after P sorption suggests that precipitation played an important role in P removal by the engineered biochar produced from Mg-enriched plant tissues.

It is interesting to draw attention to the XPS spectrum of P 2p3/2 on the surface of the P-laden biochar (Figure 6-5b). The binding energies of P 2p3/2 peak represent three compounds. The binding energy at 132.3 eV corresponds to $MgHPO_4$ (11.2%), while that at 135.2 eV to $Mg(H_2PO_4)_2$ (24.8%) [181, 182]. The molar ratio between $MgHPO_4$ and $Mg(H_2PO_4)_2$ is 0.45, which is similar to that of the XPS analysis of Mg 1s (0.49). The most intense component at a high binding energy of 138.16 eV associated with the presence of P analog (64.0%) in which there is no reaction between P anions and metallic cations. Therefore, the extremely high content of PO_4 analog can be attributed to the surface deposition mechanisms. In addition to the interaction between P and MgO particles as reported in our previous studies, the other three Mg salts including the two precipitates can also adsorb additional P analog by hydrogen bonding

[183-185]. The number of the additional P overlayers should be around two layers presumed from the fitting XPS spectrum of P 2p3/2. Findings from the XPS analysis of P 2p3/2 on post-sorption biochar indicated that, in addition to precipitation, surface deposition could also play an important role in controlling the adsorption of P on the engineered biochar.

In summary, findings from the sorption experiments and post-sorption characterizations indicated that the removal of P by the engineered biochar from Mg-enriched tomato tissues is mainly controlled by both the precipitation (strong chemical bond) and surface deposition (weak chemical bond) mechanisms (Figure 6-6). Because the majority of the P (64%) in post-sorption biochar is deposited on the Mg surface with the carbon matrix through weak chemical bonds, it may be bioavailable through desorption processes (Figure 6-6), when the exhausted biochar is applied to soils as amendment. Hence, the spent biochar may have the potential to serve as a P-fertilizer and improve soil fertility.

P Desorption from P-Laden Biochar as A Slow-Release Fertilizer.

To assess the bioavailability of P, the extractable P content of the post-sorption (P-laden) biochar was determined with the Mehlich 3 method, which is widely accepted laboratory index of plant-available P in soil. Results showed that the extractable P of the exhausted biochar was around 7555.5±10.5 mg $P \cdot kg^{-1}$, much higher than that of optimum P in soil for plant growth and crop yields, i.e. 45-50 mg $P \cdot kg^{-1}$ [186]. About 19% of total P in post-sorption biochar was Mehlich3 extractable which is consistent with findings of published studies [187]. This result suggest a high feasibility of using the engineered biochar to treat and reclaim P from wastewater and then applied the P-

laden biochar directly to soil as a fertilizer for eco-friendly and sustainable production of crops.

Desorption kinetics study of the P-laden biochar showed the slow release of the P and the equilibrium was reached after 30 hrs (Figure 6-7a). Based on the adsorption/desorption mechanisms (Figure 6-6), two layers of P are adsorbed on the biochar through weak chemical bonds (e.g., hydrogen and electrostatic bonds). Thus, desorption of the P in the two layers from the biochar can be described by the second-order kinetics:

$$\frac{dC_t}{dt} = k_{ds}(C_e - C_t) \qquad (6\text{-}3)$$

where k_{ds} is the second order rate constant (L mg^{-1} h^{-1}). The equation was then solved with a zero initial condition for C_t:

$$C_t = \frac{C_e{}^2 k_{ds} t}{C_e k_{ds} t + 1} \qquad (6\text{-}4)$$

Simulations form the equation (4) matched the experimental data well with R^2=0.916 (Table 6-1), confirming that the surface adsorption-desorption mechanism as discussed previously. Because of the strong sorption of P on the Mg surface, only small amount of P was released into the solution at equilibrium. As shown in Figure 6-7b, however, this release was repeatable when fresh solution was introduced to the system (to mimic conditions under plant growth – which depletes released P). During the 11 successive slow releasing experiments, about same amount of P (3.2% of total adsorbed P) was released at each run, indicating the exhaust biochar could be used as a slow-P-release fertilizer when applied to soils. In addition, the TGA analysis showed that the P-laden biochar has similar thermal stability to that of the original sample

(Figure 6-8), suggesting that, in addition to be a P-fertilizer, the poste-sorption biochar could also be used as a carbon sequester.

Seeds Germination and Early Stage Seedling Growth Bioassay

Bioassay of seeds germination and early stage seedlings growth is a simple and commonly used ecotoxicological test for evaluating the impact of biochar amendment on crop growth [188]. The assay results in this work showed that the P-laden biochar nanocomposite could promote seed germination. The addition of the biochar increased seed germination rate from 53% to 85% and the results are statistically significant ($p < 0.001$). After 13-day growth, the length of the grasses with biochar addition was much longer than that in control groups (Figure 6-9). Furthermore, leaves of the grasses from the biochar groups were greener and stronger. These results were consistent with findings in the literature that sufficient supply of phosphorus may not only increase the germination rate but also promote the radicle growth [189]. The assay results further confirmed that the post-sorption, P-laden engineered biochar could be used as a slow-release fertilizer to be applied to soils to improve soil quality and productivity.

Implications

The engineered biochar converted form Mg-enriched tomato tissues showed strong P removal ability. The spent biochar, which is P laden, behaved as a slow-release fertilizer and could release P into aqueous solution in multiple times (mimics slow release P source for plant uptake) to stimulate grass seeds' emergence and growth. The concept and findings form this study can be used to develop new sustainable and eco-friendly strategies to synthesize and apply the engineered biochar to reclaim P, reduce eutrophication, fertilize soils, improve soil quality, and sequester carbon.

Table 6-1. Best-fit parameter values from model simulations of P adsorption kinetics, isotherms and desorption kinetics.

	Parameter 1	Parameter 2	Parameter 3	R^2
Adsorption kinetics				
First-order	k_1 = 0.337 (h^{-1})	q_e = 11.950 ($mg \cdot g^{-1}$)		0.989
Second- order	k_2 = 0.032 ($g \cdot mg^{-1} \cdot h^{-1}$)	q_e = 13.260 ($mg \cdot g^{-1}$)		0.999
n_th-order	k_n = 0.406 ($g^{n-1} \cdot mg^{1-n} \cdot h^{-1}$)	q_e = 12.820 ($mg \cdot g^{-1}$)	n = 1.744	1.000
Elovich	β = 2.390 ($g \cdot mg^{-1}$)	α = 2.538 ($mg \cdot g^{-1} \cdot h^{-1}$)		0.975
Adsorption isotherms				
Langmuir	K = 0.090 ($L \cdot mg^{-1}$)	Q = 116.600 ($mg \cdot g^{-1}$)		0.972
Freundlich	K_f = 21.690 ($mg^{(1-n)} \cdot L^n \cdot g^{-1}$)	n = 0.342		0.850
Langmuir-Freundlich	K_{lf} = 0.023 ($L^n \cdot mg^{-n}$)	Q = 103.800 ($mg \cdot g^{-1}$)	n = 1.749	0.991
Redlich-Peterson	K_r = 0.015 ($L^n \cdot mg^{-n}$)	a = 7.082 ($L \cdot g^{-1}$)	n= 1.298	0.994
Temkin	b =129.700 ($J \cdot g \cdot mg^{-1}$)	A = 2.008 ($L \cdot mg^{-1}$)		0.912
Desorption kinetics				
Second- order	k_{ds} = 0.126 ($L \cdot mg^{-1} \cdot h^{-1}$)	Ce = 11.740 ($mg \cdot L^{-1}$)		0.916

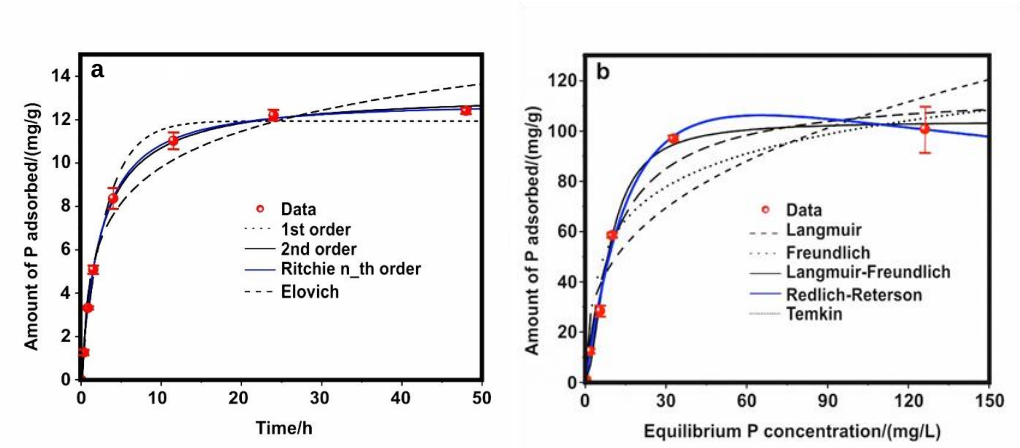

Figure 6-1. Adsorption kinetic (a) and isotherm (b) data and modeling for phosphate on the engineered biochar. Symbols are experimental data and lines are model results.

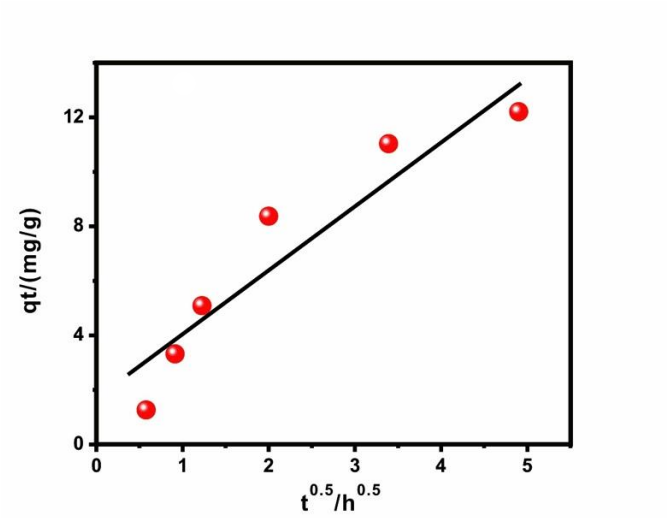

Figure 6-2. Kinetics pre-equilibrium adsorption versus square root of time.

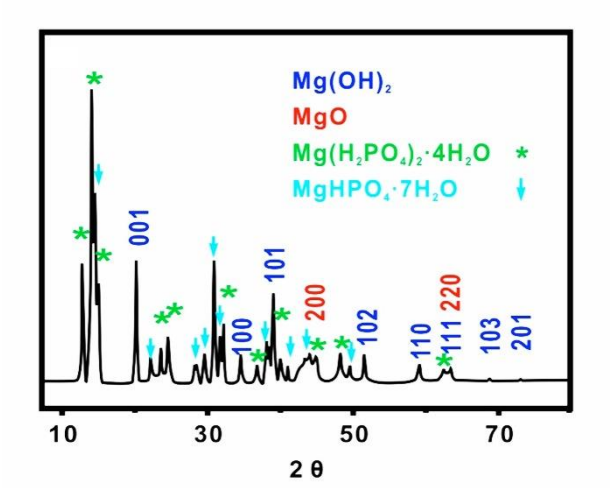

Figure 6-3. XRD spectrum of P-laden biochar.

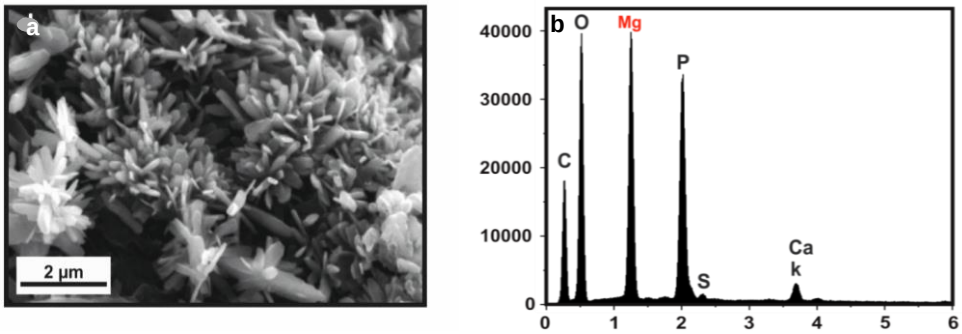

Figure 6-4. SEM image and EDX spectrum of P-laden biochar morphological structures.

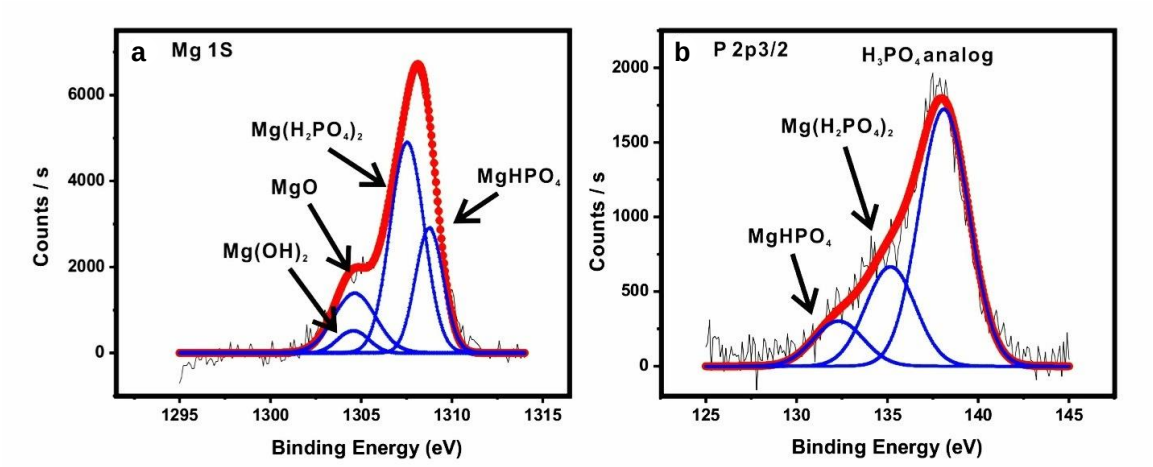

Figure 6-5. XPS spectra of the Mg 1s (a) and P 2p3/2 (b) region for P-laden biochar.

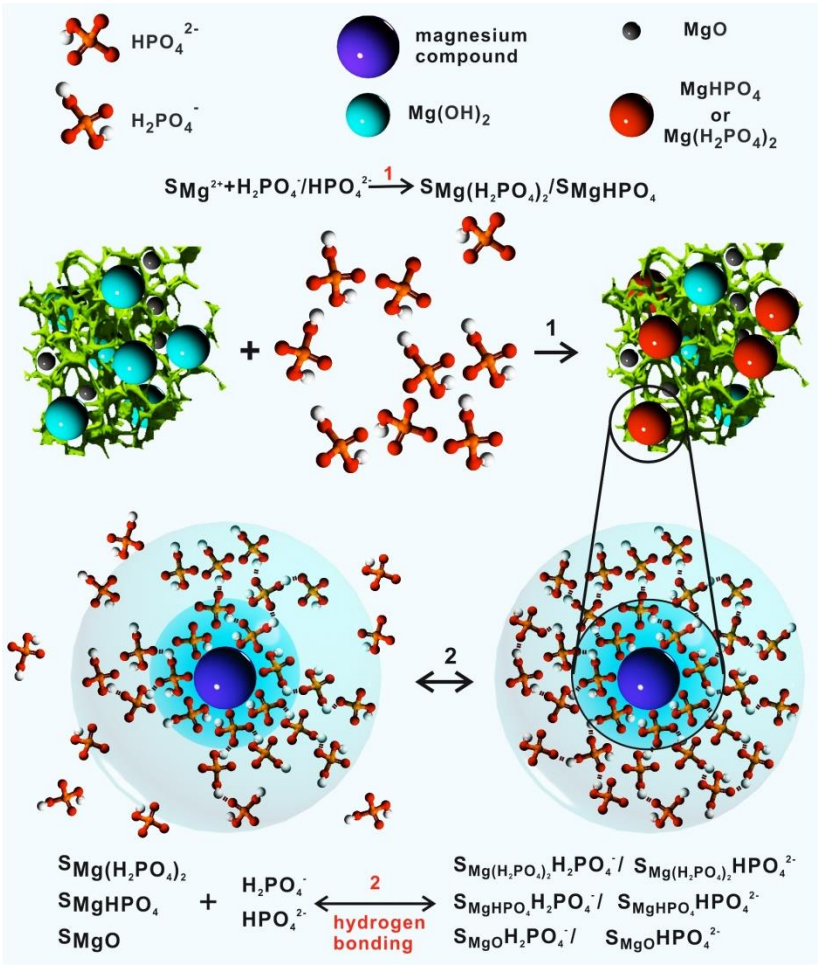

Figure 6-6. Illustration scheme of adsorption and desorption mechanisms of P on the engineered biochar surface (S).

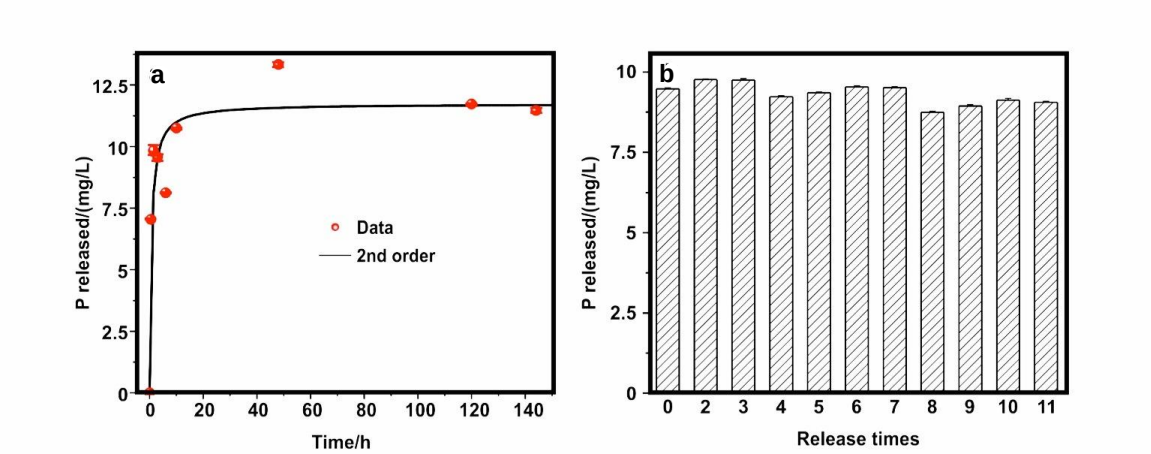

Figure 6-7. (a) Desorption kinetics, symbols are experimental data and the line is model results. (b) Successive and repeatable release of phosphate by P-laden biochar as each time fresh solution was introduced to the system to mimic conditions under plant growth.

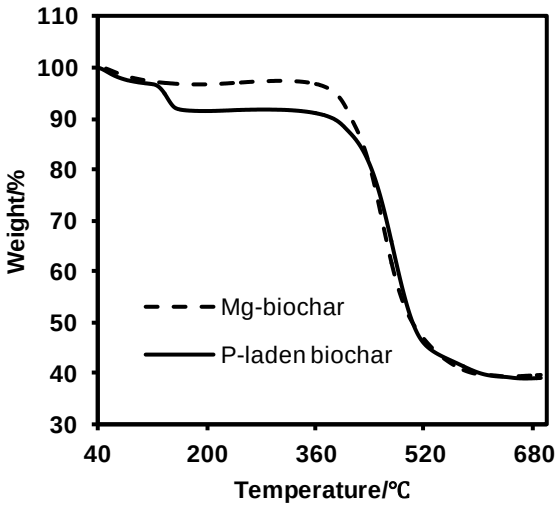

Figure 6-8. TGA curve of P-laden biochar.

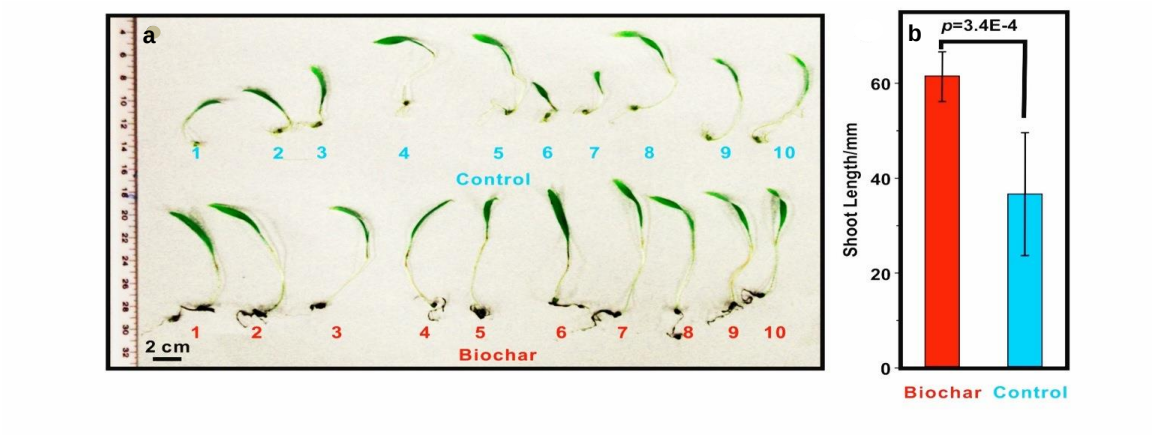

Figure 6-9. Comparison of grass seedlings between P-laden biochar and control groups.

CHAPTER 7
ADSORPTION OF SULFAMETHOXAZOLE ON BIOCHAR AND ITS IMPACT ON RECLAIMED WATER IRRIGATION[1]

Introduction

Water stress and scarcity resulting from rapid population growth, global climate change, and pollution is among the greatest environmental problems today [49]. In the past decade, freshwater consumption by agriculture had been rising due not only to water-thirsty vegetables and meat, but also to the increase in biofuel crops [50]. Reclaimed water has been used for both agricultural and landscape irrigation to satisfy this demand. Globally, about 20 million ha of land is now irrigated with reclaimed water and this has become a key strategy in fighting water shortages [190, 191].

However, the benefits and hazards associated with the application of reclaimed water must be considered. On one hand, reclaimed water typically contains some nutrient elements, such as nitrogen, so its application to agricultural fields may bring additional benefit to soil and crop systems and reduce the need for fertilizer application [53]. On the other hand, reclaimed-water irrigation may also pose environmental risks by introducing various pollutants, including organic pollutants and heavy metals, to irrigated soils and the underlying groundwater [192]. Another major concern with irrigation and direct injection of reclaimed-water is that active/infective human enteric viruses and bacteria might be delivered with the reclaimed-water to the subsurface environment [193-195]. Pharmaceutical residues, which are recognized emerging contaminants, are frequently detected in the discharge of treated effluent from

[1] Reprinted with permission from Yao, Y.; Gao, B.; Chen, H.; Jiang, L.; Inyang, M.; Zimmerman, A. R.; Cao, X.; Yang, L.; Xue, Y.; Li, H., Adsorption of sulfamethoxazole on biochar and its impact on reclaimed water irrigation. Journal of Hazardous Materials 2012, 209, 408-413.

wastewater treatment plants (WWTP) [55]. Various technologies including physical (e.g., filtration), chemical (e.g., chlorination), and biological (e.g., activated sludge) methods have been developed and applied in WWTP [196]. However, most of the wastewater treatment methods, except member filtration technologies (e.g., Nanofilitration and Reverse Osmosis), cannot completely remove pharmaceuticals in the effluent [196]. Occurrences of pharmaceuticals in treated wastewater, surface water, and groundwater have been reported worldwide [55, 57, 58, 197]. In a field study of pharmaceuticals in soil irrigated with treated urban wastewater, Furlong et al [59] found that reclaimed-water irrigation resulted in leaching of pharmaceuticals, such as erythromycin, carbamazepine, and fluoxetine, through the vadose zone to contaminate groundwater. Soil and groundwater contaminations by reclaimed-water irrigation in agriculture caused by pharmaceuticals, such as antibiotics and hormones, have also been demonstrated in several other studies [60, 192, 197].

Sulfamethoxazole (SMX) is one of the most frequently detected pharmaceuticals in reclaimed water and other environmental samples [59, 197]. As a sulfonamide bacteriostatic antibiotic, SMX is extensively used for treatment and prevention of both human and animal diseases [198]. It has been ubiquitously found in the high ng/L range in discharges from WWTP and in the low ng/L range in rivers and groundwater [199]. SMX is characterized as relatively unreactive to soil surfaces and shows high mobility in soils [200]. If released into aquatic systems through discharges from WWTP, SMX may have toxic effects on aquatic organisms and also may induce drug resistance in pathogens [201, 202]. Occurrences of SMX in groundwater have been reported in the U.S. and other countries [60, 197, 203], so it is important to limit SMX leaching through

the vadose zone during reclaimed-water irrigation. As suggested by Munoz et al. [197], there is a critical need to develop new methods or technologies for reclaimed-water irrigation in agriculture to reduce the contamination risk of pharmaceuticals, particularly with respect to SMX.

Recent development in biochar technology may provide such an opportunity to reduce the risk of pharmaceutical contamination of groundwater from reclaimed-water irrigation. Biochar, sometimes called agrichar, is a charcoal derived from the thermal decomposition of carbon-rich biomass. When biochar is used in agriculture as a soil amendment, it can effectively increase soil fertility and create a carbon sink to mitigate global warming [67, 77, 204]. In addition, a number of investigations have also revealed biochar's potential to be a low-cost adsorbent to control pollutant migration in soils [205, 206]. Biochar converted from agricultural residues has demonstrated strong sorption ability for a variety of contaminants through various mechanisms [8, 207, 208]. Previous studies have showed that biochar has strong affinities for soil organic matters and organic pollutants such as phenanthrene (PHE), phenols, polycyclic aromatic hydrocarbons (PAHs), and polychlorinated biphenyls (PCBs) [8, 10]. Although pharmaceuticals are emerging organic contaminants, very little research, if any, has been conducted to investigate the ability of biochar to remove pharmaceuticals from water. If shown to have sufficient sorption ability for pharmaceuticals such as SMX, biochar amendment could limit pharmaceuticals leaching from soil into groundwater or surface water in addition to improving soil fertility and carbon sequestration. This would increase the safety and feasibility of using reclaimed water for agricultural and landscape irrigation.

The overarching objective of this work was to develop a new technology to reduce the contamination risk of reclaimed-water irrigation. It is our central hypothesis that biochar, when amended in soils irrigated with reclaimed water, can sorb pharmaceutical contaminants to protect the soils and groundwater. To test this hypothesis and achieve the overarching objective, a series of laboratory experiments were conducted to study the adsorption of SMX, a common pharmaceutical contaminant in reclaimed water, on biochar and its impact on reclaimed-water irrigation. The specific objectives were to: (1) test the ability of different types of biochar to sorb aqueous SMX; (2) determine the leaching and retention of SMX in simulated reclaimed water through soils amended with selected biochar; and (3) evaluate the effect of SMX-laden biochar on the growth of *E. coli*.

Materials and Methods

Materials

A total of 8 biochar samples were produced from four commonly used feedstock materials: bamboo (BB), Brazilian pepper wood (BP), sugarcane bagasse (BG), and hickory wood (HW). The raw materials were converted into biochar through slow pyrolysis inside a furnace (Olympic 1823HE) in a N_2 environment at temperatures of 450 and 600˚C. The resulted biochar samples are here referred as BB450, BB600, BP450, BP600, BG450, BG600, HW450, and HW600. The biochar samples were then crushed and sieved yielding a uniform 0.5-1 mm size fraction. After washing with deionized (DI) water for several times to remove impurities, such as ash, the biochar samples were oven dried (80˚C) and sealed in a container for later use. Detailed information about biochar production procedures can be found in a previously published study [209].

Sandy soil was collected from an agricultural station at the University of Florida in Gainesville, FL. The soil was sieved through a 1mm mesh (No. 18) and dried (60˚C) in an oven overnight and sealed in a container prior to use. Basic properties of the soil can be found in the Supporting Information (Table S1).

Sulfamethoxazole (SMX, ACS 732-46-6) was purchased from Applichem (Germany). The physicochemical properties of SMX are summarized in the Supporting Information (Table S2). All the other chemicals were analytical reagents supplied by Fisher Scientific. Artificial reclaimed water was synthesized to simulate a typical Florida conserve II reclaimed water and its major element chemical composition can be found in the Supporting Information (Table S3) [53, 210].

Characterization of Sorbents

A range of physicochemical properties of the biochar samples were determined. The pH was measured using a biochar to deionized (DI) water mass ratio of 1:20 followed by shaking and an equilibration time of 5 minutes before measurement with a pH meter (Fisher Scientific Accumet Basic AB15). Elemental C, H, and N abundances were determined using a CHN Elemental Analyzer (Carlo-Erba NA-1500) via high-temperature catalyzed combustion followed by infrared detection of the resulting CO_2, H_2 and NO_2 gases, respectively [67]. Major inorganic elements were determined using the APHA standard method of acid digesting the samples for multi-elemental analysis by inductively-coupled plasma emission spectroscopy (ICP-AES) [211]. The surface area of the biochar was determined on Micromeretics Autosorb1 and using the Brunauer-Emmett-Teller (BET) method in the 0.01 to 0.3 relative pressure range of the N_2 sorption isotherm [212].

Sorption of SMX

Batch sorption experiments were conducted to compare the sorption of SMX by the eight biochar samples in 68 mL digestion vessels (Environmental Express) at room temperature (22 ± 0.5 ˚C). Approximately 0.1 g of each biochar sample (accurately weighted) was added into the vessels and mixed with 50 mL 10 mg/L SMX solution in DI water. To show the effectiveness of the sorbents, the concentration of SMX solution used in this work (mg/L) was much higher than that in real environmental samples (i.e., μg/L or ng/L) [57]. This approach has been successfully used in several studies to examine the sorption of SMX on various sorbents [57, 213, 214]. The mixtures were shaken at 55 rpm in a mechanical shaker for 24 h, and the vials were then withdrawn. Vessels without either biochar or SMX were included as experimental controls. Following the sorption period, the mixtures were filtered through 0.22 μm nylon membrane filters (GE cellulose nylon membrane) and the pH of the supernatant was measured. The concentration of SMX in the supernatant was measured with a dual beam UV/VIS spectrophotometer (Thermo Scientific, EVO 60) [215]. The SMX detection wavelengths were set at 280 nm (BB450, BP450), 267 nm (BB600, BP600, BG600, HW450 and HW600), and 290 nm (BG450) to minimize the effect of background absorbance and the detection limit was about 0.1 mg/L. The pH of the standard solutions was adjusted to match that of each supernatant and the correlation coefficients (r^2) for all the spectrophotometric standard curves were higher than or equal to 0.999. Sorbed SMX concentration was calculated based on the difference between initial and final aqueous SMX concentration. Solid-water distribution coefficients (K_d), defined as the ratio between adsorbed concentration on solid phase divided by the

equilibrium concentration in solution, were used to compare the SMX sorption abilities of the various biochar types.

All the experimental treatments were performed in duplicate and the average values are reported. Additional analyses were conducted whenever two measurements showed a difference larger than 5%.

Transport of SMX in Reclaimed Water through Soil Columns

Two biochar samples, BG450 and BB450, were selected to study their effect on SMX retention and transport in combination with soil. Simulated reclaimed water spiked with SMX was applied to laboratory soil columns to simulate reclaimed-water irrigation. The soil columns were made of acrylic cylinders measuring 16.5 cm in height and 4.0 cm in internal diameter, and the bottom of the columns were covered with a stainless steel mesh with 60 μm pore size to prevent soil loss. The sandy soil with or without biochar was wet-packed into the column following the procedures reported by Tian et al. [216]. Three types of soil columns, in duplicate, were used: (1) soil amended with 2% BB450 (by weight), (2) soil amended with 2% BG450 (by weight), and (3) soil with no biochar. The total amount of soil or biochar-amended soil in the columns was a uniform 200 g. About one pore-volume of artificial reclaimed wastewater (i.e., 51 mL) was first poured into the soil columns each day for two days to precondition the column. On days 3 and 4, same amount of reclaimed wastewater spiked with 2 mg/L SMX was applied to the soil columns. After that, the columns were flushed with one pore-volume SMX-free reclaimed water each day for another five days. The leaching process in each day took less than an hour, and all the leachate samples were collected from the outlet at the bottom of the columns and immediately filtered through 0.22 μm filters for further analyses.

Reverse phase high-performance liquid chromatography (HPLC, Waters 2695, Milford, MA) equipped with a Phenomenex Gemini C18 column (150 mm × 4.6 mm I.D., 5 µm) at room temperature was used to determine SMX concentration in the leachate samples. A Waters 2489 ultraviolet detector was used to detect SMX at a wavelength of 270 nm. The SMX detection limit of this method was 20 µg/L and the working range was 50–1000 µg/L with linear correlation coefficients $R^2 > 0.99$.

TCLP Extraction

The toxicity characteristic leaching procedure (TCLP) was applied to the soil and soil-biochar mixtures following column experiments and entails extracting the adsorbed SMX following the USEPA Method 1311 [217]. The TCLP has been used to determine the mobility and bioavailability of both organic and inorganic contaminants in soils [206]. Soil was removed from the columns and air-dried and homogenized after the transport experiments. Extraction fluid of the TCLP was prepared by adding 5.7 ml glacial acetic acid and 64.3 ml of 1N NaOH separately into 500 ml reagent water and then diluting to a volume of 1L. The pH of the extraction fluid was 4.9. Solid-phase samples were then mixed with the extraction fluid at a weight ratio of 1:20, respectively, in standard extraction vessels. The vessels were shaken for 18 h at room temperature and the liquid component was separated from solid phases by filtering through 0.7 µm pore size borosilicate glass fiber filters. The filtrates were analyzed for SMX concentration by HPLC as described previously. Three independent extraction experiments were conducted for each soil sample and a one-way ANOVA test with a significance level of 0.05 ($p<0.05$) was used to check for differences between treatments.

Growth Inhibition

To obtain SMX-laden biochar for the growth inhibition experiments, 0.1 g of BB450 or BG450 was mixed with 50 mL SMX solution of three different concentrations (20, 30, and 50 mg/L) and the mixture was shaken for 24 hr. After filtration, SMX-laden biochar samples were collected and oven dried at 80 ^{o}C. The SMX-laden biochar was labeled as BB450S20, BB450S30, BB450S50, BG450S20, BG450S30, and BG450S50 based on the initial SMX concentration.

E. coli DH5α was used in the test and was cultured overnight at 35˚C by constant agitation in a biochemical incubator. Biochar and SMX-laden biochar samples were sterilized in an autoclave to kill native bacteria in the samples. Pre-experiment comparing the growth inhibition effects of SMX and sterilized SMX showed the autoclave treatment had no effect on the antibiotic properties of SMX because of its good thermal stability as reported in the literature [218, 219]. 83 mg BG450S20 and BB450S20, 56 mg BG450S30 and BB450S30, and 33 mg BG450S50 and BB450S50 were then added to 5 mL fresh nutrient broth medium to test their effect on bacterial growth. The amount of the adsorbed SMX in each of BG treatments was around 0.15 mg, which was much higher than that of BB treatments (0.10 mg each). SMX-free biochar (33 mg) and blank controls without biochar were also included in the experiment. The pour-plate method was used to enumerate *E. coli* following APHA standard procedures [211]. Briefly, 0.5 ml of the diluted *E. coli* sample was placed on the center of a sterile petri dish (100 mm diameter) using a sterile pipette. Sterile, molten plate count agar (45 to 50°C) including biochar and SMX-laden biochar or blank controls was added and mixed with the sample by swirling the plate. The mixture was allowed to cool at room temperature until solidified and then were incubated

(SenxinGRP-9160, Shanghai, China) at 35°C for 48 hrs. Colonies in the medium were counted to determine bacterial concentration following the standard procedures [211]. The growth experiments were repeated six times for all tested samples and results were statistically analyzed with the t-test and one-way ANOVA with a significance level of 0.05 ($p < 0.05$).

Results and Discussion

Biochar Properties

CHN analysis indicated that all the eight biochar samples prepared and used in this work were carbon rich and contained 75.6-83.6% carbon (Table 7-1), which is typical of pyrolyzed biomass [67, 208]. The oxygen and hydrogen contents of all the samples ranged 11.5-18.1% and 2.2-3.6%, respectively, some of which are likely as surface functional groups, which are commonly found on biochar surfaces [208]. The biochar samples contained relatively small amount of nitrogen (0.1-0.9%), but most of those values are still much higher than that of most of the natural soils in the US [220]. Element analysis showed that all the biochar samples had relatively low levels of phosphorous and metal elements, except the two BP biochar had more than 2% of Calcium (Table 7-1).

Measurements of the pH indicated that all the biochar were alkaline (8.04-9.67) (Table 7-1), suggesting that they could be used as amendments to reduce soil acidity. The BET surface area measurements showed that biochar produced at 450 ^{o}C had very low surface areas (0.7-13.6 m^2/g), which is common for low-temperature wood and grass biochar (Table 7-1) [87]. When the pyrolytic temperature increased to 600 ^{o}C, the surface area of the biochar increased dramatically to 243.7-401.0 m^2/g. Strong positive

correlation between N_2-measured surface area and pyrolytic temperature was also observed in several previous biochar studies [87, 88].

Sorption of SMX

All the tested biochar showed certain ability to remove aqueous SMX. The solid-water distribution coefficient (K_d) of the biochar ranged 2-104 L/kg with HW450 having the lowest sorption ability (Figure 6-1). The BG biochar had the highest K_d values of 104 and 94 L/kg for BG450 and BG600, respectively. Other than for the biochar made from HW, biochar made at 450 ^oC showed better adsorption ability than the 600 ^oC biochar. This contrasts with the findings of Kasozi et al [8] showing an increase in biochar sorption of catechol with increasing combustion temperature but similar to the same study in their finding that grass biochar sorb catechol to a greater extent than hard wood biochar. Because biochar made at lower temperature may contain more surface functional groups than that prepared at a higher temperature [87, 221, 222], the higher sorption of SMX onto lower temperature biochar suggests that surface function groups on biochar may play a more important role in interactions between SMX and biochar than other factors such as surface area or hydrophobicity. Previous studies have indicated that, in soil, SMX has very small K_d values (0.6-3.1 L/kg) and is highly mobile [200, 214]. The K_d values of seven out of eight biochar used in this work were an order of magnitude greater than that of soils, suggesting that those biochar, when amended in soils, can reduce the mobility of SMX in the soil matrix.

Transport in Soil Columns

Two types of biochar, BG450 (K_d= 104 L/kg) and BB450 (K_d= 64 L/kg), which had relatively high sorption ability for SMX, were used in the column experiments. As expected, both biochar reduced the transport of SMX in reclaimed water through the

soils (Figure 7-2). When the SMX-free artificial reclaimed water was added to the soil columns, there was no detectable SMX in all the leachate, suggesting no background SMX in the soil or biochar-soil mixtures (Figure 7-2). Although the SMX-spiked reclaimed water was added to the columns on day-3, SMX was not detected immediately as the solution simply replaced the soil pore water. SMX was detected in all column leachates on day-4, but the breakthrough concentration of SMX in BG450-(5 µg/L) and BB450-(54 µg/L) amended columns were several orders lower than that of the unamended soil columns (329 µg/L). The breakthrough concentration of SMX in the unamended soil on day-5 was the highest (819 µg/L), and was more than 40% of the input concentration (i.e., 2 mg/L). The average peak breakthrough concentrations of the SMX in the biochar-amended soil columns were much lower (i.e., 139 and 25 µg/L for BB450-and BG450-amended soil columns). The BG450-amended soil columns had the lowest SMX breakthrough concentration, which was consistent with the results obtained from the sorption experiments. When the SMX-free reclaimed water was used to flush the columns on day-6, the SMX concentration of all leachates decreased (Figure 7-2). Compared to the biochar-amended columns, however, the unamended soil columns still showed much higher SMX breakthrough concentration. Mass balance calculation indicated that more than 60% of the SMX in the reclaimed water was transported through the unamended soil column by the end of the experiment, confirming that SMX has a high mobility in soils. The transport of SMX in the biochar-amended soil columns, however, was much lower, with only about 15% and 2% of the SMX in the reclaimed water transported through the soil columns amended with BB450 and BG450, respectively. The leaching column experimental results suggest that biochar can be

used as an amendment in agricultural soils irrigated with reclaimed water to adsorb SMX and to limit its mobility in the vadose zone, thus protecting groundwater quality.

TCLP Extraction

Although there was much more SMX retained by the biochar-amended soils, the TCLP-extractable SMX levels in the biochar-amended soils was significantly less than that of the unamended soils (Figure 7-3) with the one-way ANOVA analysis showing the differences among the tested samples was statistically significant ($p = 0.028$). The average SMX concentration in the TCLP extraction from the two biochar-amended soils was only about 76% (BB450) and 14% (BG450) of that from the unamended soils. This result suggests that, in addition to reducing SMX mobility in soil, the bioavailability of SMX in soils will be reduced by biochar amendment, even if it is highly accumulated in the biochar. The effect of biochar on reducing the mobility and bioavailability of organic contaminants, such as pesticides, in soils was also observed in several recent studies [206, 223, 224]. In a recent study, Cao et al. [206] found that biochar prepared from animal manure could reduce atrazine and lead concentrations in the TCLP extractions by 53-77% and 70-89%, respectively.

Growth Inhibition

The growth response of *E coli* varied among the different samples, but all showed growth of bacterial colonies reaching colony forming units (cfu) on the order of 10^5 to 10^8 cfu/ml (Figure 7-4). The average number of bacteria in the blank control was 4.0×10^8 cfu/mL, which was almost identical to that of the BG450-treated growth media (4.0×10^8 cfu/mL) and was slightly higher than that in BB450 media (3.7×10^8 cfu/mL). The one-way ANOVA analysis showed there were no significant differences in the bacterial growth number among these three treatments ($p = 0.664$), suggesting that the

SMX-free biochar does not have any antibiotic effect on *E coli*. Previous studies showed that biochar amendment can often benefit soil microorganisms by providing them suitable habitats, and additional organic carbon and mineral nutrient sources [86, 225]. The statistical analysis of the bacterial growth numbers among all the nine tested treatments (i.e., one control, two blank biochar, and six SMX-laden biochar); however, showed statistically significant differences ($p = 0.014$). Those results indicated that some of the SMX-laden biochar may inhibit the growth of the bacteria.

Comparisons of treatments of three SMX-laden BB biochar to that of the controls showed that the SMX-laden BB biochar had no inhibition effect on *E. coli* growth ($p = 0.208$). The average *E coli* number in the BB450S30 treated growth medium (4.0×10^8 cfu/mL) was even slightly higher than that in the control and SMX-free BB450 media. The one-way ANOVA analysis of the growth experimental data of the BG biochar, however, indicated that the three of the SMX-laden BG biochar showed statistically significant inhibition of the growth of the bacteria ($p < 0.001$). The average *E coli* numbers in the BG450S20, BG450S30, and BG450S50 treated growth medium were 2.4×10^8, 2.3×10^8, and 2.6×10^8 cfu/ml, respectively. This suggests that high levels of immobilized pharmaceuticals in biochar could cause adverse effect to the microbial population which is important for soil and plant health. When selecting biochar as a soil amendment to reduce the environmental impacts of reclaimed water irrigation, biochar with the highest pharmaceutical sorption abilities may not be the best choice. As shown in this study, although BB450 showed lower sorption ability to SMX, it could be a better amendment than BG450 to soil irrigated with reclaimed water. Because the biochar (BB450) with higher amount of SMX showed slight antibiotic effect on the tested

bacteria, it could potentially affect the indigenous soil microbial community when applied to soils irrigated with reclaimed water. Further investigations are still needed to test the effect of pharmaceutical-laden biochar to the soil ecosystems including the microecosystems.

Implications

Biochar land application has been suggested to be an effective way to sequester carbon as well as improving soil quality [204]. Our results suggest that biochar soil amendment also has the potential to be used as a safeguard against the leaching of pharmaceuticals into surface or ground waters, which is of particular concern during application of reclaimed water to irrigate landscapes and agricultural fields. We found that mobility and bioavailability of SMX in biochar-amended soils were lower than that of unamended soils. Biochar soil amelioration, therefore, should be promoted in areas where reclaimed water or wastewater is used for irrigation. Because high-level accumulation of pharmaceuticals in biochar could cause adverse effect on the indigenous soil microbial community, comprehensive environmental risk assessments are recommended when selecting biochar to amend soils irrigated with reclaimed water.

Table 7-1. Properties and elemental composition of biochar used in this study.

	BET surface area	pH	Elemental composition (%, mass based)											
			C	H	O [a]	N	P	K	Ca	Mg	Zn	Cu	Fe	Al
BB450	10.2	8.70	76.89	3.55	18.10	0.23	0.36	0.35	0.29	0.19	0.01	-[b]	-[b]	0.04
BB600	375.5	8.93	80.89	2.43	14.86	0.15	0.54	0.52	0.34	0.23	0.01	-[b]	-[b]	0.04
BP450	0.7	9.36	75.63	3.59	17.22	0.28	0.08	0.29	2.59	0.26	0.01	-[b]	0.01	0.04
BP600	234.7	9.67	76.99	2.18	17.65	0.10	0.09	0.26	2.42	0.25	0.01	-[b]	0.01	0.04
BG450	13.6	8.95	78.60	3.52	15.45	0.92	0.07	0.25	0.83	0.18	0.01	-[b]	0.06	0.11
BG600	388.3	7.70	77.91	2.42	17.76	0.41	0.08	0.15	0.91	0.21	0.01	-[b]	0.05	0.11
HW450	12.9	8.04	83.62	3.24	11.45	0.17	0.02	0.33	0.92	0.18	0.01	-[b]	0.01	0.06
HW600	401.0	9.36	81.81	2.17	14.02	0.73	0.02	0.24	0.82	0.13	-[b]	-[b]	0.01	0.06

a: Determined by weight difference assumed that the total weight of the samples was made up of the tested elements only. b: < 0.01%.

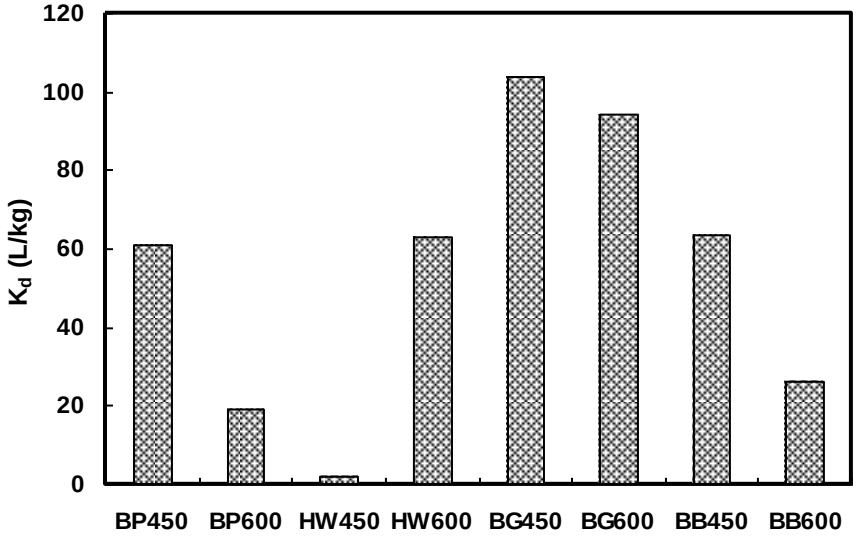

Figure 7-1. The solid-water distribution coefficients (K_d) of SMX adsorption on different types of biochar.

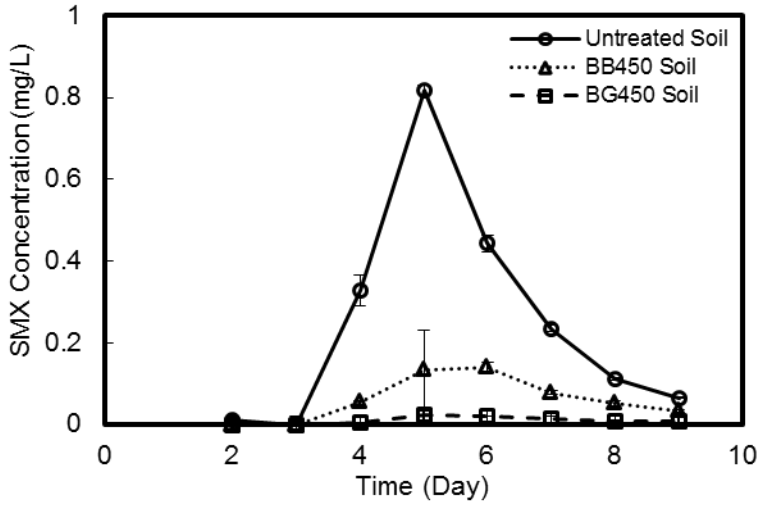

Figure 7-2. Concentration of SMX in simulated reclaimed water leachates transported through biochar-amended and unamended soil columns.

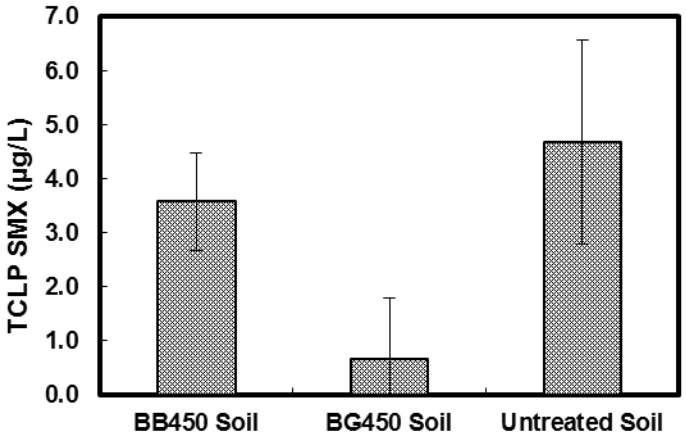

Figure 7-3. Concentration of SMX in TCLP extracts of biochar-amended and unamended soils irrigated with simulated reclaimed water with SMX.

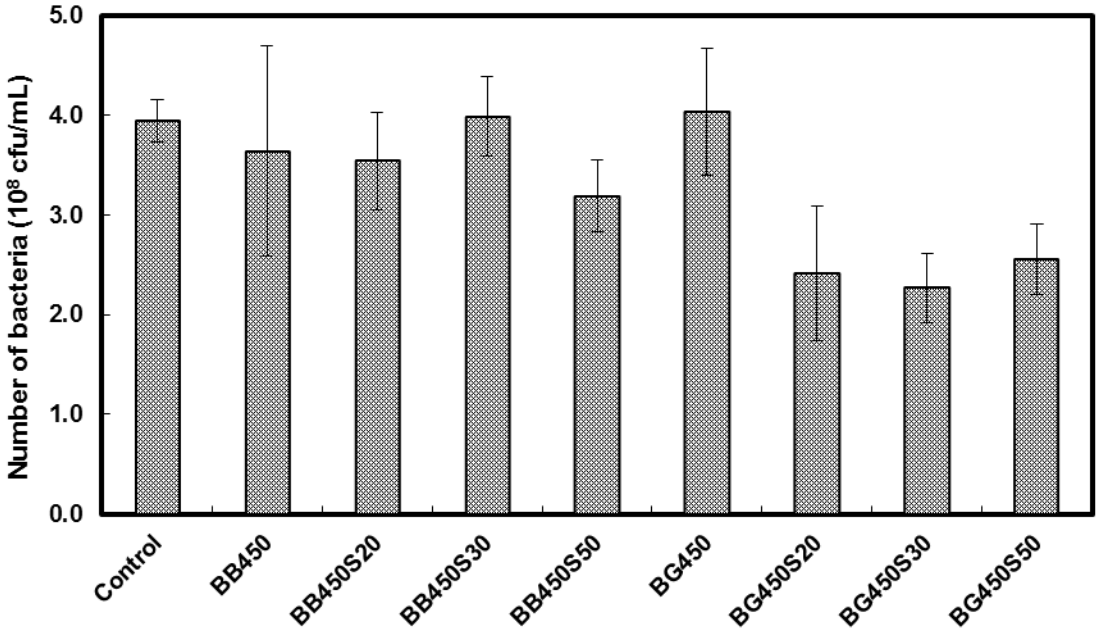

Figure 7-4. Concentration of SMX in TCLP extracts of biochar-amended and unamended soils irrigated with simulated reclaimed water with SMX.

CHAPTER 8
REMOVAL OF METHYLENE BLUE FROM AQUEOUS SOLUTION BY CLAY MODIFIED BIOCHAR

Introduction

Biochar, produced from agricultural and forest residues, has received much attention recently because of its potential application as a soil amendment as well as a carbon fixer to benefit the environment. When it is amended into soils, biochar may improve soil fertility, enhance agricultural productivity, increase soil nutrients and water holding capacity, and reduce emissions of other greenhouse gases [131-133, 170]. Recent studies also suggest that biochar can be used as an alternative low-cost sorbent to remove various contaminants from water [2, 93, 133, 138, 139, 226]. Because the functions of biochar are strongly depending on the properties of the feedstock and the processing method, several engineering methods have been developed to modify biochar and enhance its sorption ability to various contaminants in aqueous solutions [76, 80, 135, 164].

In recent years, clay minerals have been widely used as low-cost materials in various fields such as agriculture, industry engineering, petroleum discovery, and recovery and refining. Important characteristics relating to applications of clay minerals are particle size, surface chemistry, particle shape, surface area, and other physical and chemical properties [227]. Due to their interesting properties of lamellar structure, high surface area, and high ion exchange capacity, clay minerals have great potential to fix various pollutants, such as heavy metals, dyes, and organic compounds [38, 228]. Among the studied clays, montmorillonite and kaolinite as low-cost adsorbents have received considerable recognition. Montmorillonite, expandable-layered silicates, consists of two tetrahedral and one octahedral unit forming a platelet approximately 10

A˚ thick [229]. One important property is that the layers are negatively charged and this negative charge is normally balanced by hydrated cations placed in the interlayer spaces [230]. Kaolinite is a layered silicate mineral, with one tetrahedral sheet linked through oxygen atoms to one octahedral sheet of alumina octahedral. The exchange sites of kaolinite are located on the surface and it has no interlayer exchange sites [231]. High cation exchange capacity and the adsorption properties of both clays may play an effective role in adsorbing inorganic and organic pollutants from aqueous solutions.

Engineered methods such as surface modification have been promoted to create biochar-based materials (i.e., engineered biochars) with enhanced functions for environmental applications [163]. To take advantage of the recent developments of biochar technology and high adsorption capacity of clay, a group of new engineered biochars (i.e., clay-modified biochar) could have the potential to remove various inorganic and organic cationic contaminants as well as improve carbon sequestration, soil fertility and water holding capacity.

More than 7×10^5 tons of industrial dyes are produced annually and over 100,000 commercially available dyes exist, with a considerable fraction being discharged directly into aqueous effluent [71]. Many of these dyes are toxic and even carcinogenic and this poses a serious hazard to aquatic living organisms as well as diminishing the transparency of the water [71, 72]. Adsorption techniques have been widely applied to the dye wastewater treatment. The removal of cationic dyes such as methylene blue (MB) by clays and their interaction have been extensively studied [38, 73]. MB has long been used as a model for the adsorption of organic dyes from

aqueous solution and can be attracted toward the clays' anionic layers and are, therefore, quite suitable for investigating the properties of new engineered carbon in aqueous suspensions [74].

The overarching objective of this work was to develop a low-cost method to produce clay-modified biochar for environmental applications, especially for removal of cationic contaminants (MB) from wastewater. 6 new clay-modified engineered biochar were produced in laboratory through slow pyrolysis of clay (montmorillonite and kaolinite) pretreated biomass (bamboo, bagasse, hickory chips). Physicochemical properties of the clay-modified biochar were characterized and a MB adsorption experiment was conducted. The objectives were as follows: 1) develop a novel approach for preparing low-cost clay-modified engineered carbon, 2) characterize the physicochemical properties of the engineered biochar, and 3) assess the MB removal ability by the clay-modified biochar and the sorption mechanisms.

Materials and Methods

Biochar Production

Montmorillonite (MMT), Kaolin (KLN) and methylene blue ($C_{16}H_{18}ClN_3S$, molecular weight, 319.9 g/mol) were purchased from Southern Clay Products, Inc., Thiele Kaolin Co., and Sigma–Aldrich, respectively.

A stable clay suspension was prepared by adding 2 g Montmorillonite and/or Kaolin powder to 500 ml deionized (DI) water followed by sonication of the mixture for 30 min with ultrasonicator (3510R-DTH, Bransonic Ultrasonics Corporation). The obtained clay suspensions were first modified on the biomass feedstock, bamboo (BB), bagasse (BG), hickory chips (HC), which were milled into powders of ~2 mm prior to use. 10 g of the feedstocks were dipped into the clay suspensions and stirred for 1 hour.

The feedstocks were then separated from the mixture and oven dried at 80 ^{o}C. The clay treated biomass feedstocks were placed in a quartz tube inside a tube furnace (MTI, Richmond, CA) to produce the clay-modified biochars through slow pyrolysis (annealing) in a N_2 environment at temperatures of 600˚C for one hour. Untreated raw materials (bamboo, bagasse, hickory chips) were also used as feedstocks to produce biochars without clay modification in the furnace with the same pyrolysis conditions. The resulting biochar samples were washed with DI water several times to remove impurities, oven dried, and sealed in a container for further testing. The resulting clay-modified and untreated biochar samples were henceforth referred to as BB-MMT, BG-MMT, HC-MMT, BB-KLN, BG-KLN, HC-KLN, BB, BG, HC, respectively.

Characterizations

The N_2 surface areas of the engineered biochar were obtained using NOVA 1200 surface area analyzer. C, H, N analyses were conducted using a CHN Elemental Analyzer (Carlo-Erba NA-1500) via high-temperature catalyzed combustion followed by infrared detection of the resulting CO_2, H_2 and NO_2 gases, respectively. Major elements of biochars were determined by acid digestion of the samples followed by inductively-coupled plasma atomic emission spectroscopy (ICP-AES) analysis. Biochar oxygen contents were determined by a mass balance assuming the total weight of all measured elements sum up to 1. Scanning electron microscope (SEM) imaging analysis of the biochars was conducted using a JEOL JSM-6400 Scanning Microscope. Surface elemental analysis was also conducted simultaneously with the SEM at the same surface locations using energy dispersive X-ray spectroscopy (EDX, Oxford Instruments Link ISIS). X-ray diffraction (XRD) analysis was carried out using a computer-controlled X-ray diffractometer (Philips Electronic Instruments) equipped with a stepping motor and

graphite crystal monochromator. Thermogravimetric analysis (TGA) of biochars was conducted with a Mettler Toledo's TGA/DSC1 analyzer under a stream of air/nitrogen atmosphere, with heating from 30 ^{o}C to 750 ^{o}C (10 ^{o}C/min).

Methylene Blue Sorption

The methylene blue sorption ability of 9 biochars were examined using 68 mL digestion vessels (Environmental Express) at room temperature (22±0.5 ˚C) with a 1:500 (0.1g biochar in 50ml solution) biochar / solution (20 mg/L methylene blue) ratio for 24 h. The samples were withdrawn from a mechanical shaker and immediately filtered through 0.22 µm pore size nylon membrane filters (GE cellulose nylon membrane) to determine adsorbed methylene blue concentrations by inductively-coupled plasma atomic emission spectroscopic (ICP-AES).

Adsorption Kinetics and Isotherm

Adsorption kinetics and isotherm of methylene blue onto BG-MMT were examined using similar method as described above. 20 mg/L methylene blue solutions and time intervals of 5 min, 30 min, 1, 2, 6, 12, 24, 36, and 48 h were used for adsorption kinetics study. Adsorption isotherm was determined with different methylene blue solution concentrations ranging from 1 to 150 mg/L for 48 h. The samples were withdrawn from a mechanical shaker and immediately filtered to determine adsorbed methylene blue concentrations by ICP-AES. All the experimental treatments were performed in duplicate and the average values are reported. Additional analyses were conducted whenever two measurements showed a difference larger than 5%.

Regeneration Experiments

Adsorbent regeneration studies were carried out by using the MB saturated BG-MMT biochar obtained from isotherm experiment after discarding the supernatant dye

solution. The resulted sorbent was then washed three times with DI water for removing non-adsorbed dye, and agitated with 50 ml of 0.50 mol l^{-1} KCl solution for 2 h. The regenerated biochar was separated and oven dried at 80˚C for further MB sorption test with same procedure described above. This sorption-regeneration procedure was repeated for multiple times.

Results and Discussion

Surface Area and Elemental Analysis

All the nine engineered biochars had large surface areas expect HC-KLN (Table 8-1). The order of surface area were as follows: bagasse category > bamboo category > hickory category (Table 8-1). Raw material treated with clays decreased the surface area especially with kaolinite, probably because clays covered the surface pores on the biochars.

CHN analysis indicated that all nine biochar samples prepared and used in this work were carbon rich with carbon content ranging from 70.2~ 83.3% (mass based) (Table 8-1), which is typical of pyrolyzed biomass [67, 208]. The carbon contents of the bagasse-based biochars (i.e., BG-MMT, BG-KLN, BG) were lower than that of bamboo/hickory-based biochars, and they corresponded to their raw materials instead of clay categories, which showed that biochars carbon level wasn't changed by clay modification and raw material type was the determinant. The hydrogen and nitrogen contents of all the samples were comparable with each other and ranged 2.1~ 2.9% and 0.2~ 0.8%, respectively, some of which are likely as surface functional groups, which are commonly found on biochar surfaces [208]. The oxygen contents of biochars from same type of raw material were comparable with each other, while that of kaolinite modified biochars was slightly increased probably owing to high oxygen level in

kaolinite. The level of oxygen in 3 raw material categories was: bagasse > hickory > bamboo, which means biochar oxygen level is based on the raw material type, while clay modification only slightly improve it.

Both montmorillonite and kaolinite are layered silicate minerals, with the chemical composition $(Na,Ca)_{0.33}(Al,Mg)_2(Si_4O_{10})(OH)_2 \cdot nH_2O$ and $Al_2Si_2O_5(OH)_4$, respectively. Hence, modification of the minerals could change the metal contents of the engineered biochars. Element analysis showed that both montmorillonite and kaolinite modification dramatically increased the biochars' aluminum content (Table 8-1), which is a main element of the clays. Also, the iron contents of the clay-modified biochars were higher than that of untreated biochars due to varying amounts of iron element in both clays (Table 8-1). It is consistent with the literature, where Segad et al.[229] indicated that iron is a common substitute in montmorillonite, and Al(III) could be exchanged with Fe(II) and hence get negatively charged, and Mestdagh et al.[232] reported varying amounts of iron can be accommodated within the octahedral sheet of kaolinite. The significantly increased aluminum and iron contents of engineered biochars indicated both montmorillonite and kaolinite were successfully added on the biochars. All other elements contents within the nine biochar samples were relatively low and comparable with each other (Table 8-1).

Thermogravimetric Analysis (TGA) Of Clay-Modified and Untreated Biochars

The TGA analysis under air atmosphere showed that the clay-modified biochars had similar and comparable thermal stability to that of the untreated samples (Figure 8-1a-c). Although the onset decomposition temperatures of the clay-modified biochars for all three types of raw materials were slightly decreased, the new engineered samples were still thermally stable as clay has long been used to improve materials' thermal

properties [233]. In addition, the residues of all the clay-modified biochars were higher than that of untreated samples, with the kaolinite-modified sample's residue slightly higher than that of the montmorillonite-modified one, due to the presence of large amount of silicon within both of the clays. The TGA analysis of the engineered and untreated biochars further confirmed that our clay modification method has successfully combined biochar and clay together and the products have high thermal stability.

In a nitrogen atmosphere, TGA analysis of MMT-modified and untreated bagasse feedstocks was conducted with heating rate of 10 ^{o}C/min from 30 ^{o}C to 600 ^{o}C and staying at 600 ^{o}C for 1 hour to simulate biochar production process. Figure 8-8-2d showed TGA curves were comparable to each other which reveals that the presence of montmorillonite into bagasse feedstocks doesn't alter formation of the char, and slightly increases biochar production rate.

Methylene Blue Removal Ability of Clay-Modified Biochars

The nine biochars' ability to adsorb MB from aqueous solution was tested and the results are shown in Figure 8-2. Generally speaking, the bagasse category biochars had a better MB removal rate than the other two categories, probably due to its large surface area. All three biochars from untreated raw materials (i.e., BB, BG, and HC) showed very low MB removal of about 9.0 ~ 25.6% (Figure 8-2), which is consistent with reported studies [234]. Surface modification with both clays did improve MB adsorption for bagasse and hickory. Especially for bagasse, the montmorillonite modification improved the MB removal rate from 25.6% to 84.3%, while 30.0% for kaolinite modification. This dramatic improvement with clay modification might be because of the large bagasse surface area, which could facilitate clay attachment, and also because of

the superior cationic ion sorption ability of montmorillonite, which has been widely studied [38, 236, 237].

As BG-MMT demonstrated the highest MB removal ability, it was then selected for further investigations including adsorption kinetics and isotherm, and sorption mechanisms.

Adsorption Kinetics

Kinetics and isotherm studies were carried out and a number of well-known sorption models were applied in order to better understand the processes governing the adsorption of MB to the engineered BG-MMT biochar. The kinetics experiment data shows a rapid initial uptake followed by smooth increase, with equilibrium reached in less than 48 h (Figure 8-3). Different mathematical models including pseudo-first-order, pseudo-second order, the Ritchie nth-order, and the Elovich models were used to fit the kinetics data, and the governing equations are

$$\frac{dq_t}{dt} = k_1(q_e - q_t) \quad \text{first-order (8-1a)}$$

$$\frac{dq_t}{dt} = k_2(q_e - q_t)^2 \quad \text{second-order (8-1b)}$$

$$\frac{dq_t}{dt} = k_n(q_e - q_t)^N \quad \text{N\_th-order (8-2c)}$$

$$\frac{dq_t}{dt} = \alpha \exp(-\beta q_t) \quad \text{Elovich (8-3d)}$$

where q_t and q_e are the amount of MB adsorbed at time t and equilibrium, respectively; k_1, k_2, and k_n are adsorption rate constants; α is the initial adsorption rate; and β is the desorption constant. More details can be found in Yao et al.[238]. The best-fit kinetics models parameters are listed in Table 8-1. Among the four kinetic models tested, the Ritchie nth-order and Elovich models fit the experimental data better with coefficients of

determination (R^2) of 0.931 and 0.950, respectively, revealing that MB sorption to the engineered biochar BG-MMT could be controlled by multiple mechanisms.

Previous studies have suggested intraparticle diffusion processes as a dominant mechanism accounting for sorption contaminants on carbon materials [176, 239, 240]. In this study, the linearized plots of Qt vs. $t^{0.5}$ for the adsorption of MB on BG-MMT biochar are shown in Figure 8-3b. The high linear dependency on the square root of time (R^2=0.983) revealed the sorption kinetics of MB on BG-MMT might be strongly affected by the intraparticle diffusion mechanism. The intraparticle diffusion parameter K_{id} is defined as the slope of the plot, which was 0.975 mg $g^{-1}h^{-0.5}$ in this study (Figure 8-3b). On the other hand, the straight line didn't pass through the origin but with a significant intercept of 2.919 mg g^{-1}. This is because of the wide distribution of pore size for the engineered carbon studied [241]. This large intercept indicated the high contribution of the surface sorption in the rate-controlling step, because the intercept of the plot reflects the boundary layer effect (film diffusion) [242]. Hence, the rate-controlling parameter in the study is dominated by both intraparticle and film diffusion mechanisms.

Adsorption isotherms

The adsorption equilibrium isotherm is important for describing how the adsorbate molecules distribute between the liquid and the solid phases under equilibrium state [72]. The isotherm experiment results, as shown in Figure 8-4, indicated montmorillonite modification greatly enhanced the MB sorption ability of the biochar, with maximum MB sorption capacities of more than 10 mg g^{-1} and ~2 mg g^{-1} for BG-MMT and BG, respectively (Figure 8-4). Hence, the clay surface modification method in this study

could be effectively used to promote adsorbent's properties. Besides, four well-known models were used to fit the isotherm experimental data that is essential to practical operation, and the governing equations are [128, 145]

$$q_e = \frac{KQC_e}{1+KC_e} \quad \text{Langmuir (8-2a)}$$

$$q_e = K_f C_e^{\,n} \quad \text{Freundlich (8-2b)}$$

$$q_e = \frac{KQC_e^{\,n}}{1+KC_e^{\,n}} \quad \text{Langmuir-Freundlich (8-2c)}$$

$$q_e = \frac{K_r C_e}{1+aC_e^{\,n}} \quad \text{Redlich-Peterson (8-2d),}$$

where K, K_f, K_{lf}, and K_r represents the four models' coefficient, respectively; Q ($mg \cdot g^{-1}$) denotes the maximum capacity; C_e ($mg \cdot L^{-1}$) is the sorbate concentration at equilibrium; and n and a are constants for Freundlich and Redlich-Peterson models, respectively [128]. See details in Yao et al.[238] All four tested isotherm models fit the experimental data fairly well and the parameters are also shown in Table 8-2. Freundlich and Redlich-Peterson models had slightly better fitting performance than the other two, with R^2 of 0.940 and 0.937, respectively. Hence, MB sorption should be onto a heterogeneous surface, and the process could be governed by multiple mechanisms, which is consistent with kinetics study results.

SEM-EDX and XRD

SEM imaging of the BG-MMT (500 X and 2000X) showed that the biochar surface was widely covered by thin film structures (Figure 8-5a, b). After zooming in at 8997X magnification, the films showed layered surfaces (Figure 8-5c), which is a common montmorillonite structural morphology reported in literatures [243, 244]. The surface coverage with montmorillonite was confirmed by EDX analysis. The spectrum of

EDX of the surface at the same spot with SEM imaging identified extremely high peak of silicon and aluminum, as well as sodium, calcium, magnesium, and iron, all of which are typical of the elemental composition of montmorillonite (Figure 8-5d). The layered montmorillonite on the surface of the engineered biochar could contribute to the lower surface area of the material because it could cover the surface pores, which is consistent with the findings from the N_2 surface area measurement.

XRD analysis of the BG-MMT revealed the presence of mineral crystals. In the spectrum, the four strong peaks at 6.4^o (d = 13.840 Å), 6.9^o (d = 12.803 Å), 19.9^o (d = 4.449 Å) and 35.1^o (d = 2.555 Å) were identified as expansible phyllosilicate, i.e., montmorillonite (Figure 8-6). The XRD result concurs to the SEM-EDX analyses that the surface modification method in the work has successfully added montmorillonite on the surface of biochar, and it is the main reason of biochar's MB adsorption ability enhancement. Quartz (SiO_2), as a common mineral within biochars, were also found in BG-MMT, which is consistent with the EDX results [80].

Regeneration of Exhausted BG-MMT Sorbent

Regeneration study was carried out to evaluate the cyclic performance of BG-MMT as an adsorbent by performing multiple cycle adsorption experiments. At first, the MB adsorption capacity of BG-MMT was 11.26 mg g^{-1}. Multiple cycle dye adsorption revealed that the regenerated biochar continue to adsorb MB after each adsorption-regeneration cycle, with a stable capacity of around 7.90 mg g^{-1} (Figure 8-7), which account for 70.11% of initial capacity. Considering the MB sorption experiment results discussed above, BG and BG-MMT removed 25.60% and 84.33% MB, respectively (Figure 8-2). In other words, BG biochar accounts for 30.35% dye sorption while MMT explains for the remaining 69.65%, which is a perfect match with the regeneration study

results. Hence, biochar itself is capable of the uptake of a small part of MB from solution. However, the process is nonreversible. The mechanism could be explained considering the electrostatic interaction between the surface of the biochar, which is usually negatively charged, with the positively charged MB [141, 245]. Montmorillonite is the main factor for MB uptake (70.11%) which could be desorbed by KCl solution. When also taking into consideration the high CEC of montmorillonite (119 meq/100 g), the adsorption mechanism of montmorillonite could therefore be cation exchange [246-248].

After multiple cycle adsorptions, the BG-MMT material is still stable, which is consistent with TGA results. The sorbent could be regenerated easily by KCl solution and recovered most of its MB removal ability reveals that the BG-MMT provides the potential to be recycled and reused after MB dye adsorption.

Implications

A new engineered biochar with clay modification has been successfully developed. Both biochar and clay are relatively cheap due to their accessibility and abundance compared to activated carbons [230]. Besides its low cost, the clay-modified biochar has much higher sorption ability to cationic dye (MB) than the original char. Due to stability and cycle performance, the engineered biochar has the potential to be regenerated and reused for repeated dye sorption.

Table 8-1. Elemental analysis of biochars produced in this study (mass %)a. BG-MMT, BB-MMT, HC-MMT, BG-KLN, BB-KLN, HC-KLN, BG, BB, HC are biochars produced from clay-modified and untreated feedstocks, respectively.

Sample ID	%, mass based																		
	C	H	N	O	K	Na	Mg	Ca	Cu	Cr	Fe	Al	As	Cd	Ag	P	Mn	Pb	Zn
BB-MMT	83.27	2.26	0.25	12.41	0.33	0.14	0.14	0.21	0.01	-	0.23	0.68	-	-	-	0.08	-	-	0.01
BG-MMT	75.31	2.25	0.75	18.87	0.32	0.13	0.22	0.85	0.01	-	0.47	0.75	-	-	-	0.03	0.01		0.01
HC-MMT	80.93	2.21	0.28	15.14	0.11	0.04	0.19	0.57	0.01	-	0.15	0.32	-	-	-	0.00	0.04	-	0.00
BB-KLN	81.02	2.15	0.25	15.85	0.07	-	0.05	0.19	0.01	-	0.08	0.30	-	-	-	0.03	0.00	-	0.00
BG-KLN	70.20	2.44	0.74	24.44	0.06	-	0.16	0.88	0.02	-	0.46	0.53	-	-	-	0.03	0.05	-	0.00
HC-KLN	78.08	2.11	0.33	18.12	0.05	-	0.18	0.52	0.01	-	0.07	0.51	-	-	-	0.00	0.03	-	0.00
BB	80.89	2.43	0.15	14.86	0.52		0.23	0.34	0.00		0.00	0.04				0.54			0.01
BG	76.45	2.93	0.79	18.32	0.15		0.21	0.91	0.00		0.05	0.11				0.08			0.01
HC	81.81	2.17	0.73	14.02	0.24		0.13	0.82	0.00		0.01	0.06				0.02			0.00

'-' below detection limit.

Table 8-2. Best-fit kinetics and isotherms models parameters for MB adsorption to BG-MMT biochar.

	Parameter 1	Parameter 2	Parameter 3	R^2
Adsorption kinetics				
First-order	k_1 = 0.928 (h^{-1})	q_e = 6.888 ($mg \cdot g^{-1}$)		0.769
Second- order	k_2 = 0.201 ($g \cdot mg^{-1} \cdot h^{-1}$)	q_e = 7.265 ($mg \cdot g^{-1}$)		0.852
n_th-order	k_n = 3.215 ($g^{n-1} \cdot mg^{1-n} \cdot h^{-1}$)	q_e = 9.298 ($mg \cdot g^{-1}$)	n = 5.000	0.931
Elovich	β = 0.872 ($g \cdot mg^{-1}$)	α = 160.019 ($mg \cdot g^{-1} \cdot h^{-1}$)		0.950
Adsorption isotherms				
Langmuir	K = 0.373 ($L \cdot mg^{-1}$)	Q = 11.940 ($mg \cdot g^{-1}$)		0.908
Freundlich	K_f = 5.640 ($mg^{(1-n)} \cdot L^n \cdot g^{-1}$)	n = 0.169		0.940
Langmuir-Freundlich	K_{lf} = 0.494 ($L^n \cdot mg^{-n}$)	Q = 15.000 ($mg \cdot g^{-1}$)	n = 0.449	0.928
Redlich-Peterson	K_r = 3.211 ($L \cdot g^{-1}$)	a = 20.000 ($L^n \cdot mg^{-n}$)	n= 0.852	0.937

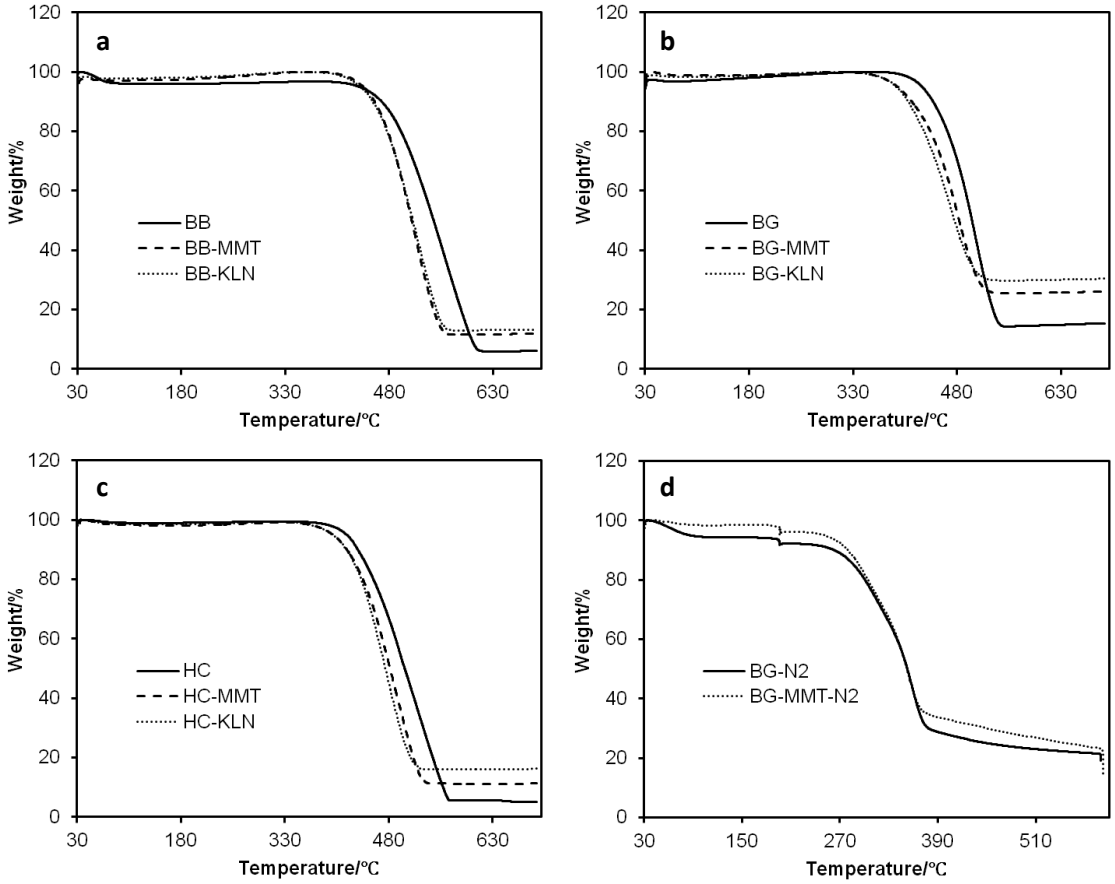

Figure 8-1. TGA curves comparison of clay-modified and untreated biochars under air (a-c) or nitrogen (d) atmosphere.

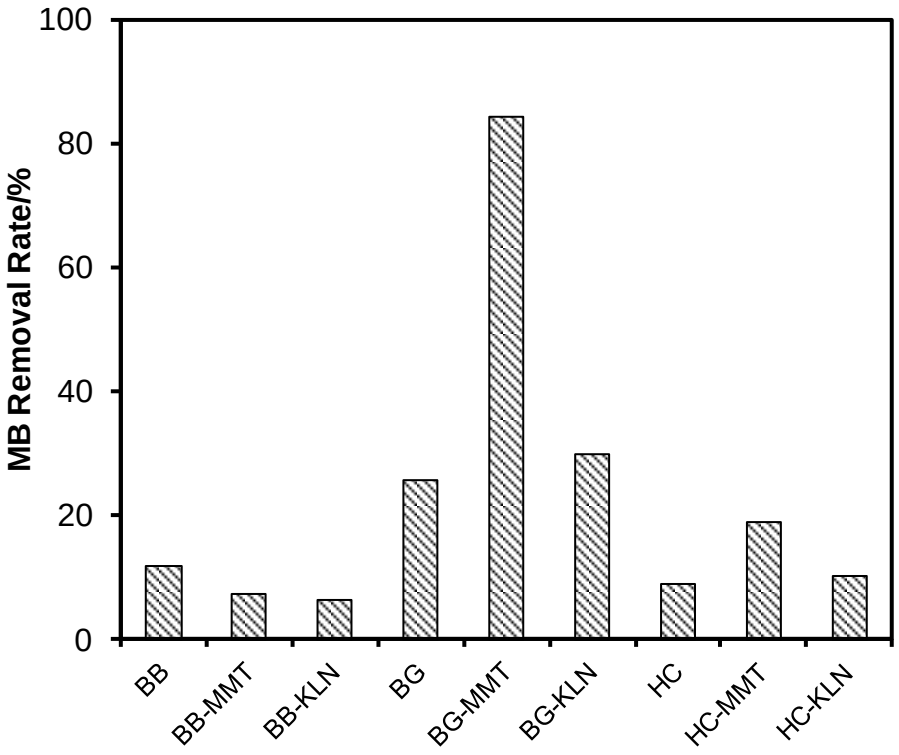

Figure 8-2. Comparison of methylene blue (MB) adsorption ability of nine biochars produced in this study.

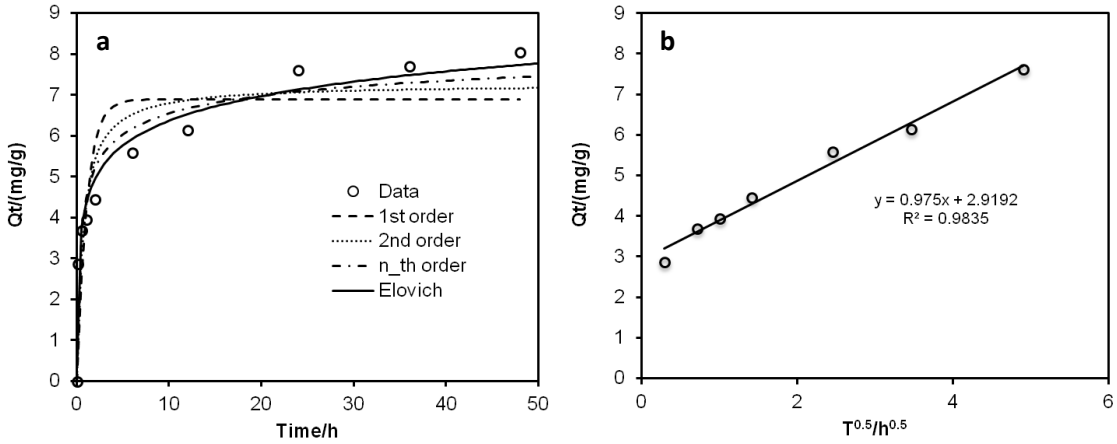

Figure 8-3. Adsorption kinetics data and modeling (a), and intraparticle diffusion plot for methylene blue (MB) on BG-MMT biochar. Symbols are experimental data and lines are model results.

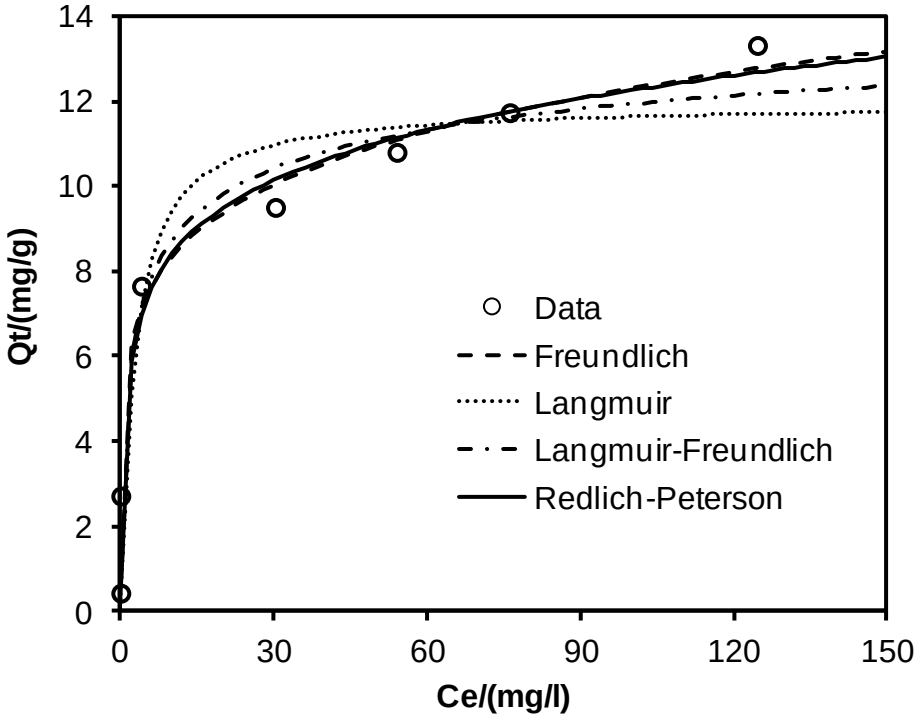

Figure 8-4. Adsorption isotherm data and modeling for methylene blue (MB) on BG-MMT biochar. Symbols are experimental data and lines are model results.

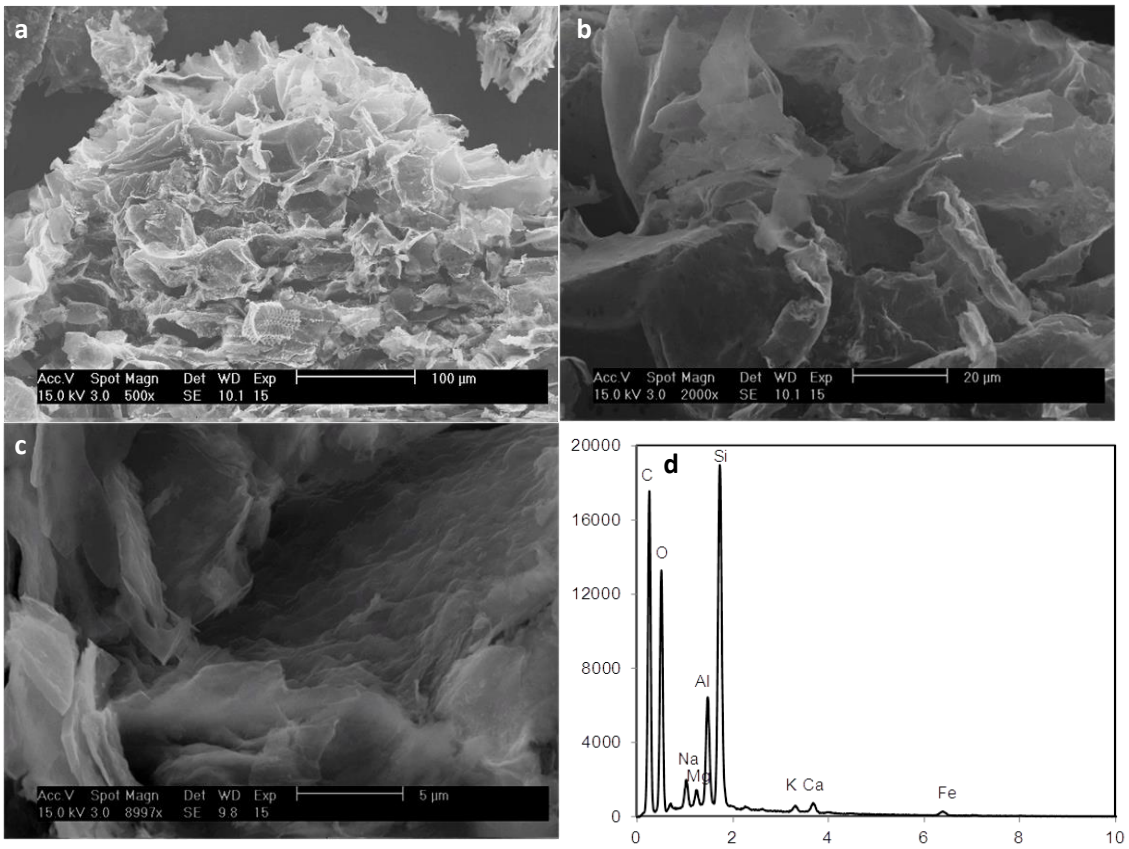

Figure 8-5. SEM image (a-c) and EDX spectrum (d) of BG-MMT biochar.

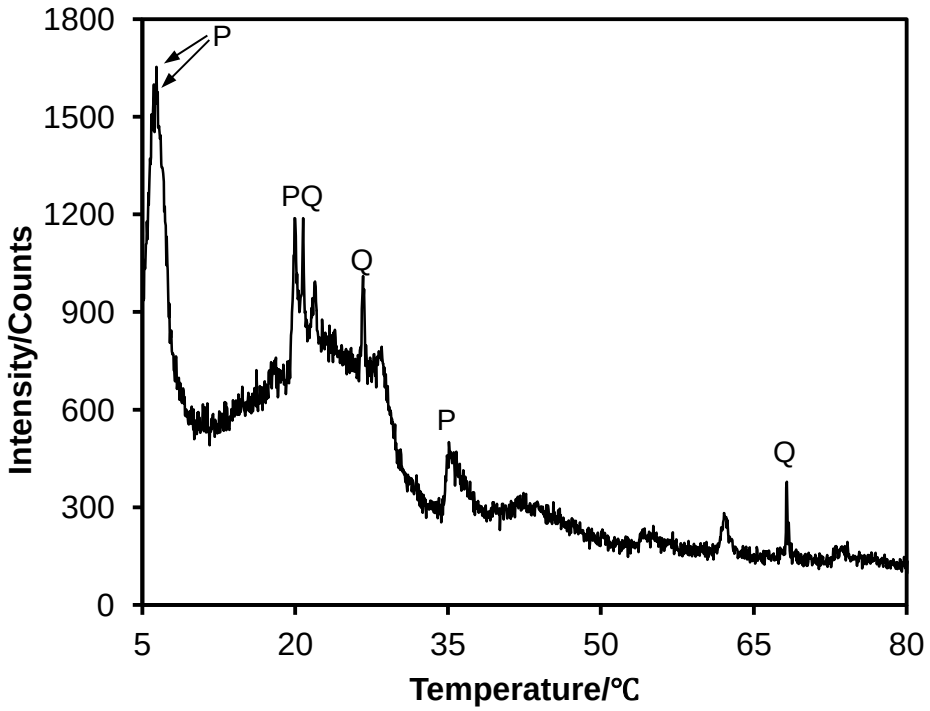

Figure 8-6. XRD spectrum of BG-MMT biochar.

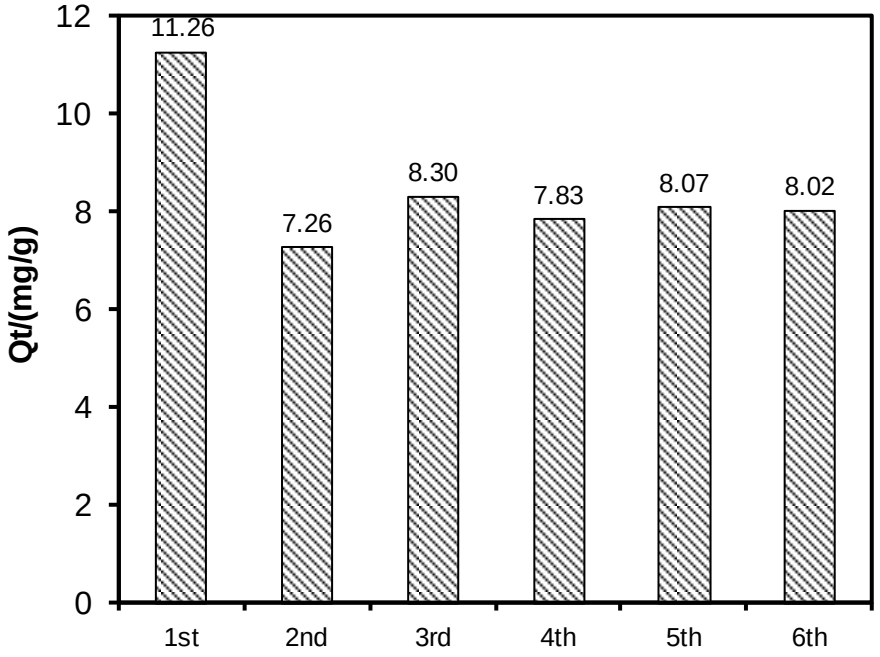

Figure 8-7. Regeneration and cycle performance of BG-MMT sorbent.

CHAPTER 9
CONCLUSIONS

Biochar converted from agricultural residues or other carbon-rich wastes may provide new solutions for environmental management, particularly with respect to carbon sequestration and contaminant remediation. This Ph.D. dissertation systematically investigated the application of various biochars to remove various contaminants, including nutrients, antibiotics, and cationic dye from aqueous solutions and its implications.

In Chapter 2, I studied whether and how biochar can affect soil nutrients (nitrate, ammonium, and phosphate) leaching. The effect of biochar on the retention and release of nutrient ions (i.e., nitrate, ammonium, and phosphate) varies with nutrient and biochar type. Of the thirteen biochars tested in this study, most of them showed little to no nitrate or phosphate sorption ability. However, nine biochars removed aqueous ammonium. When two selected biochars (BP600, PH600) with relatively good sorption ability were used in soil columns, they could effective reduce the leaching of nitrate and ammonium. Only one biochar, however, could reduce the leaching of phosphate from the soil columns. The results obtained from the leaching column study were consistent with finding from the sorption experiments, suggesting the effect of biochar on nutrients in soils could be determined through laboratory batch sorption studies. It is also recommended that sorption ability of biochars to nutrients should be determined before their applications to soils as amendment.

In Chapter 3, based on the characterization of DSTC biochar physicochemical properties and the preliminary phosphate sorption assessment,

it is evident that (1) residue from the anaerobic digestion of sugar beet tailings can be used as a feed stock for biochar production, (2) some of the physicochemical properties (e.g., pH and surface functional groups) of the two biochars are similar, but only the anaerobically digested sugar beet tailing biochar has colloidal and nano-sized periclase (MgO) on its surface, and (3) anaerobic digestion enhances the phosphate adsorption ability of biochar produced from digested sugar beet tailings relative to undigested ones.

In Chapter 4, biochar converted from anaerobically digested sugar beet tailings (DSTC) demonstrated superior ability to remove phosphate from water under a range of pH and competitive ion conditions. Batch sorption experiments and post-sorption characterizations suggested that phosphate removal was mainly controlled by adsorption onto colloidal and nano-sized MgO particles on the DSTC surface. Because both the original and anaerobically digested sugar beet tailings are waste materials, the cost to make DSTC should be very low. However, the use of pre-digested sugar beet tailings has the benefit of additional energy generation and more efficient production (with less CO_2 release during production). Thus, DSTC should be considered a promising alternative water treatment or environmental remediation technology for phosphate removal. In addition, when used as an adsorbent to reclaim phosphate from water, the exhausted biochar can be directly applied to agricultural fields as a fertilizer to improve soil fertility because the P-loaded biochar contains abundance of valuable nutrients. Potential additional environmental benefits from this approach

include fuel or energy produced during both the anaerobic digestion and pyrolysis and carbon sequestration due to biochar's refractory nature.

In Chapter 5, an innovative method has been developed to produce engineered biochar directly (without pretreatment) from plant tissues enriched with Mg. The results from the initial P sorption evaluation and biochar characterization indicated that this novel approach successfully created Mg-biochar composites, containing both nanosized MgO and $Mg(OH)_2$ particles within the matrix, which can be used as a high-efficiency adsorbent to remove P form aqueous solutions.

In Chapter 6, engineered biochar converted form Mg-enriched tomato tissues showed strong P removal ability. The spent biochar, which is P laden, behaved as a slow-release fertilizer and could release P into aqueous solution in multiple times (mimics slow release P source for plant uptake) to stimulate grass seeds' emergence and growth. The concept and findings form this study can be used to develop new sustainable and eco-friendly strategies to synthesize and apply the engineered biochar to reclaim P, reduce eutrophication, fertilize soils, improve soil quality, and sequester carbon.

In Chapter 7, biochar soil amendment as a safeguard against the leaching of pharmaceuticals into surface or ground waters, which is of particular concern during application of reclaimed water to irrigate landscapes and agricultural fields, was investigated. I found that mobility and bioavailability of SMX in biochar-amended soils were lower than that of unamended soils. Biochar soil amelioration, therefore, should be promoted in areas where reclaimed water or

waste water is used for irrigation. Because high-level accumulation of pharmaceuticals in biochar could cause adverse effect on the indigenous soil microbial community, comprehensive environmental risk assessments are recommended when selecting biochar to amend soils irrigated with reclaimed water.

In Chapter 8, new engineered biochars with clay modification has been successfully developed using two low-cost materials, which combined advantages of both biochar and clay. The clay-modified biochar has much higher sorption ability to cationic dye (MB) than the original char. The regeneration experiment reveals that the clay-modified biochar has the potential for recycle and reuse after dye adsorption and sorption mechanisms are cation exchange and electrostatic interaction. My results suggest that the simple surface modification method with clay modification in this study could be used to prepare sorbent with enhanced capacity and high regeneration performance.

The results of this dissertation indicate that biochar, as alternative sorbent, could effectively remove nutrients (phosphate), antibiotics (SMX) and cationic dye (MB) from aqueous solutions. New preparation methods, such as anaerobically digestion, plant nutrient enrichment, and surface modification could further enhance the sorption ability of biochars and thus promote their environmental applications.

LIST OF REFERENCES

1. Verheijen, F.; Jeffery, S.; Bastos, A. C.; Velde, M. v. d.; Diafas, I., *Biochar application to soils - a critical scientific review of effects on soil properties, processes and functions*. EUR 24099 EN, Office for the Official Publications of the European Communities, Luxemburg, 149pp: 2009.

2. Lehmann, J.; Gaunt, J.; Rondon, M., Bio-char sequestration in terrestrial ecosystems – a review. *Mitigation and Adaptation Strategies for Global Change* **2006**, (11), 403–427.

3. Major, J.; Rondon, M.; Molina, D.; Riha, S. J.; Lehmann, J., Maize yield and nutrition during 4 years after biochar application to a Colombian savanna oxisol. *Plant and Soil* **2010,** *333*, (1-2), 117-128.

4. Glaser, B.; Lehmann, J.; Zech, W., Ameliorating physical and chemical properties of highly weathered soils in the tropics with charcoal - a review. *Biology and Fertility of Soils* **2002,** *35*, (4), 219-230.

5. Singh, B. P.; Hatton, B. J.; Singh, B.; Cowie, A. L.; Kathuria, A., Influence of Biochars on Nitrous Oxide Emission and Nitrogen Leaching from Two Contrasting Soils. *Journal Of Environmental Quality* **2010,** *39*, (4), 1224-1235.

6. Yang, Y. N.; Sheng, G. Y., Enhanced pesticide sorption by soils containing particulate matter from crop residue burns. *Environmental Science & Technology* **2003,** *37*, (16), 3635-3639.

7. Chen, B. L.; Chen, Z. M., Sorption of naphthalene and 1-naphthol by biochars of orange peels with different pyrolytic temperatures. *Chemosphere* **2009,** *76*, (1), 127-133.

8. Kasozi, G. N.; Zimmerman, A. R.; Nkedi-Kizza, P.; Gao, B., Catechol and humic acid sorption onto a range of laboratory-produced black carbons (biochars). *Environmental Science & Technology* **2010,** *44*, (16), 6189-6195.

9. Valix, M.; Cheung, W. H.; McKay, G., Preparation of activated carbon using low temperature carbonisation and physical activation of high ash raw bagasse for acid dye adsorption. *Chemosphere* **2004,** *56*, (5), 493-501.

10. Cornelissen, G.; Gustafsson, O.; Bucheli, T. D.; Jonker, M. T. O.; Koelmans, A. A.; Van Noort, P. C. M., Extensive sorption of organic compounds to black carbon, coal, and kerogen in sediments and soils: Mechanisms and consequences for distribution, bioaccumulation, and biodegradation. *Environmental Science & Technology* **2005,** *39*, (18), 6881-6895.

11. Cao, X. D.; Ma, L. N.; Gao, B.; Harris, W., Dairy-Manure Derived Biochar Effectively Sorbs Lead and Atrazine. *Environmental Science & Technology* **2009,** *43*, (9), 3285-3291.

12. Uchimiya, M.; Lima, I. M.; Klasson, K. T.; Chang, S. C.; Wartelle, L. H.; Rodgers, J. E., Immobilization of Heavy Metal Ions (Cu-II, Cd-II, Ni-II, and Pb-II) by Broiler Litter-Derived Biochars in Water and Soil. *Journal Of Agricultural And Food Chemistry* **2010,** *58*, (9), 5538-5544.

13. Beesley, L.; Moreno-Jimenez, E.; Gomez-Eyles, J. L., Effects of biochar and greenwaste compost amendments on mobility, bioavailability and toxicity of inorganic and organic contaminants in a multi-element polluted soil. *Environmental Pollution* **2010,** *158*, (6), 2282-2287.

14. Bhargava, D. S.; Sheldarkar, S. B., Use of Tnsac in Phosphate Adsorption Studies and Relationships - Literature, Experimental Methodology, Justification and Effects of Process Variables. *Water Research* **1993,** *27*, (2), 303-312.

15. Ozacar, M., Adsorption of phosphate from aqueous solution onto alunite. *Chemosphere* **2003,** *51*, (4), 321-327.

16. Karaca, S.; Gurses, A.; Ejder, M.; Acikyildiz, M., Kinetic modeling of liquid-phase adsorption of phosphate on dolomite *Journal of Colloid and Interface Science* **2004,** *277*, (2), 257-263.

17. Huang, C. P., Removal of Phosphate by Powdered Aluminum-Oxide Adsorption. *Journal Water Pollution Control Federation* **1977,** *49*, (8), 1811-1817.

18. Namasivayam, C.; Sangeetha, D., Equilibrium and kinetic studies of adsorption of phosphate onto ZnCl2 activated coir pith carbon. *Journal of Colloid and Interface Science* **2004,** *280*, (2), 359-365.

19. Xing, X.; Gao, B.-Y.; Zhong, Q.-Q.; Yue, Q.-Y.; Li, Q., Sorption of nitrate onto amine-crosslinked wheat straw: Characteristics, column sorption and desorption properties. *Journal of Hazardous Materials* **2011,** *186*, (1), 206-211.

20. Yeoman, S.; Stephenson, T.; Lester, J. N.; Perry, R., The Removal of Phosphorus During Waste-Water Treatment - a Review. *Environmental Pollution* **1988,** *49*, (3), 183-233.

21. Patureau, D.; Helloin, E.; Rustrian, E.; Bouchez, T.; Delgenes, J. P.; Moletta, R., Combined phosphate and nitrogen removal in a sequencing batch reactor using the aerobic denitrifier, Microvirgula aerodenitrificans. *Water Research* **2001,** *35*, (1), 189-197.

22. Gieseke, A.; Arnz, P.; Amann, R.; Schramm, A., Simultaneous P and N removal in a sequencing batch biofilm reactor: insights from reactor- and microscale investigations. *Water Research* **2002,** *36*, (2), 501-509.

23. de-Bashan, L. E.; Bashan, Y., Recent advances in removing phosphorus from wastewater and its future use as fertilizer (1997-2003). *Water Research* **2004,** *38*, (19), 4222-4246.

24. Altundogan, H. S.; Tumen, F., Removal of phosphates from aqueous solutions by using bauxite. I: Effect of pH on the adsorption of various phosphates. *Journal of Chemical Technology and Biotechnology* **2002,** *77*, (1), 77-85.

25. Singh, M.; Srivastava, R. K., Sequencing batch reactor technology for biological wastewater treatment: a review. *Asia-Pacific Journal of Chemical Engineering* **2010**, n/a-n/a.

26. Ovez, B.; Ozgen, S.; Yuksel, M., Biological denitrification in drinking water using Glycyrrhiza glabra and Arunda donax as the carbon source. *Process Biochemistry* **2006,** *41*, (7), 1539-1544.

27. Clark, T.; Stephenson, T.; Pearce, A., Phosphorus removal by chemical precipitation in a biological aerated filter. *Water Research* **1997,** *31*, (10), 2557-2563.

28. Neufeld, R. D.; Thodos, G., REMOVAL OF ORTHOPHOSPHATES FROM AQUEOUS SOLUTIONS WITH ACTIVATED ALUMINA. *Environmental Science & Technology* **1969,** *3*, (7), 661-&.

29. Momberg, G. A.; Oellermann, R. A., The Removal of Phosphate by Hydroxyapatite and Struvite Crystallization in South-Africa. *Water Science and Technology* **1992,** *26*, (5-6), 987-996.

30. Biswas, B. K.; Inoue, K.; Ghimire, K. N.; Harada, H.; Ohto, K.; Kawakita, H., Removal and recovery of phosphorus from water by means of adsorption onto orange waste gel loaded with zirconium. *Bioresource Technology* **2008,** *99*, (18), 8685-8690.

31. Ben Ali, M. A.; Rakib, M.; Laborie, S.; Viers, P.; Durand, G., Coupling of bipolar membrane electrodialysis and ammonia stripping for direct treatment of wastewaters containing ammonium nitrate. *Journal of Membrane Science* **2004,** *244*, (1-2), 89-96.

32. Della Rocca, C.; Belgiorno, V.; Meric, S., Overview of in-situ applicable nitrate removal processes. *Desalination* **2007,** *204*, (1-3), 46-62.

33. Chabani, M.; Amrane, A.; Bensmaili, A., Kinetics of nitrates adsorption on Amberlite IRA 400 resin. *Desalination* **2007,** *206*, (1-3), 560-567.

34. Saad, R.; Belkacemi, K.; Hamoudi, S., Adsorption of phosphate and nitrate anions on ammonium-functionalized MCM-48: Effects of experimental conditions. *Journal of Colloid and Interface Science* **2007,** *311*, (2), 375-381.

35. Kumar, P.; Sudha, S.; Chand, S.; Srivastava, V. C., Phosphate Removal from Aqueous Solution Using Coir-Pith Activated Carbon. *Separation Science and Technology* **2010,** *45*, (10), 1463-1470.

36. Yamada, H.; Kayama, M.; Saito, K.; Hara, M., A Fundamental Research on Phosphate Removal by Using Slag. *Water Research* **1986,** *20*, (5), 547-557.

37. Agyei, N. M.; Strydom, C. A.; Potgieter, J. H., An investigation of phosphate ion adsorption from aqueous solution by fly ash and slag. *Cement and Concrete Research* **2000,** *30*, (5), 823-826.

38. G√ºrses, A.; Do*ƒ*üar, á.; Yal√ß*ƒ*±n, M.; A√ß*ƒ*±ky*ƒ*±ld*ƒ*±z, M.; Bayrak, R.; Karaca, S., **The adsorption kinetics of the cationic dye, methylene blue, onto clay**. *Journal of hazardous materials* **2006,** *131*, (1), 217-228.

39. Liu, C. J.; Li, Y. Z.; Luan, Z. K.; Chen, Z. Y.; Zhang, Z. G.; Jia, Z. P., Adsorption removal of phosphate from aqueous solution by active red mud. *Journal of Environmental Sciences-China 19*, 1166-1170.

40. Xue, Y. J.; Hou, H. B.; Zhu, S. J., Characteristics and mechanisms of phosphate adsorption onto basic oxygen furnace slag. *Journal of Hazardous Materials 162*, (2-3), 973-980.

41. Chun, Y.; Sheng, G. Y.; Chiou, C. T.; Xing, B. S., Compositions and sorptive properties of crop residue-derived chars. *Environmental Science & Technology* **2004,** *38*, (17), 4649-4655.

42. Chen, B. L.; Zhou, D. D.; Zhu, L. Z., Transitional adsorption and partition of nonpolar and polar aromatic contaminants by biochars of pine needles with different pyrolytic temperatures. *Environmental Science & Technology* **2008,** *42*, (14), 5137-5143.

43. Uchimiya, M.; Lima, I. M.; Klasson, K. T.; Wartelle, L. H., Contaminant immobilization and nutrient release by biochar soil amendment: Roles of natural organic matter. *Chemosphere* **2010,** *80*, (8), 935-940.

44. Yao, Y.; Gao, B.; Inyang, M.; Zimmerman, A. R.; Cao, X.; Pullammanappallil, P.; Yang, L., Removal of Phosphate from Aqueous Solution by Biochar Derived from Anaerobically Digested Sugar Beet Tailings: I. Biochar Characterization and Preliminary Assessment **2011**, (Submitted).

45. Roberts, K. G.; Gloy, B. A.; Joseph, S.; Scott, N. R.; Lehmann, J., Life Cycle Assessment of Biochar Systems: Estimating the Energetic, Economic, and Climate Change Potential. *Environmental Science & Technology* **2010,** *44*, (2), 827-833.

46. Cao, X. D.; Harris, W., Properties of dairy-manure-derived biochar pertinent to its potential use in remediation. *Bioresource Technology* **2010,** *101*, (14), 5222-5228.

47. Yang, Y. N.; Sheng, G. Y., Pesticide adsorptivity of aged particulate matter arising from crop residue burns. *Journal Of Agricultural And Food Chemistry* **2003,** *51*, (17), 5047-5051.

48. Inyang, M.; Gao, B.; Pullammanappallil, P.; Ding, W. C.; Zimmerman, A. R., Biochar from anaerobically digested sugarcane bagasse. *Bioresource Technology* **2010,** *101*, (22), 8868-8872.

49. Hochstrat, R.; Wintgens, T.; Melin, T.; Jeffrey, P., Assessing the European wastewater reclamation and reuse potential - a scenario analysis. *Desalination* **2006,** *188*, (1-3), 1-8.

50. Fingerman, K. R.; Berndes, G.; Orr, S.; Richter, B. D.; Vugteveen, P., Impact assessment at the bioenergy-water nexus. *Biofuels Bioproducts & Biorefining-Biofpr* **2011,** *5*, (4), 375-386.

51. Li, F.; Wichmann, K.; Otterpohl, R., Evaluation of appropriate technologies for grey water treatments and reuses. *Water Science and Technology* **2009,** *59*, (2), 249-260.

52. Hamilton, A. J.; Stagnitti, F.; Xiong, X. Z.; Kreidl, S. L.; Benke, K. K.; Maher, P., Wastewater irrigation: The state of play. *Vadose Zone Journal* **2007,** *6*, (4), 823-840.

53. Morgan, K. T.; Wheaton, T. A.; Parsons, L. R.; Castle, W. S., Effects of reclaimed municipal waste water on horticultural characteristics, fruit quality, and soil and leaf mineral concentration of citrus. *Hortscience* **2008,** *43*, (2), 459-464.

54. Al-Khashman, O., Chemical Evaluation of Ma'an Sewage Effluents and its Reuse in Irrigation Purposes. *Water Resources Management* **2009,** *23*, (6), 1041-1053.

55. Daughton, C. G.; Ternes, T. A., Pharmaceuticals and personal care products in the environment: Agents of subtle change? *Environmental Health Perspectives* **1999,** *107*, 907-938.

56. Munoz, I.; Gomez-Ramos, M. J.; Aguera, A.; Garcia-Reyes, J. F.; Molina-Diaz, A.; Fernandez-Alba, A. R., Chemical evaluation of contaminants in wastewater effluents and the environmental risk of reusing effluents in agriculture. *Trac-Trends in Analytical Chemistry* **2009,** *28*, (6), 676-694.

57. Caliskan, E.; Gokturk, S., Adsorption Characteristics of Sulfamethoxazole and Metronidazole on Activated Carbon. *Separation Science And Technology* **2010,** *45*, (2), 244-255.

58. Hernando, M. D.; Mezcua, M.; Fernandez-Alba, A. R.; Barcelo, D., Environmental risk assessment of pharmaceutical residues in wastewater effluents, surface waters and sediments. *Talanta* **2006,** *69*, (2), 334-342.

59. Furlong, E. T.; Kinney, C. A.; Werner, S. L.; Cahill, J. D., Presence and distribution of wastewater-derived pharmaceuticals in soil irrigated with reclaimed water. *Environmental Toxicology and Chemistry* **2006,** *25*, (2), 317-326.

60. Fenet, H.; Mahjoub, O.; Escande, A.; Rosain, D.; Casellas, C.; Gomez, E., Estrogen-like and dioxin-like organic contaminants in reclaimed wastewater: transfer to irrigated soil and groundwater. *Water Science and Technology* **2011,** *63*, (8), 1657-1662.

61. Ying, G. G.; Chen, F.; Kong, L. X.; Wang, L.; Zhao, J. L.; Zhou, L. J.; Zhang, L. J., Distribution and accumulation of endocrine-disrupting chemicals and pharmaceuticals in wastewater irrigated soils in Hebei, China. *Environmental Pollution* **2011,** *159*, (6), 1490-1498.

62. Thiele-Bruhn, S., Pharmaceutical antibiotic compounds in soils - a review. *Journal of Plant Nutrition and Soil Science-Zeitschrift Fur Pflanzenernahrung Und Bodenkunde* **2003,** *166*, (2), 145-167.

63. Chen, H.; Gao, B.; Li, H.; Ma, L., Effects of pH and Ionic Strength on Sulfamethoxazole and Ciprofloxacin Transport in Saturated Porous Media. *Journal Of Contaminant Hydrology* **2011**, doi:10.1016/j.jconhyd.2011.06.002.

64. Barnes, K. K.; Christenson, S. C.; Kolpin, D. W.; Focazio, M.; Furlong, E. T.; Zaugg, S. D.; Meyer, M. T.; Barber, L. B., Pharmaceuticals and other organic waste water contaminants within a leachate plume downgradient of a municipal landfill. *Ground Water Monitoring and Remediation* **2004,** *24*, (2), 119-126.

65. Lin, C. Y.; Huang, S. D., Application of liquid-liquid-liquid microextraction and high-performance liquid-chromatography for the determination of sulfonamides in water. *Analytica Chimica Acta* **2008,** *612*, (1), 37-43.

66. Lehmann, J.; Gaunt, J.; Rondon, M., Bio-char sequestration in terrestrial ecosystems - a review. *Mitigation and Adaptation Strategies for Global Change* **2006,** *11*, (2), 403-427.

67. Zimmerman, A. R.; Gao, B.; Ahn, M. Y., Positive and negative carbon mineralization priming effects among a variety of biochar-amended soils. *Soil Biology & Biochemistry* **2011,** *43*, (6), 1169-1179.

68. Cao, X. D.; Ma, L. N.; Liang, Y.; Gao, B.; Harris, W., Simultaneous immobilization of lead and atrazine in contaminated soils using dairy-manure biochar. *Environmental Science & Technology* **2011,** *45*, (11), 4884-4889.

69. Yao, Y.; Gao, B.; Inyang, M.; Zimmerman, A. R.; Cao, X.; Pullammanappallil, P.; Yang, L., Removal of phosphate from aqueous solution by biochar derived from anaerobically digested sugar beet tailings. *Journal Of Hazardous Materials* **2011,** *190*, (1-3), doi:10.1016/j.jhazmat.2011.03.083.

70. Yao, Y.; Gao, B.; Inyang, M.; Zimmerman, A. R.; Cao, X.; Pullammanappallil, P.; Yang, L., Removal of phosphate from aqueous solution by biochar derived from anaerobically digested sugar beet tailings. *Journal of Hazardous Materials* **2011,** *190*, (1-3), 501-507.

71. Crini, G., Non-conventional low-cost adsorbents for dye removal: a review. *Bioresource Technology* **2006,** *97*, (9), 1061-1085.

72. Almeida, C.; Debacher, N.; Downs, A.; Cottet, L.; Mello, C., Removal of methylene blue from colored effluents by adsorption on montmorillonite clay. *Journal of colloid and interface science* **2009,** *332*, (1), 46.

73. Rytwo, G.; Nir, S.; Margulies, L., Interactions of monovalent organic cations with montmorillonite: adsorption studies and model calculations. *Soil Science Society of America Journal* **1995,** *59*, (2), 554-564.

74. Chandrasekhar, S.; Pramada, P., Rice husk ash as an adsorbent for methylene blue,Äîeffect of ashing temperature. *Adsorption* **2006,** *12*, (1), 27-43.

75. Laird, D.; Fleming, P.; Wang, B.; Horton, R.; Karlen, D., Biochar impact on nutrient leaching from a Midwestern agricultural soil. *Geoderma* **2010,** *158*, (3-4), 436-442.

76. Inyang, M.; Gao, B.; Pullammanappallil, P.; Ding, W.; Zimmerman, A. R., Biochar from anaerobically digested sugarcane bagasse. *Bioresource Technology* **2010,** *101*, (22), 8868-8872.

77. Van Zwieten, L.; Kimber, S.; Morris, S.; Chan, K. Y.; Downie, A.; Rust, J.; Joseph, S.; Cowie, A., Effects of biochar from slow pyrolysis of papermill waste on agronomic performance and soil fertility. *Plant And Soil* **2010,** *327*, (1-2), 235-246.

78. Lehmann, J.; Pereira da Silva, J.; Steiner, C.; Nehls, T.; Zech, W.; Glaser, B., Nutrient availability and leaching in an archaeological Anthrosol and a Ferralsol of the Central Amazon basin: fertilizer, manure and charcoal amendments. *Plant and Soil* **2003,** *249*, (2), 343-357.

79. Ding, Y.; Liu, Y.-X.; Wu, W.-X.; Shi, D.-Z.; Yang, M.; Zhong, Z.-K., Evaluation of biochar effects on nitrogen retention and leaching in multi-layered soil columns. *Water Air and Soil Pollution* **2010,** *213*, (1-4), 47-55.

80. Yao, Y.; Gao, B.; Inyang, M.; Zimmerman, A. R.; Cao, X.; Pullammanappallil, P.; Yang, L., Biochar derived from anaerobically digested sugar beet tailings: Characterization and phosphate removal potential. *Bioresource Technology* **2011,** *102*, (10), 6273-6278.

81. APHA; AWWA; WEF, *Standard methods for the examination of water and wastewater*. American Public Health Association.: 1992; Vol. 2.

82. USEPA, ESS method 310.1: Ortho-phosphorus, dissolved automated, ascorbic acid. Environmental Sciences Section Inorganic chemistry unit, Wisconsin State Lab of Hygiene. In 1992.

83. Tian, Y. A.; Gao, B.; Silvera-Batista, C.; Ziegler, K. J., Transport of engineered nanoparticles in saturated porous media. *Journal of Nanoparticle Research* **2010,** *12*, (7), 2371-2380.

84. Novak, J. M.; Lima, I.; Xing, B.; Gaskin, J. W.; Steiner, C.; Das, K.; Ahmedna, M.; Rehrah, D.; Watts, D. W.; Busscher, W. J., Characterization of designer biochar produced at different temperatures and their effects on a loamy sand. *Annals of Environmental Science* **2009,** *3*, (1), 2.

85. Antal, M. J.; Gronli, M., The art, science, and technology of charcoal production. *Industrial & Engineering Chemistry Research* **2003,** *42*, (8), 1619-1640.

86. Lehmann, J.; Joseph, S., *Biochar for environmental management: science and technology*. Earthscan London/Washington DC, 2009.

87. Mukherjee, A.; Zimmerman, A. R.; Harris, W., Surface chemistry variations among a series of laboratory-produced biochars. *Geoderma* **2011,** *163*, (3-4), 247-255.

88. Brown, R. A.; Kercher, A. K.; Nguyen, T. H.; Nagle, D. C.; Ball, W. P., Production and characterization of synthetic wood chars for use as surrogates for natural sorbents. *Organic Geochemistry* **2006,** *37*, (3), 321-333.

89. Li, Z.; Katsumi, T.; Inui, T., Application of grass char for Cd (II) treatment in column leaching test. *Journal of Hazardous Materials* **2011,** *185*, (2), 768-775.

90. Inyang, M.; Gao, B.; Ding, W.; Pullammanappallil, P.; Zimmerman, A. R.; Cao, X., Enhanced lead sorption by biochar derived from anaerobically digested sugarcane bagasse. *Separation Science and Technology* **2011,** *46*, (12), 1950-1956.

91. Uchimiya, M.; Chang, S.; Klasson, K. T., Screening biochars for heavy metal retention in soil: Role of oxygen functional groups. *Journal Of Hazardous Materials* **2011,** *190*, (1-3), 432-441.

92. Mizuta, K.; Matsumoto, T.; Hatate, Y.; Nishihara, K.; Nakanishi, T., Removal of nitrate-nitrogen from drinking water using bamboo powder charcoal. *Bioresource Technology* **2004,** *95*, (3), 255-257.

93. Beesley, L.; Moreno-Jimenez, E.; Gomez-Eyles, J. L.; Harris, E.; Robinson, B.; Sizmur, T., A review of biochars' potential role in the remediation, revegetation and restoration of contaminated soils. *Environmental Pollution* **2011,** *159*, (12), 3269-3282.

94. Lehmann, J.; Rillig, M. C.; Thies, J.; Masiello, C. A.; Hockaday, W. C.; Crowley, D., Biochar effects on soil biota - A review. *Soil Biology & Biochemistry* **2011,** *43*, (9), 1812-1836.

95. Steiner, C.; Glaser, B.; Teixeira, W. G.; Lehmann, J.; Blum, W. E. H.; Zech, W., Nitrogen retention and plant uptake on a highly weathered central Amazonian Ferralsol amended with compost and charcoal. *Journal of Plant Nutrition and Soil Science-Zeitschrift Fur Pflanzenernahrung Und Bodenkunde* **2008,** *171*, (6), 893-899.

96. Steiner, C.; Garcia, M.; Zech, W., Effects of charcoal as slow release nutrient carrier on N-P-K dynamics and soil microbial population: pot experiments with Ferralsol substrate. In *Amazonian dark earths: Wim Sombroek's vision*, Woods, W. I.; Teixeira, W. G.; Lehmann, J.; Steiner, C.; WinklerPrins, A.; Rebellato, L., Eds. Springer: 2009; p 325.

97. Sposito, G., *The chemistry of soils*. Oxford University: New York, 1989.

98. Liang, B.; Lehmann, J.; Solomon, D.; Kinyangi, J.; Grossman, J.; O'Neill, B.; Skjemstad, J. O.; Thies, J.; Luizao, F. J.; Petersen, J.; Neves, E. G., Black Carbon increases cation exchange capacity in soils. *Soil Science Society Of America Journal* **2006,** *70*, (5), 1719-1730.

99. Atkinson, C. J.; Fitzgerald, J. D.; Hipps, N. A., Potential mechanisms for achieving agricultural benefits from biochar application to temperate soils: a review. *Plant And Soil* **2010,** *337*, (1-2), 1-18.

100. Liu, W.; Pullammanappallil, P. C.; Chynoweth, D. P.; Teixeira, A. A., Thermophilic anaerobic digestion of sugar beet tailings. *Transactions of the Asabe* **2008,** *51*, (2), 615-621.

101. Johnson, P. R.; Sun, N.; Elimelech, M., Colloid transport in geochemically heterogeneous porous media: Modeling and measurements. *Environmental Science & Technology* **1996,** *30*, (11), 3284-3293.

102. Martins, R. C.; Bahia, M. G. A.; Buono, V. T. L., Surface analysis of ProFile instruments by scanning electron microscopy and X-ray energy-dispersive spectroscopy: a preliminary study. *International Endodontic Journal* **2002,** *35*, (10), 848-853.

103. Thirunavukkarasu, O. S.; Viraraghavan, T.; Subramanian, K. S., Arsenic removal from drinking water using granular ferric hydroxide. *Water Sa* **2003,** *29*, (2), 161-170.

104. Chen, W. F.; Parette, R.; Zou, J. Y.; Cannon, F. S.; Dempsey, B. A., Arsenic removal by iron-modified activated carbon. *Water Research* **2007,** *41*, (9), 1851-1858.

105. Huang, X.; Liao, X. P.; Shi, B., Adsorption removal of phosphate in industrial wastewater by using metal-loaded skin split waste (vol 166, pg 1261, 2009). *Journal of Hazardous Materials* **2010,** *178*, (1-3), 1146-1146.

106. Demirbas, A.; Pehlivan, E.; Altun, T., Potential evolution of Turkish agricultural residues as bio-gas, bio-char and bio-oil sources. *International Journal of Hydrogen Energy* **2006,** *31*, (5), 613-620.

107. Hanay, O.; Hasar, H.; Kocer, N. N.; Aslan, S., Evaluation for agricultural usage with speciation of heavy metals in a municipal sewage sludge. *Bulletin of Environmental Contamination and Toxicology* **2008,** *81*, (1), 42-46.

108. Gu, X. Y.; Wong, J. W. C., Identification of inhibitory substances affecting bioleaching of heavy metals from anaerobically digested sewage sludge. *Environmental Science & Technology* **2004,** *38*, (10), 2934-2939.

109. Krishnan, K. A.; Haridas, A., Removal of phosphate from aqueous solutions and sewage using natural and surface modified coir pith. *Journal of Hazardous Materials* **2008,** *152*, (2), 527-535.

110. Eberhardt, T. L.; Min, S. H.; Han, J. S., Phosphate removal by refined aspen wood fiber treated with carboxymethyl cellulose and ferrous chloride *Bioresource Technology* **2006,** *97*, (18), 2371-2376.

111. deJonge, H.; MittelmeijerHazeleger, M. C., Adsorption of CO2 and n(2) on soil organic matter: Nature of porosity, surface area, and diffusion mechanisms. *Environmental Science & Technology* **1996,** *30*, (2), 408-413.

112. Chiou, C. T.; Lee, J. F.; Boyd, S. A., THE SURFACE-AREA OF SOIL ORGANIC-MATTER - REPLY. *Environmental Science & Technology* **1992,** *26*, (2), 404-406.

113. Kopinke, F. D.; Stottmeister, U., Adsorption of CO2 and N-2 on soil organic matter: Nature of porosity, surface area, and diffusion mechanism. *Environmental Science & Technology* **1996,** *30*, (12), 3634-3635.

114. Kwon, S.; Pignatello, J. J., Effect of natural organic substances on the surface and adsorptive properties of environmental black carbon (char): Pseudo pore blockage by model lipid components and its implications for N-2-probed surface properties of natural sorbents. *Environmental Science & Technology* **2005,** *39*, (20), 7932-7939.

115. Chomaa, J.; Jaroniecb, M., Characterization of Nanoporous Carbons by Using Gas Adsorption Isotherms. In *Activated Carbon Surfaces in Environmental Remediation*, Bandosz, T. J., Ed. ELSEVIER Ltd: Oxford, UK, 2006.

116. Binh Thanh, N.; Lehmann, J.; Kinyangi, J.; Smernik, R.; Riha, S. J.; Engelhard, M. H., Long-term black carbon dynamics in cultivated soil. *Biogeochemistry* **2009,** *92*, (1/2), 163-176.

117. Suhas; Carrott, P. J. M.; Carrott, M. M. L. R., Lignin - from natural adsorbent to activated carbon: a review. *Bioresource Technology* **2007,** *98*, (12), 2301-2312.

118. Ozcimen, D.; Karaosmanoglu, F., Production and characterization of bio-oil and biochar from rapeseed cake. *Renewable Energy* **2004,** *29*, (5), 779-787.

119. Purevsuren, B.; Avid, B.; Tesche, B.; Davaajav, Y., A biochar from casein and its properties. *Journal of Materials Science* **2003,** *38*, (11), 2347-2351.

120. Rutherford, D. W., Wershaw, Robert L. and Cox, Larry G. , Changes in Composition and Porosity Occurring During the Thermal Degradation of Wood and Wood Components. *U.S. Department of the Interior, U.S. Geological Survey, Denver* **2004,** *2004-5292*.

121. Volceanov, E.; Georgescu, M.; Volceanov, A.; Mihalache, F., Zirconium phosphate binder for periclase refractories. *Silicates Industriels* **2003,** *68*, (3-4), 31-36.

122. Chernyakhovskii, V. A., Technology of Unfired Periclase-Spinel Parts with a Phosphate Binder. *Refractories* **1985,** *26*, (1-2), 41-44.

123. Yao, Y.; Gao, B.; Inyang, M.; Zimmerman, A. R.; Cao, X.; Pullammanappallil, P.; Yang, L., Removal of Phosphate from Aqueous Solution by Biochar Derived from Anaerobically Digested Sugar Beet Tailings: II. Adsorption Mechanisms and Characteristics. **2011**, (Submitted).

124. Manning, B. A.; Goldberg, S., Modeling competitive adsorption of arsenate with phosphate and molybdate on oxide minerals. *Soil Science Society Of America Journal* **1996,** *60*, (1), 121-131.

125. Schindler, P. W.; Stumm, W., The surface chemistry of oxides, hydroxides, and oxide minerals. In *Aquatic surface chemistry - chemical processes at the particle-water interface.*, Stumm, W., Ed. John Wiley & Sons: New York, 1987.

126. Kosmulski, M., *Surface charging and points of zero charge*. Taylor & Francis Group: Boca Raton, FL, 2009.

127. Shin, E. W.; Han, J. S.; Jang, M.; Min, S. H.; Park, J. K.; Rowell, R. M., Phosphate adsorption on aluminum-impregnated mesoporous silicates: Surface structure and behavior of adsorbents. *Environmental Science & Technology* **2004,** *38*, (3), 912-917.

128. Gerente, C.; Lee, V. K. C.; Le Cloirec, P.; McKay, G., Application of chitosan for the removal of metals from wastewaters by adsorption - Mechanisms and models review. *Critical Reviews in Environmental Science and Technology* **2007,** *37*, (1), 41-127.

129. Axe, L.; Trivedi, P., Intraparticle surface diffusion of metal contaminants and their attenuation in microporous amorphous Al, Fe, and Mn oxides. *Journal Of Colloid And Interface Science* **2002,** *247*, (2), 259-265.

130. Weerasooriya, R.; Tobschall, H. J.; Seneviratne, W.; Bandara, A., Transition state kinetics of Hg(II) adsorption at gibbsite-water interface. *Journal of Hazardous Materials* **2007,** *147*, (3), 971-978.

131. Marris, E., Putting the carbon back: Black is the new green. *Nature* **2006,** *442*, (7103), 624-626.

132. Woolf, D.; Amonette, J. E.; Street-Perrott, F. A.; Lehmann, J.; Joseph, S., Sustainable biochar to mitigate global climate change. *Nature Communications* **2010,** *1*.

133. Lehmann, J., A handful of carbon. *Nature* **2007,** *447*, (7141), 143-144.

134. Zhang, M.; Gao, B.; Varnoosfaderani, S.; Hebard, A. F.; Yao, Y.; Inyang, M., Preparation and characterization of a novel magnetic biochar for arsenic removal. *Bioresource Technology* **2012,** *doi: 10.1016/j.biortech.2012.11.132*.

135. Xue, Y.; Gao, B.; Yao, Y.; Inyang, M.; Zhang, M.; Zimmerman, A. R.; Ro, K. S., Hydrogen peroxide modification enhances the ability of biochar (hydrochar) produced from hydrothermal carbonization of peanut hull to remove aqueous heavy metals: Batch and column tests. *Chemical Engineering Journal* **2012,** *200*, 673-680.

136. Inyang, M. D.; Gao, B.; Ding, W. C.; Pullammanappallil, P.; Zimmerman, A. R.; Cao, X. D., Enhanced lead sorption by biochar derived from anaerobically digested sugarcane bagasse. *Separation Science And Technology* **2011,** *46*, (12), 1950-1956.

137. Inyang, M.; Gao, B.; Yao, Y.; Xue, Y.; Zimmerman, A. R.; Pullammanappallil, P.; Cao, X., Removal of heavy metals from aqueous solution by biochars derived from anaerobically digested biomass. *Bioresource Technology* **2012,** *110*, 50-56.

138. Schelske, C. L., Eutrophication: focus on phosphorus. *Science* **2009,** *324*, (5928), 722-722.

139. Conley, D. J.; Paerl, H. W.; Howarth, R. W.; Boesch, D. F.; Seitzinger, S. P.; Havens, K. E.; Lancelot, C.; Likens, G. E., Controlling eutrophication: nitrogen and phosphorus. *Science (Washington)* **2009,** *323*, (5917).

140. Strahm, B. D.; Harrison, R. B., Nitrate sorption in a variable-charge forest soil of the Pacific Northwest. *Soil science* **2006,** *171*, (4), 313-321.

141. Yao, Y.; Gao, B.; Zhang, M.; Inyang, M.; Zimmerman, A. R., Effect of biochar amendment on sorption and leaching of nitrate, ammonium, and phosphate in a sandy soil. *Chemosphere* **2012**.

142. Chen, W.; Parette, R.; Zou, J.; Cannon, F. S.; Dempsey, B. A., Arsenic removal by iron-modified activated carbon. *Water research* **2007,** *41*, (9), 1851-1858.

143. Gu, Z.; Fang, J.; Deng, B., Preparation and evaluation of GAC-based iron-containing adsorbents for arsenic removal. *Environmental Science & Technology* **2005,** *39*, (10), 3833-3843.

144. Zhang, M.; Gao, B.; Yao, Y.; Xue, Y.; Inyang, M., Synthesis of porous MgO-biochar nanocomposites for removal of phosphate and nitrate from aqueous solutions. *Chemical Engineering Journal* **2012,** *210*, 26-32.

145. Yao, Y.; Gao, B.; Inyang, M.; Zimmerman, A. R.; Cao, X. D.; Pullammanappallil, P.; Yang, L. Y., Removal of phosphate from aqueous solution by biochar derived from anaerobically digested sugar beet tailings. *Journal Of Hazardous Materials* **2011,** *190*, (1-3), 501-507.

146. BBhargava, D. S.; Sheldarkar, S. B., Use of Tnsac in Phosphate Adsorption Studies and Relationships - Isotherm Relationships and Utility in the Field. *Water Research* **1993,** *27*, (2), 325-335.

147. Chen, B.; Chen, Z.; Lv, S., A novel magnetic biochar efficiently sorbs organic pollutants and phosphate. *Bioresource Technology* **2011,** *102*, (2), 716-723.

148. Karley, A. J.; White, P. J., Moving cationic minerals to edible tissues: potassium, magnesium, calcium. *Current Opinion In Plant Biology* **2009,** *12*, (3), 291-298.

149. Ma, L. Q.; Komar, K. M.; Tu, C.; Zhang, W. H.; Cai, Y.; Kennelley, E. D., A fern that hyperaccumulates arsenic - A hardy, versatile, fast-growing plant helps to remove arsenic from contaminated soils. *Nature* **2001,** *409*, (6820), 579-579.

150. Song, W. Y.; Sohn, E. J.; Martinoia, E.; Lee, Y. J.; Yang, Y. Y.; Jasinski, M.; Forestier, C.; Hwang, I.; Lee, Y., Engineering tolerance and accumulation of lead and cadmium in transgenic plants. *Nature Biotechnology* **2003,** *21*, (8), 914-919.

151. Rugh, C. L.; Wilde, H. D.; Stack, N. M.; Thompson, D. M.; Summers, A. O.; Meagher, R. B., Mercuric ion reduction and resistance in transgenic Arabidopsis thaliana plants expressing a modified bacterial merA gene. *Proceedings of the National Academy of Sciences of the United States of America* **1996,** *93*, (8), 3182-3187.

152. Patterson, A., The Scherrer formula for x-ray particle size determination. *Physical Review* **1939,** *56*, (10), 978.

153. Holzwarth, U.; Gibson, N., The Scherrer equation versus the'Debye-Scherrer equation'. *Nature Nanotechnology* **2011,** *6*, (9), 534-534.

154. Almeelbi, T.; Bezbaruah, A., Aqueous phosphate removal using nanoscale zero-valent iron. *Journal of Nanoparticle Research* **2012,** *14*, (7), 1-14.

155. Smith, V. H., Eutrophication of freshwater and coastal marine ecosystems - A global problem. *Environmental Science and Pollution Research* **2003,** *10*, (2), 126-139.

156. Penn, C. J.; Warren, J. G., Investigating phosphorus sorption onto kaolinite using isothermal titration calorimetry. *Soil Science Society of America Journal* **2009,** *73*, (2), 560-568.

157. USEPA, Ecological restoration: a tool to manage stream quality, Report EPA 841-F-95-007. *US EPA, Washington,DC, USA* **1995**.

158. Dodds, W. K.; Bouska, W. W.; Eitzmann, J. L.; Pilger, T. J.; Pitts, K. L.; Riley, A. J.; Schloesser, J. T.; Thornbrugh, D. J., Eutrophication of US freshwaters: analysis of potential economic damages. *Environmental Science & Technology* **2008,** *43*, (1), 12-19.

159. Zhang, M.; Gao, B.; Yao, Y.; Xue, Y.; Inyang, M., Synthesis, characterization, and environmental implications of graphene-coated biochar. *Science Of The Total Environment* **2012,** *435-436*, 567-572.

160. Yao, Y.; Gao, B.; Zhang, M.; Inyang, M.; Zimmerman, A. R., Effect of biochar amendment on sorption and leaching of nitrate, ammonium, and phosphate in a sandy soil. *Chemosphere* **2012,** *89*, (11), 1467-1471.

161. Chen, B. L.; Chen, Z. M.; Lv, S. F., A novel magnetic biochar efficiently sorbs organic pollutants and phosphate. *Bioresource Technology* **2011,** *102*, (2), 716-723.

162. Yao, Y.; Gao, B.; Inyang, M.; Zimmerman, A. R.; Cao, X.; Pullammanappallil, P.; Yang, L., Engineered carbon (biochar) prepared by direct pyrolysis of mg-accumulated tomato tissues: Characterization and phosphate removal potential. *Bioresource Technology* **2013**, doi: 10.1016/j.biortech.2013.03.057.

163. Zhang, M.; Gao, B.; Yao, Y.; Xue, Y. W.; Inyang, M., Synthesis of porous MgO-biochar nanocomposites for removal of phosphate and nitrate from aqueous solutions. *Chemical Engineering Journal* **2012,** *210*, 26-32.

164. Zhang, M.; Gao, B.; Varnoosfaderani, S.; Hebard, A. F.; Yao, Y.; Inyang, M., Preparation and characterization of a novel magnetic biochar for arsenic removal. *Bioresource Technology* **2013,** *130*, 457-462.

165. Zhang, M.; Gao, B.; Yao, Y.; Inyang, M., Phosphate removal ability of biochar/MgAl-LDH ultra-fine composites prepared by liquid-phase deposition. *Chemosphere* **2013**, doi: 10.1016/j.chemosphere.2013.02.050.

166. Yan, L. G.; Xu, Y. Y.; Yu, H. Q.; Xin, X. D.; Wei, Q.; Du, B., Adsorption of phosphate from aqueous solution by hydroxy-aluminum, hydroxy-iron and hydroxy-iron-aluminum pillared bentonites. *Journal of Hazardous Materials 179*, (1-3), 244-250.

167. Chouyyok, W.; Wiacek, R. J.; Pattamakomsan, K.; Sangvanich, T.; Grudzien, R. M.; Fryxell, G. E.; Yantasee, W., Phosphate Removal by Anion Binding on Functionalized Nanoporous Sorbents. *Environmental Science & Technology* **2010,** *44*, (8), 3073-3078.

168. Biswas, B. K.; Inoue, K.; Ghimire, K. N.; Ohta, S.; Harada, H.; Ohto, K.; Kawakita, H., The adsorption of phosphate from an aquatic environment using metal-loaded orange waste. *Journal of Colloid and Interface Science 312*, (2), 214-223.

169. Huang, X.; Liao, X. P.; Shi, B., Adsorption removal of phosphate in industrial wastewater by using metal-loaded skin split waste. *Journal of Hazardous Materials* **2009,** *166*, (2-3), 1261-1265.

170. Harvey, O. R.; Kuo, L.-J.; Zimmerman, A. R.; Louchouarn, P.; Amonette, J. E.; Herbert, B. E., An Index-Based Approach to Assessing Recalcitrance and Soil Carbon Sequestration Potential of Engineered Black Carbons (Biochars). *Environmental Science & Technology* **2012,** *46*, (3), 1415-1421.

171. Masiello, C.; Druffel, E., Black carbon in deep-sea sediments. *Science* **1998,** *280*, (5371), 1911-1913.

172. Czimczik, C. I.; Masiello, C. A., Controls on black carbon storage in soils. *Global Biogeochemical Cycles* **2007,** *21*, (3), GB3005.

173. Nguyen, B. T.; Lehmann, J.; Kinyangi, J.; Smernik, R.; Riha, S. J.; Engelhard, M. H., Long-term black carbon dynamics in cultivated soil. *Biogeochemistry* **2009,** *92*, (1), 163-176.

174. Liang, B.; Lehmann, J.; Solomon, D.; Sohi, S.; Thies, J. E.; Skjemstad, J. O.; Luizão, F. J.; Engelhard, M. H.; Neves, E. G.; Wirick, S., Stability of biomass-derived black carbon in soils. *Geochimica et Cosmochimica Acta* **2008,** *72*, (24), 6069-6078.

175. Mehlich, A., Mehlich 3 soil test extractant: A modification of Mehlich 2 extractant. *Communications in Soil Science & Plant Analysis* **1984,** *15*, (12), 1409-1416.

176. Weerasooriya, R.; Tobschall, H. J.; Seneviratne, W.; Bandara, A., Transition state kinetics of Hg (II) adsorption at gibbsite‚Äìwater interface. *Journal of hazardous materials* **2007,** *147*, (3), 971-978.

177. Fournier, V.; Marcus, P.; Olefjord, I., Oxidation of magnesium. *Surface and interface analysis* **2002,** *34*, (1), 494-497.

178. Song, Y.; Shan, D.; Chen, R.; Zhang, F.; Han, E. H., Formation mechanism of phosphate conversion film on Mg-8.8 Li alloy. *Corrosion Science* **2009,** *51*, (1), 62-69.

179. Lv, J.; Qiu, L.; Qu, B., Controlled growth of three morphological structures of magnesium hydroxide nanoparticles by wet precipitation method. *Journal of Crystal Growth* **2004,** *267*, (3), 676-684.

180. Henrist, C.; Mathieu, J. P.; Vogels, C.; Rulmont, A.; Cloots, R., Morphological study of magnesium hydroxide nanoparticles precipitated in dilute aqueous solution. *Journal of Crystal Growth* **2003,** *249*, (1), 321-330.

181. Zhang, W.; Tian, B.; Du, K. Q.; Zhang, H. X.; Wang, F. H., Preparation and Corrosion Performance of PEO Coating With Low Porosity on Magnesium Alloy AZ91D In Acidic KF System. *Int. J. Electrochem. Sci* **2011,** *6*, 5228-5248.

182. Song, Y.; Shan, D.; Chen, R.; Zhang, F.; Han, E. H., A novel phosphate conversion film on Mg-8.8 Li alloy. *Surface and Coatings Technology* **2009,** *203*, (9), 1107-1113.

183. Chusuei, C.; Goodman, D.; Van Stipdonk, M.; Justes, D.; Loh, K.; Schweikert, E., Solid-liquid adsorption of calcium phosphate on TiO2. *Langmuir* **1999,** *15*, (21), 7355-7360.

184. Vanderkooi, G., Crystal-refined hydrogen-bond potentials for interactions involving the phosphate group. *The Journal of Physical Chemistry* **1983,** *87*, (25), 5121-5129.

185. Burget, U.; Zundel, G., Glutamic acid-dihydrogen phosphate hydrogen-bonded networks: their proton polarizability as a function of cations present. Infrared investigations. *Biophysical journal* **1987,** *52*, (6), 1065-1070.

186. Pierzynski, G. M., Methods of phosphorus analysis for soils, sediments, residuals, and waters. In North Carolina State University Raleigh: 2000.

187. Gaskin, J.; Steiner, C.; Harris, K.; Das, K.; Bibens, B., Effect of low-temperature pyrolysis conditions on biochar for agricultural use. *Transactions of the Asabe* **2008,** *51*, (6), 2061-2069.

188. Solaiman, Z. M.; Murphy, D. V.; Abbott, L. K., Biochars influence seed germination and early growth of seedlings. *Plant and Soil* **2012**, 1-15.

189. Austin, R. B., GROWTH OF WATERCRESS (RORIPPA NASTURTIUM AQUATICUM (L) HAYEK) FROM SEED AS AFFECTED BY PHOSPHORUS NUTRITION OF PARENT PLANT. *Plant and Soil* **1966,** *24*, (1), 113-&.

190. Hamilton, A. J.; Stagnitti, F.; Xiong, X. Z.; Kreidl, S. L.; Benke, K. K.; Maher, P., Wastewater irrigation: The state of play. *Vadose Zone J* **2007,** *6*, (4), 823-840.

191. Evanylo, G.; Ervin, E.; Zhang, X., Reclaimed Water for Turfgrass Irrigation. *Water* **2010**, (2), 685-701.

192. Al-Khashman, O., Chemical evaluation of Ma'an sewage effluents and its reuse in irrigation purposes. *Water Resour Manag* **2009,** *23*, (6), 1041-1053.

193. Masciopinto, C.; La Mantia, R.; Chrysikopoulos, C. V., Fate and transport of pathogens in a fractured aquifer in the Salento area, Italy. *Water Resources Research* **2008,** *44*, (1).

194. Chrysikopoulos, C. V.; Masciopinto, C.; La Mantia, R.; Manariotis, I. D., Removal of Biocolloids Suspended in Reclaimed Wastewater by Injection into a Fractured Aquifer Model. *Environmental Science & Technology* **2010,** *44*, (3), 971-977.

195. Anders, R.; Chrysikopoulos, C. V., Virus fate and transport during artificial recharge with recycled water. *Water Resources Research* **2005,** *41*, (10).

196. Drewes, J. E.; Sedlak, D.; Snyder, S.; dickenson, E., *Development of indicators and surrogates for chemical contaminant removal during wastewater treatment and reclamation*. Water Reuse Foundation: Alexandria, VA, 2008; p 169.

197. Munoz, I.; Gomez-Ramos, M. J.; Aguera, A.; Garcia-Reyes, J. F.; Molina-Diaz, A.; Fernandez-Alba, A. R., Chemical evaluation of contaminants in wastewater effluents and the environmental risk of reusing effluents in agriculture. *Trends Analyt Chem* **2009,** *28*, (6), 676-694.

198. Thiele-Bruhn, S., Pharmaceutical antibiotic compounds in soils - a review. *J Pl Nutr Soil Sci* **2003,** *166*, (2), 145-167.

199. Helgeson, T., *A reconnaissance-level quantitative comparison of reclaimed water, surface water, and groundwater*. Water Reuse Foundation: Alexandria, VA, 2009; p 141.

200. Chen, H.; Gao, B.; Li, H.; Ma, L., Effects of pH and Ionic Strength on Sulfamethoxazole and Ciprofloxacin Transport in Saturated Porous Media. *J Contam Hydrol* **2011**, doi:10.1016/j.jconhyd.2011.06.002.

201. Barnes, K. K.; Christenson, S. C.; Kolpin, D. W.; Focazio, M.; Furlong, E. T.; Zaugg, S. D.; Meyer, M. T.; Barber, L. B., Pharmaceuticals and other organic waste water contaminants within a leachate plume downgradient of a municipal landfill. *Ground Wat Monit Remediat* **2004,** *24*, (2), 119-126.

202. Lin, C. Y.; Huang, S. D., Application of liquid-liquid-liquid microextraction and high-performance liquid-chromatography for the determination of sulfonamides in water. *Analyt Chim Acta* **2008,** *612*, (1), 37-43.

203. Barnes, K. K.; Kolpin, D. W.; Furlong, E. T.; Zaugg, S. D.; Meyer, M. T.; Barber, L. B., A national reconnaissance of pharmaceuticals and other organic wastewater contaminants in the United States - I) Groundwater. *Science Of The Total Environment* **2008,** *402*, (2-3), 192-200.

204. Lehmann, J.; Gaunt, J.; Rondon, M., Bio-char sequestration in terrestrial ecosystems - a review. *Mitig Adapt Strat Global Change* **2006,** *11*, (2), 403-427.

205. Inyang, M.; Gao, B.; Pullammanappallil, P.; Ding, W.; Zimmerman, A. R., Biochar from anaerobically digested sugarcane bagasse. *Bioresource Technol* **2010,** *101*, (22), 8868-8872.

206. Cao, X.; Ma, L. N.; Liang, Y.; Gao, B.; Harris, W., Simultaneous immobilization of lead and atrazine in contaminated soils using dairy-manure biochar. *Environmental Science & Technology* **2011,** *45*, (11), 4884-4889.

207. Yao, Y.; Gao, B.; Inyang, M.; Zimmerman, A. R.; Cao, X.; Pullammanappallil, P.; Yang, L., Removal of phosphate from aqueous solution by biochar derived from anaerobically digested sugar beet tailings. *J. Hazard Mater* **2011,** *190*, (1-3), doi:10.1016/j.jhazmat.2011.03.083.

208. Inyang, M.; Gao, B.; Ding, W.; Pullammanappallil, P.; Zimmerman, A. R.; Cao, X., Enhanced lead sorption by biochar derived from anaerobically digested sugarcane bagasse. *Separation Science And Technology* **2011**, doi: 10.1080/01496395.2011.584604.

209. Yao, Y.; Gao, B.; Inyang, M.; Zimmerman, A. R.; Cao, X.; Pullammanappallil, P.; Yang, L., Biochar derived from anaerobically digested sugar beet tailings: Characterization and phosphate removal potential. *Bioresource Technol* **2011,** *102*, (10), 6273-6278.

210. Parsons, L. R.; Wheaton, T. A.; Castle, W. S., High application rates of reclaimed water benefit citrus tree growth and fruit production. *Hortscience* **2001,** *36*, (7), 1273-1277.

211. APHA, Standard methods for the examination of water and wastewater (19th edition). *American Public Health Association, Washington, D.C* **1995**.

212. Hammes, K.; Smernik, R. J.; Skjemstad, J. O.; Schmidt, M. W. I., Characterisation and evaluation of reference materials for black carbon analysis using elemental composition, colour, BET surface area and C-13 NMR spectroscopy. *Applied Geochemistry* **2008,** *23*, (8), 2113-2122.

213. Pan, B.; Huang, P.; Wua, M.; Wang, Z.; Wang, P.; Jiao, X.; Xing, B., Physicochemical and sorption properties of thermally-treated sediments with high organic matter content. *Bioresource Technology* **2012,** *103*, 367-373.

214. Tolls, J., Sorption of veterinary pharmaceuticals in soils: A review. *Environmental Science & Technology* **2001,** *35*, (17), 3397-3406.

215. Shamsa, F.; Amani, L., Determination of Sulfamethoxazole and Trimethoprim in Pharmaceuticals by Visible and UV Spectrophotometry. *Iranian Journal of Pharmaceutical Research* **2006**, (1), 31-36.

216. Tian, Y. A.; Gao, B.; Silvera-Batista, C.; Ziegler, K. J., Transport of engineered nanoparticles in saturated porous media. *J Nanopart Res* **2010,** *12*, (7), 2371-2380.

217. USEPA, T. C. L. P., EPA method 1311. *Washington, US* **1990**.

218. Wallace, R. J.; Wiss, K.; Bushby, M. B.; Hollowell, D. C., Invitro Activity of Trimethoprim and Sulfamethoxazole against the Nontuberculous Mycobacteria. *Reviews of Infectious Diseases* **1982,** *4*, (2), 326-331.

219. Fernandes, N. S.; Carvalho, M. A. D.; Mendes, R. A.; Ionashiro, M., Thermal decomposition of some chemotherapic substances. *Journal Of The Brazilian Chemical Society* **1999,** *10*, (6), 459-462.

220. Schacklette, H. T.; Boerngen, J. G., Element concentrations is soils and other surfical materials of the conterminous United States. *USGS Professional Paper 1270* **1984**.

221. Guo, Y.; Rockstraw, D. A., Physicochemical properties of carbons prepared from pecan shell by phosphoric acid activation. *Bioresource Technol* **2007,** *98*, (8), 1513-1521.

222. Gaskin, J.; Steiner, C.; Harris, K.; Das, K.; Bibens, B., Effect of low-temperature pyrolysis conditions on biochar for agricultural use. *Trans. ASABE* **2008,** *51*, (6), 2061-2069.

223. Wang, H. L.; Lin, K. D.; Hou, Z. N.; Richardson, B.; Gan, J., Sorption of the herbicide terbuthylazine in two New Zealand forest soils amended with biosolids and biochars. *Journal Of Soils And Sediments* **2010,** *10*, (2), 283-289.

224. Yang, X. B.; Ying, G. G.; Peng, P. A.; Wang, L.; Zhao, J. L.; Zhang, L. J.; Yuan, P.; He, H. P., Influence of Biochars on Plant Uptake and Dissipation of Two Pesticides in an Agricultural Soil. *Journal Of Agricultural And Food Chemistry* **2010,** *58*, (13), 7915-7921.

225. Steinbeiss, S.; Gleixner, G.; Antonietti, M., Effect of biochar amendment on soil carbon balance and soil microbial activity. *Soil Biol Biochem* **2009,** *41*, (6), 1301-1310.

226. Sohi, S. P.; Krull, E.; Lopez-Capel, E.; Bol, R., A Review of Biochar and Its Use and Function in Soil. *Advances in Agronomy* **2010,** *105*, 47-82.

227. Murray, H. H., Overview,Äîclay mineral applications. *Applied Clay Science* **1991,** *5*, (5), 379-395.

228. Bilgi√ß, C., Investigation of the factors affecting organic cation adsorption on some silicate minerals. *Journal of colloid and interface science* **2005,** *281*, (1), 33-38.

229. Segad, M.; JoÃànsson, B.; √Ökesson, T.; Cabane, B., Ca/Na montmorillonite: Structure, forces and swelling properties. *Langmuir* **2010,** *26*, (8), 5782-5790.

230. Gurses, A.; Dogar, C.; Yalcin, M.; Acikyildiz, M.; Bayrak, R.; Karaca, S., The adsorption kinetics of the cationic dye, methylene blue, onto clay. *Journal of Hazardous Materials* **2006,** *131*, (1-3), 217-228.

231. Ghosh, D.; Bhattacharyya, K. G., Adsorption of methylene blue on kaolinite. *Applied Clay Science* **2002,** *20*, (6), 295-300.

232. Mestdagh, M.; Vielvoye, L.; Herbillon, A., Iron in kaolinite: II. The relationship between kaolinite crystallinity and iron content. *Clay Minerals* **1980,** *15*, (1), 1-13.

233. Gong, F.; Feng, M.; Zhao, C.; Zhang, S.; Yang, M., Thermal properties of poly (vinyl chloride)/montmorillonite nanocomposites. *Polymer Degradation and Stability* **2004,** *84*, (2), 289-294.

234. Aygun, A.; Yenisoy-Karakas, S.; Duman, I., Production of granular activated carbon from fruit stones and nutshells and evaluation of their physical, chemical and adsorption properties. *Microporous and Mesoporous Materials* **2003,** *66*, (2-3), 189-195.

235. Ayg√ºn, A.; Yenisoy-Karaka≈ü, S.; Duman, I., Production of granular activated carbon from fruit stones and nutshells and evaluation of their physical, chemical and adsorption properties. *Microporous and Mesoporous Materials* **2003,** *66*, (2), 189-195.

236. Klika, Z.; Pustkova, P.; Dudova, M.; Capkova, P.; Klikova, C.; Matys Grygar, T., The adsorption of methylene blue on montmorillonite from acid solutions. *Clay Minerals* **2011,** *46*, (3), 461-471.

237. Ma, Y.-L.; Xu, Z.-R.; Guo, T.; You, P., Adsorption of methylene blue on Cu (II)-exchanged montmorillonite. *Journal of colloid and interface science* **2004,** *280*, (2), 283-288.

238. Yao, Y.; Bin Gao, J. C., Ming Zhang, Mandu Inyang, Yuncong Li, Ashok Alva, Liuyan Yang, An engineered biochar reclaims phosphate from aqueous solutions: mechanisms and potential application as a slow-release fertilizer. **2013**.

239. Pignatello, J. J.; Xing, B., Mechanisms of slow sorption of organic chemicals to natural particles. *Environmental Science & Technology* **1995,** *30*, (1), 1-11.

240. Brusseau, M. L.; Jessup, R. E.; Rao, P. S. C., Nonequilibrium sorption of organic chemicals: Elucidation of rate-limiting processes. *Environmental Science & Technology* **1991,** *25*, (1), 134-142.

241. Wu, F.-C.; Tseng, R.-L.; Juang, R.-S., Initial behavior of intraparticle diffusion model used in the description of adsorption kinetics. *Chemical Engineering Journal* **2009,** *153*, (1), 1-8.

242. Kalavathy, M. H.; Karthikeyan, T.; Rajgopal, S.; Miranda, L. R., Kinetic and isotherm studies of Cu (II) adsorption onto H3PO4-activated rubber wood sawdust. *Journal of colloid and interface science* **2005,** *292*, (2), 354.

243. Zhou, L.; Chen, H.; Jiang, X.; Lu, F.; Zhou, Y.; Yin, W.; Ji, X., Modification of montmorillonite surfaces using a novel class of cationic gemini surfactants. *Journal of colloid and interface science* **2009,** *332*, (1), 16-21.

244. Wang, S.; Hu, Y.; Zong, R.; Tang, Y.; Chen, Z.; Fan, W., Preparation and characterization of flame retardant ABS/montmorillonite nanocomposite. *Applied Clay Science* **2004,** *25*, (1), 49-55.

245. Pavan, F. A.; Lima, E. C.; Dias, S. L.; Mazzocato, A. C., Methylene blue biosorption from aqueous solutions by yellow passion fruit waste. *Journal of hazardous materials* **2008,** *150*, (3), 703-12.

246. Chen, G.; Pan, J.; Han, B.; Yan, H., Adsorption of methylene blue on montmorillonite. *Journal of dispersion science and technology* **1999,** *20*, (4), 1179-1187.

247. Wang, L.; Zhang, J.; Wang, A., Removal of methylene blue from aqueous solution using chitosan-< i> g</i>-poly (acrylic acid)/montmorillonite superadsorbent nanocomposite. *Colloids and Surfaces A: Physicochemical and Engineering Aspects* **2008,** *322*, (1), 47-53.

248. Usuki, A.; Kawasumi, M.; Kojima, Y.; Okada, A.; Kurauchi, T.; Kamigaito, O., Swelling behavior of montmorillonite cation exchanged for x-amino acids by e-caprolactam. *J. Mater. Res* **1993,** *8*, (5), 1174-1178.

BIOGRAPHICAL SKETCH

Ying Yao was born 1984 in Handan, China. She received the Bachelor of Science in Environmental Science from Southwest University in China in 2007 and the Master of Science in Environmental Science from the Nanjing University in 2010. She was awarded the National Oversea Scholarship of Chinese Government in 2009.

She enrolled as a PhD student in the Agricultural and Biological Engineering Department at University of Florida in 2009. Her doctoral research, under the direction of Dr. Bin Gao, focused on using biochar technology to improve environment sustainability, particularly with respect to using biochar as a low-cost adsorbent to reclaim nutrients from wastewater. As a reward to her high quality research, She has published nine peer-review journal articles (five first author papers) in top ranking international journals. She was also a recipient of outstanding international student academic achievement award at University of Florida. After graduation, she will pursue an academia career in China.